Port Engineering

Liu, Zhou; Burcharth, Hans F.

PORT ENGINEERING

Zhou Liu and Hans F. Burcharth

2. udgave, januar 1999
Laboratoriet for Hydraulik og Havnebygning
Aalborg Universitet

Contents

1 PLANNING AND LAYOUT OF PORTS

1.1 Components of a port

A port is composed optionally the following components, cf. Figs.1 and 2.

1) Breakwater : A rubble mound or vertical structure to protect the harbour from wave attacks.

2) Harbour : A protected water area which provides safe and suitable accommodation for ships to transfer cargo and passenger, to be refueled and repaired. A harbour includes

   Entrance.

   Navigation channel.

   Turning area : A place where ships can turn.

   Anchorage area : A place where ships wait for their turn at berth or for more favorable weather conditions.

   Berthing area : A place where ships berth for loading and unloading operations.

3) Berth structure and land area.

   Berth structure : A structure built to berth ships for loading and unloading operations. It includes mooring equipments such as fenders and bollards.

   Apron : An area between the berth line and the yard for loading and unloading of cargo.

   Yard : A storage area where cargo are sorted and stored temporarily.

   Berth structures can be divided into:

   Quay or wharf : A berth structure which is parallel to the shore.

   Jetty or pier : A berth structure which projects into the water from the shore.

   Dolphin : A berth structure isolated on open sea for mooring and berthing the ship.

4) Outside harbour: Navigation channel, anchorage area, dolphin and shore protection.

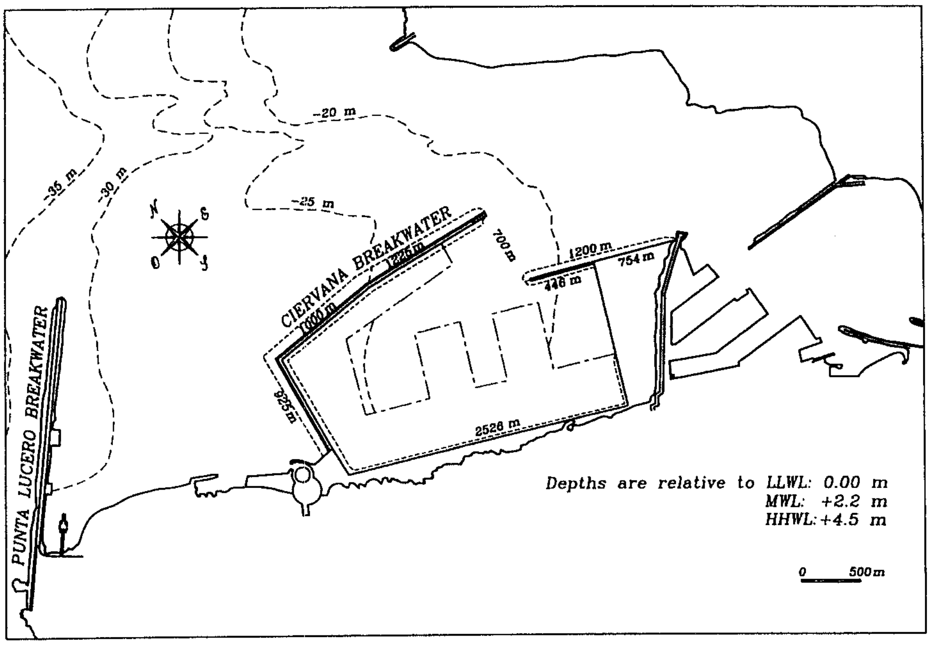

Fig.1. Layout of the Port of Bilbao, Spain.

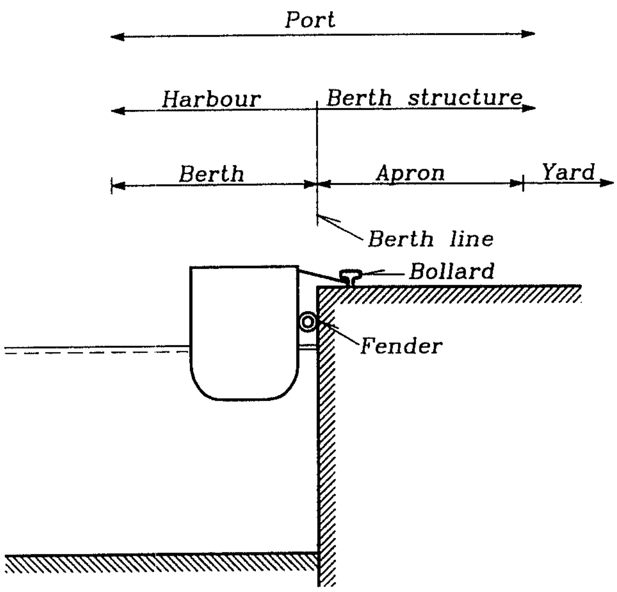

Fig.2. Definitions of port components.

1.2 Ships

Existing ships, ships being built and ships expected to be built in the future are bound to influence the plan for improvement and new construction of ports. On the other hand, the existing facilities and physical and economical constrains may influence the types and sizes of ships which will use the facilities at present and in the future.

During the last two decades, the dramatic development has taken place in regard to size of the ships, as well as the introduction of new specialized ships, the most important of which are the container ships and huge oil tank. The transport cost per tonne-nautical miles decreases with increasing carrying capacity of ships. However, general cargo ships have not changed very much in size.

1.2.1 Definition of ship dimension

The definition of the dimension of ships are shown in Fig.3.

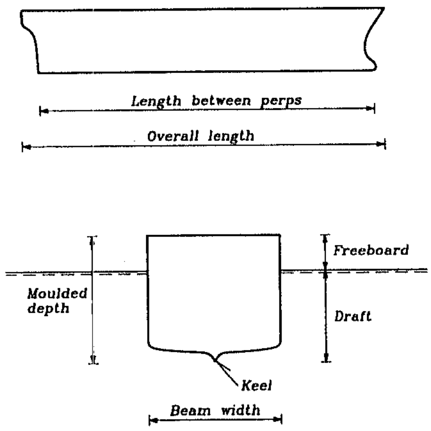

Fig.3. Definition of ship dimension.

1.2.2 Size of ships

The size of the ship is normally expressed as

- DWT Deadweight Tonnage: The carrying capacity of the ship, namely the total weight of cargo, fuel, fresh water etc.
- GRT Gross Registered Tonnage: Total volume of the ship (in m^3) divided by 2.83 m^3.
- NRT Net Registered Tonnage: available volume for cargo, i.e. GRT minus the volume of engine room, compartments for operation and ballast tanks.
- DT Displacement tonnage: The total weight of the ship, i.e. the weight of the sea water displaced by the ship.

It is normal that the dimensions of the ships are not clearly known at the design stage of the port. Table 1 lists the average dimensions of various types of ships

Table. 1 Average dimensions of various types of ships.

Type	GRT	DWT	DT	Overall length	Beam width	Moulded depth	Max. draft
	ton	ton	ton	m	m	m	m.
		400000	460000	392	66.0	29.0	24.0
		300000	356000	364	59.5	27.0	22.0
Bulk cargo		200000	240000	345	51.0	25.0	19.5
(oil, ore)		100000	125000	280	41.0	21.0	15.0
		50000	60000	225	32.0	16.5	12.0
		15000	20000	165	21.0	12.0	9.5
		50000	73500	290	32.4		13.0
		42000	61000	285	32.3		12.0
Container		30000	41500	220	31.0		11.3
		20000	27000	198	28.7		10.0
		10000	13500	159	23.5		8.0
	10000	15000	20000	165	21.5	12.0	9.5
	7000	10000	14000	145	20.0	11.5	8.5
Mixed cargo	4000	6000	8000	125	16.5	9.5	7.5
(on deck)	1000	1500	2000	70	10.0	5.1	4.3
	500	700	1000	55	8.5	4.5	3.8
	40000		35000	265	29.5	18.0	10.0
	30000		30000	230	28.0	17.0	10.0
Passenger	20000		20000	200	25.0	15.0	9.2
	10000		10000	165	20.5	12.3	8.2
	5000		5000	135	17.2	8.4	6.0
	2000		2000	90	14.0	6.2	4.5
	2500		2800	90	14.0		5.9
Fishing	1000		1750	75	11.0		5.0
	200		400	40	7.0		3.5

1.2.3 Wind area of ships

Besides the size of ships, the wind area of ships is also of importance. The Port and Harbour Research Institute of Japan proposed

$$\text{Wind area of ships } (m^2) = \alpha\,(DWT)^{\beta}, \quad \text{DWT in tonnage} \tag{1}$$

where α and β values are given in Table 2.

Table.2 Values of α and β for wind area of ships.

Type of ship			General cargo		Oil tank		Ore carrier	
Range of DWT in tonnage			500 - 140,000		500 - 320,000		500 - 200,000	
Coefficient			α	β	α	β	α	β
Laterally projected	Above sea level	Fully loaded	8.770	0.496	4.964	0.552	4.390	0.548
		Ballast loaded	9.641	0.533	5.943	0.562	5.171	0.580
	Below sea level	Fully loaded	3.495	0.608	3.198	0.611	2.723	0.625
		Ballast loaded	1.404	0.627	1.629	0.610	1.351	0.633
Front area	Above sea level	Fully loaded	2.763	0.490	2.666	0.478	1.971	0.510
		Ballast loaded	3.017	0.510	2.485	0.517	1.967	0.538

1.2.4 Types of ship movement

The six components of ship movements are shown in Fig.4.

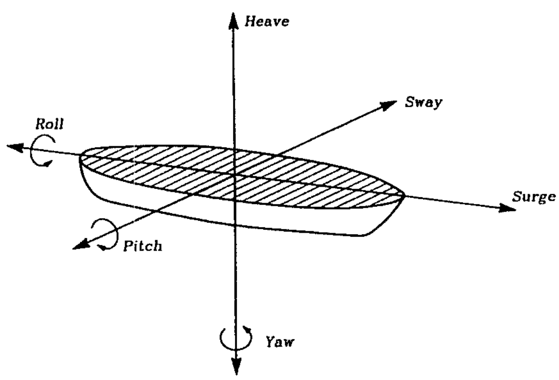

Fig.4. Types of ship movement.

1.2.5 Operation of ships inside harbour

The whole operation of a ship inside a harbour, ranging from arrival to departure, can be divided into

1) Arrival at the outer harbour basin.
2) Entering into the harbour.
3) Preparation for berthing, including possible turning of the ship.
4) Berthing, including mooring to the berth structure.
5) Loading and unloading while at berth.
6) Deberthing from the berth structure.
7) Departure from the harbour.

Fig.5 shows the approach and berthing of 80,000 DWT vessel at Hanstholm Harbour, Denmark.

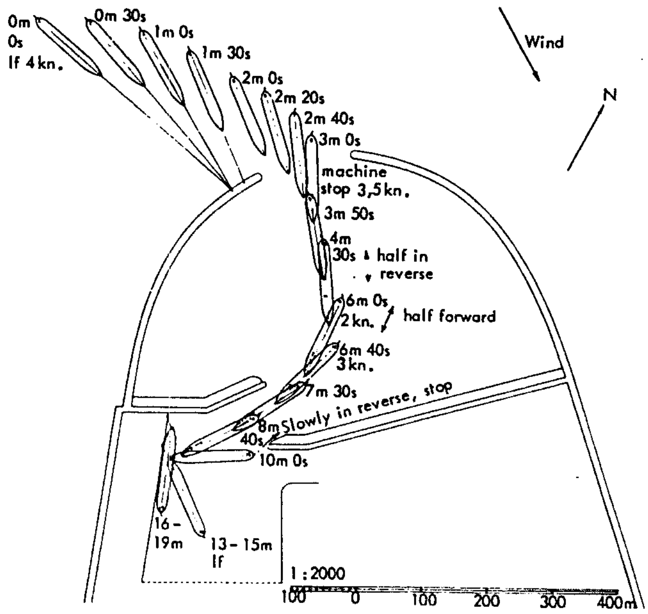

Fig.5. Approaching and berthing at Hanstholm Harbour, Denmark. (Svendsen, 1968)

1.3 Operation conditions of harbours

1.3.1 Water depth

The water depth in the navigation channel, berth basin and in front of the berth structure should be sufficient for safe manoeuvring of ships, cf. Fig.6, where the nominal water level is the level above which no obstacles to navigation exist.

The rough guide for the minimum underkeel clearance is

$$\text{Net underkeel clearance} \geq \begin{cases} 0.5 \text{ m} & \text{Soft material bottom} \\ 1.0 \text{ m} & \text{Rock bottom} \end{cases} \tag{2}$$

$$\text{Gross underkeel clearance} \geq \begin{cases} 0.30\,D & \text{Open sea area} \\ 0.25\,D & \text{Exposed channel} \\ 0.20\,D & \text{Exposed berthing area} \\ 0.15\,D & \text{Protected berthing area} \\ \multicolumn{2}{l}{D \text{ is the maximum draft of the design ship}} \end{cases} \tag{3}$$

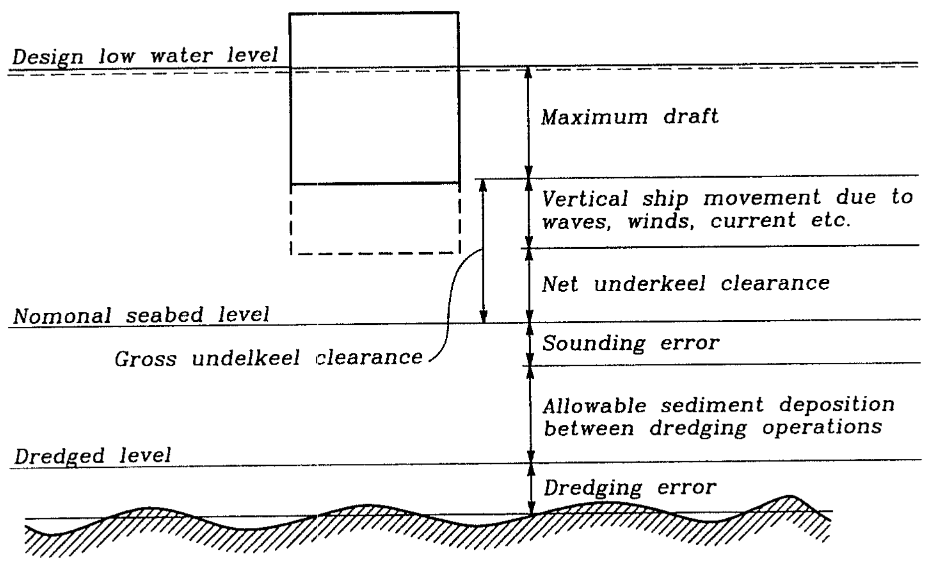

Fig.6. Components of water depth.

1.3.2 Wind

For the convenience of berthing, the berth line should be arranged as parallel as possible to the prevailing wind direction.

Wind information is often expressed into the windrose diagram showing the yearly distribution of the wind directions and speed. Wind intensity is expressed either by wind speed or by the Beaufort wind scale, cf. Fig.7, which gives also the rough guidelines of ships in the harbour based on the 10 minute mean wind speed.

The mean wind velocity and direction should be recorded 10 m above the mean water level in not less than 10 minutes. The gust ratio is the ratio of the mean wind velocity between short duration and long duration. If mean wind velocity of shorter duration is of interest, the gust ratio given in Table 3 can be applied.

Table.3. Gust ratio with respect to 1 hour mean wind velocity.

Duration	3 seconds	10 seconds	1 minute	10 minute	30 minutes	1 hour
Gust ratio	1.56	1.48	1.28	1.12	1.05	1

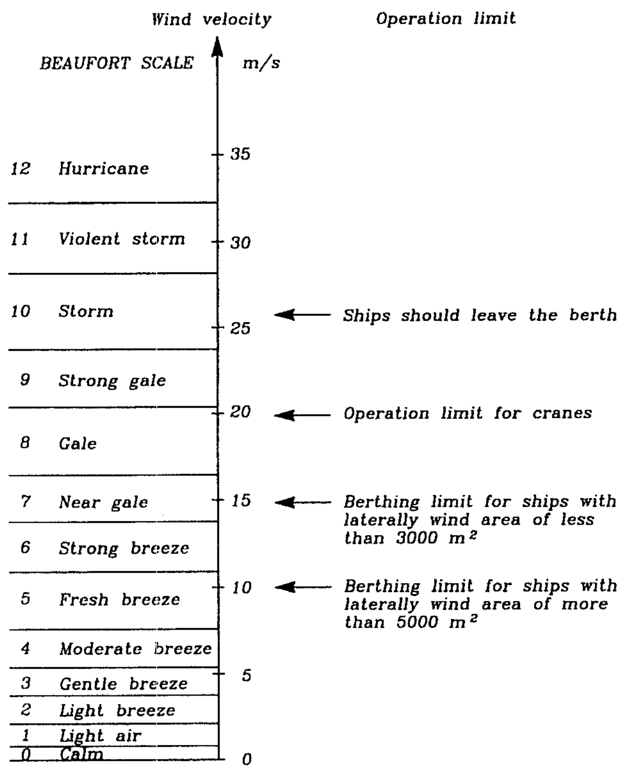

Fig.7. Rough operation guidelines for ships.

1.3.3 Waves

Waves can enter into the harbour through the entrance by diffraction, through the breakwater by penetration and overtopping. The waves are normally the main cause for the ship movement.

The generally acceptable wave height inside harbour depend on the ship size, the wave direction and the wave period. It increases with the increasing ship size.

With respect to the wave direction against the ship, the waves are classified into head-on wave, beam wave and quatering wave, cf. Fig.8. The generally acceptable wave height is the highest for the head sea and the lowest for the beam sea.

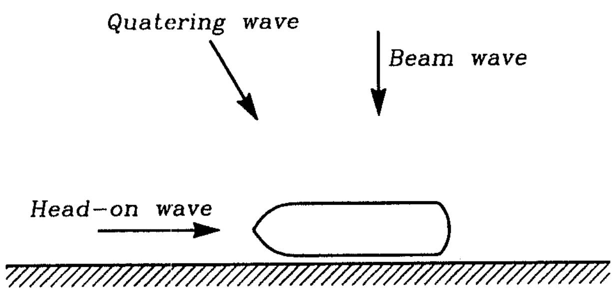

Fig.8. Wave directions.

The wave period has also influence on the generally acceptable wave heights, cf. Fig.9. For fishing boats and small ships, the short periodic waves ($\leq$ 8 seconds) is the most dangerous, and for the large ships it is the long periodic waves ($\geq$ 20 seconds).

Fig.9. Illustration of the influence of wave period on ship movement.

Table 4 is a rough guideline for the acceptable significant wave heights inside harbours with wave periods in the range of (7 $\sim$ 12) seconds.

Table.4. Guideline for acceptable significant wave height in meter ($T = 7 \sim 12$ s).

Type of ships			0^0 (head-on)	45^0 - 90^0
Fishing boat			0.15	
Passenger			0.70	
Contain			0.5	
General cargo	(DWT $\leq$ 30000)		1.0	0.8
Bulk cargo	(DWT $\leq$ 200000)	loading	1.5	1.0
		unloading	1.0	0.8
	(DWT $\leq$ 30000)		1.5	1.0
Oil tank	(DWT $\leq$ 200000)		2.5	1.2
	DWT $\geq$ 200000)		3.0	1.5

An more direct criterion would be based on the acceptable ship movement when berthing and the relation between the wave climate and ship movement.

1.3.4 Currents

Currents can arise inside a harbour due to wind transport water, tidal effect, water flow from river estuary, etc. The magnitude and direction of the current must be investigated in order to evaluate any influence on the berthing and deberthing operation of ships. The direction of current is classified in the same way as waves, cf. Fig.10.

The practical experience gives the following limit of the current velocity for the harbour operation of large ships, Table 5.

Table.5. Limit of current velocity for large ship operation inside harbour.

Current direction	0^0 (head on)	10^0	90^0
current velocity limit (m/s)	1.5	1.0	0.4

1.3.5 Visibility

The poor visibility is caused by fog, heavy rain and snow. In general the visibility of 500 to 1000 meters is required for the ship operation inside harbours.

1.3.6 Ice

Ports to be built in regions with frequent ice formation have to be designed taking into account ice problems:

- Ice inside the harbour hampers ship maneuvering.
- Drifting ice exerts impact force on port structures.
- Ice reduces the durability of port structures, especially concrete structures.

1.3.7 Availability of berth

All the items discussed in this section lead to the total availability of berth, which again can be divided into the following two cases

- Navigation availability, which describes the percentage of time the ship can enter into the harbour and berth safely.
- Operation availability, which describes the percentage of time the ship at berth can be loaded and unloaded.

Generally speaking, the yearly average availability of berth should not be less than app. 90% $\sim$ 95%. Table 6 is an example of the yearly preliminary estimate of berth availability for a 300,000 DWT oil tank.

Table.6. Example of berth availability for 300,000 DWT oil tank.

	Non-availability due to	Time frequency in percentage
Navigation	Wind above 10 m/s	4.5
	Wave above 1.5 m	0.2
	Current	0
	Visibility less than 1000 m	0.2
	Ice	0
	Tugboat non availability	0.05
Operation	Wind above 20 m/s	0.2
	wave	0
	Current	0
	Maintenance of berth structure	0.5
	$\sum$	5.55

Some of the non-availability will act together and therefore reduce the sum of the non-availability. This has not been considered in Table 6.

1.4 Design of harbour basin

The harbour basin is defined as the protected water area which should provide safe and suitable accommodations for ships. It can be divided into different areas such as berthing, turning area etc. If the harbour receives a wide range of ships, it should for economical reasons be divided into at least two zones, one for larger and the other for smaller ships. Berths for dangerous cargo like oil and gas should be located at a safe distance and clearance from other berths.

1.4.1 Entrance

The width of the entrance should be wide enough for navigation and narrow enough to protect waves from coming into harbour. It depends on the degree of wave protection required inside harbour, the navigation requirement related to not only the ship size, but also waves currents, water depth. In general,

$$\text{Width of entrance} = (0.7 \sim 1.0)\ L \tag{4}$$

L is the length of the design ship.

1.4.2 Stopping distance

The stopping distance is part of the navigation channel inside a harbour. It should be long enough for ships to stop. In general,

$$\text{Minimum stopping distance} = (7 \sim 8)\ L \tag{5}$$

1.4.3 Turning area

The turning area should be in the central area of the harbour basin. The size of the turning area will be function of the ship length and maneuverability. It will also depend on the time permitted for the execution of the turning maneuver. In general,

$$\text{Minimum diameter of turning area} = \begin{cases} 4\ L & \text{Without tug boats} \\ 2\ L & \text{With tug boats} \end{cases} \tag{6}$$

1.4.4 Anchorage area

The anchorage area is the place where ships can wait for their turn at berth or for more favorable weather condition.

The size of the anchorage area will depend on number, type and size of ships and the type of mooring systems available. A ship may be moored either with its own anchor, or to a buoy or group of buoys, or by the combination. Fig.10 shows an example of the combination mooring system and the related required anchorage area.

The water depth at an anchorage area should not exceed app. 60 meters due to the length of the anchor chain of the ships. The bottom condition must not be too hard for the anchor to stick in.

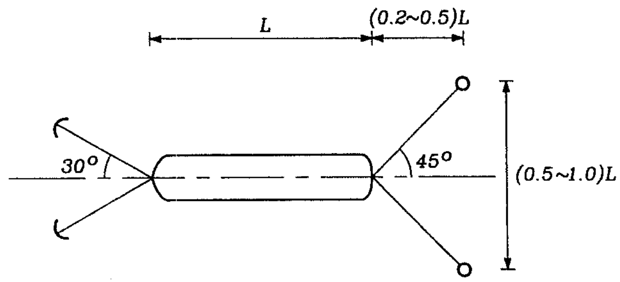

Fig.10. Combination mooring system.

1.4.5 Berthing area

Where more than one ship has to be accommodated along the berth as shown in Fig.11, a clearance length of at least 0.1 times the length of the largest ship should be provided between adjacent ships.

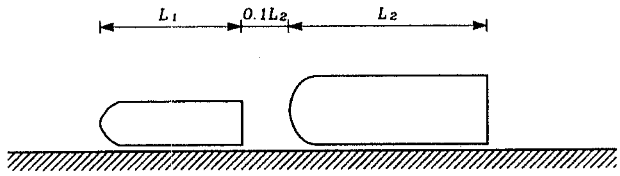

Fig.11. Clearance between ships at berth.

Pier type berth will provide the greater amount of berthing space than the quay type cf. Fig.12, where the related requirement on the berthing area is also shown.

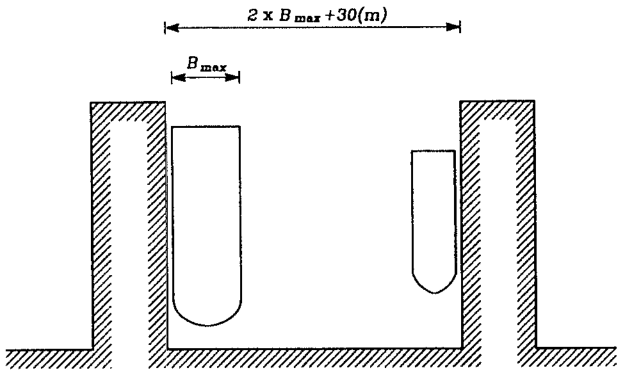

Fig.12. Required berthing area for pier type berth.

1.5 Design of navigation channel

Navigation channels or waterways can be divided into unrestricted, semi-restricted and fully restricted channels, cf. Fig.13.

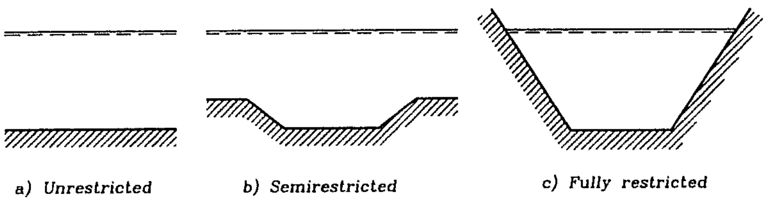

Fig.13. Types of navigation channels.

In general the layout and alignment of the channels should be such that the channels can be navigated with reasonable safety.

The required water depth in the navigation channel has been discussed in Section 1.3.1. The minimum width of the channels will primarily depend on the size of the ships, the type of the channel, the wave, the current and the wind. As a rule of thumb,

$$\text{Width of maneuvering lane} = (1.6 \sim 2.0)\ B \qquad (7)$$

$$\text{Width of clearance} = (1.0 \sim 2.0)\ B \qquad (8)$$

$$\text{With of channel} = \begin{cases} (3.6 \sim 6.0)\ B & \text{Single lane} \\ (6.2 \sim 9.0)\ B & \text{Double lanes} \end{cases} \qquad (9)$$

B is the beam width of the design ship

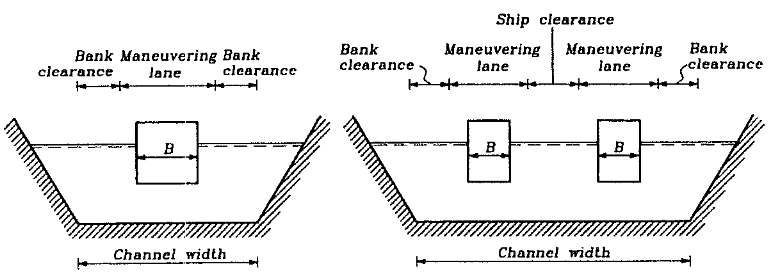

Fig.14. Channel width.

1.6 Sediment transport and dredging

Planning of a port in regions with significant sediment transport requires special care. Many ports have failed or led to unexpected high maintenance costs because of inadequate treatment of sediment transport.

There are two kinds of sediment transport caused by currents and waves, namely

Bed load	Sediment is transported in the form of rolling along sea bed.
Suspended load	Sediment is suspended by the turbulence due to wave breaking and transported.

Waves play a decisive role in coastal sediment transport process. The sediment transport capacity increases as the water gets shallow, and in the breaking zone, high concentration of suspended sediment occur. In the case where the tidal current is superimposed on the wave action, the sediment transport capacity is much higher than the current along, because the orbital wave motion at the bed generates a high concentration of sediment near the bed, which in turn is transported by the current. This mechanism is important in connection with dredged channels.

Sediment accumulation in the harbour basin can be a serious problem, because the still water in the basin provides an ideal condition for the suspended sediment passing through the entrance to settle down.

Dredging is often necessary in order to maintain the water depth in navigation channels and harbour basins. The method of dredging can be divided into

Mechanical	Sediment is picked up on board by a bucket moved by a very strong arm and boom. The sediment is then transported and dumped in another place.
Hydraulic	It is the most popular and economical method. Sediment is sucked from the sea bed and then discharged through pipes to a spoil disposal area (land or sea).

With respect to dredging economics, the variable costs, such as labor, fuel are minor compared with the fixed costs arising from new equipments, which are often manufactured specifically for the project. Moreover, the dredging efficiency is greatly influenced by the weather.

1.7 Breakwaters

The main purpose of a breakwater is to protect harbours against wave action in order to obtain acceptable mooring and maneuvering conditions for ships inside the harbour, but breakwaters are also used for protection of navigation channels and beaches against wave action and sediment transport. The breakwaters have great influence on the site selection and the layout of a port because of the relatively high cost of constructing breakwaters.

1.7.1 Types and principles of breakwaters

There are two main types of breakwaters, characterized by their seaward face, namely sloping breakwater (rubble mound breakwater) and vertical breakwater.

A sloping breakwater will force most incident waves to break on the slope due to the decreasing water depth. The energy of the incident waves are mainly dissipated by wave breaking, partly reflected back to the sea and partly transmitted into the harbour area due to penetration and overtopping, cf. Fig.15.

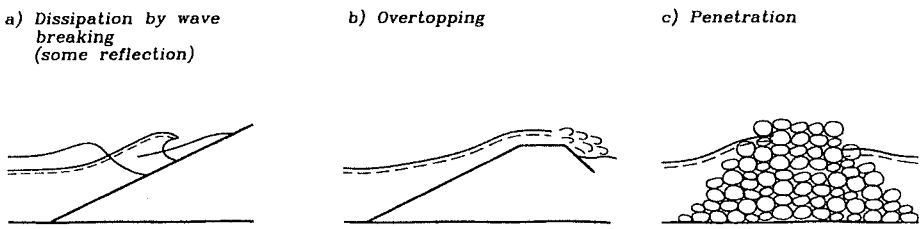

Fig.15. Illustration of incident wave energy transformation in front of a rubble mound breakwater.

In front of a vertical breakwater, the most energy of the incident waves are reflected back to the sea. Wave energy will also be dissipated due to wave breaking and transmitted into the harbour area due to overtopping, cf. Fig.16.

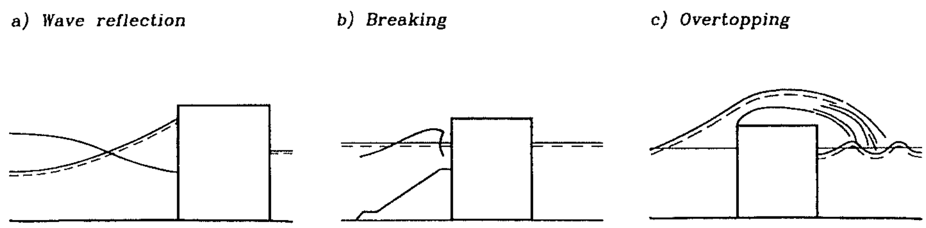

Fig.16. Illustration of incident wave energy transformation in front of a vertical breakwater.

1.7.2 Layout of breakwaters

The various functions and typical layout of breakwaters are illustrated in Fig.17.

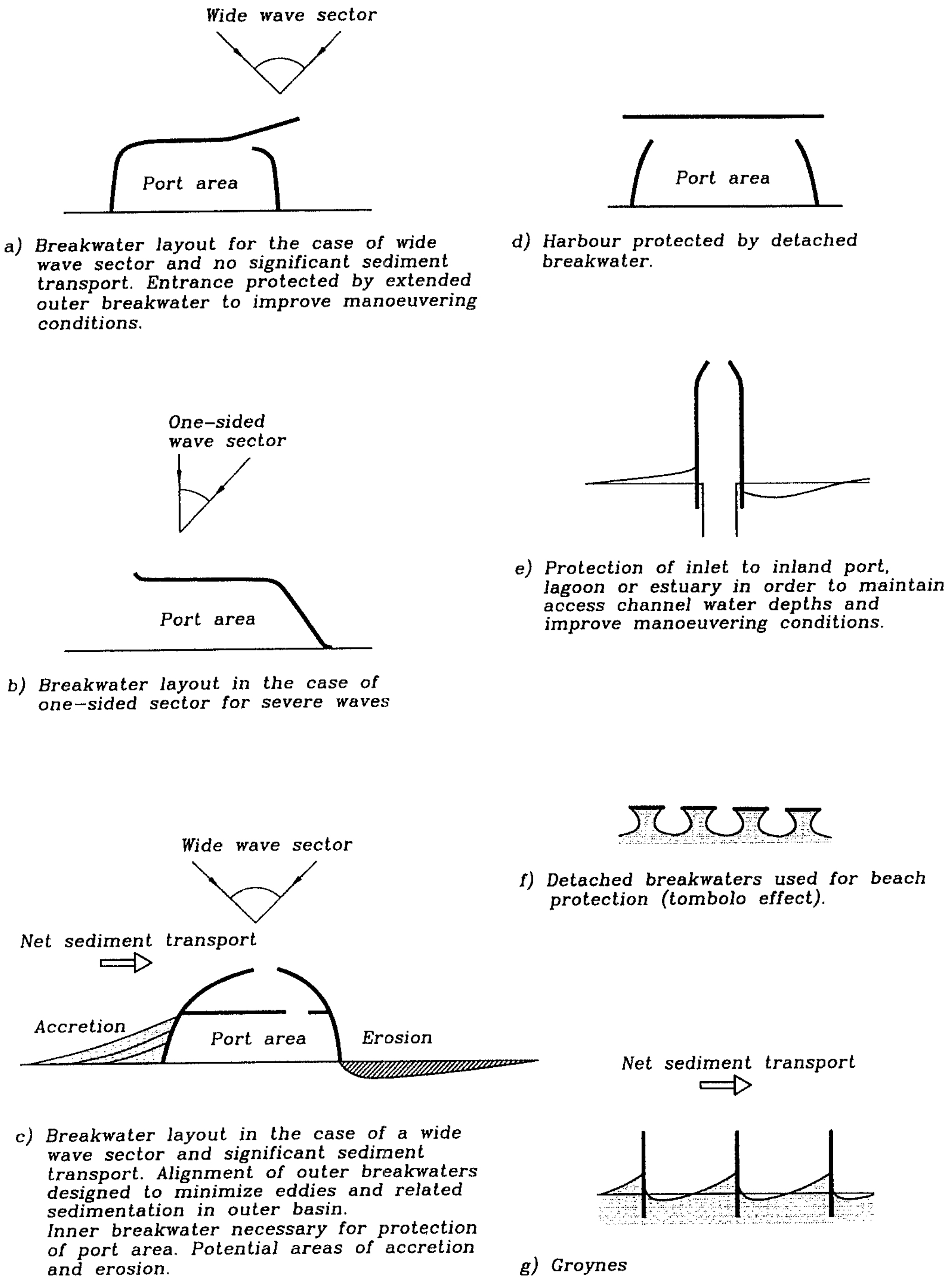

Fig.17. Illustration of typical functions and layout of breakwaters. (Burcharth, 1993)

2 EXTREME WAVE HEIGHT ANALYSIS

The determination of the design wave height, often represented by significant wave height, is usually based on the statistical analysis of a long-term wave height measurements/hindcast. The target of the extreme wave height analysis is the wave height corresponding to a certain return period.

2.1 Design level: Return period and encounter probability

Return period T

To define return period the following notations are used

X	Significant wave height, which is a random variable due to the statistical vagrancy of nature.
x	Realization of X.
$F(x)$	Cumulative distribution function of X, $F(x) = \text{Prob}(X \leq x)$.
t	Number of years of observation of X.
n	Number of observations in a period of t.
λ	Sample intensity, $\lambda = n/t$.

Fig.1 illustrates the cumulative distribution function of X. The non-exceedence probability of x is $F(x)$, or the exceedence probability of x is $(1 - F(x))$. In other words with $(1 - F(x))$ probability an observed significant wave height will be larger than x.

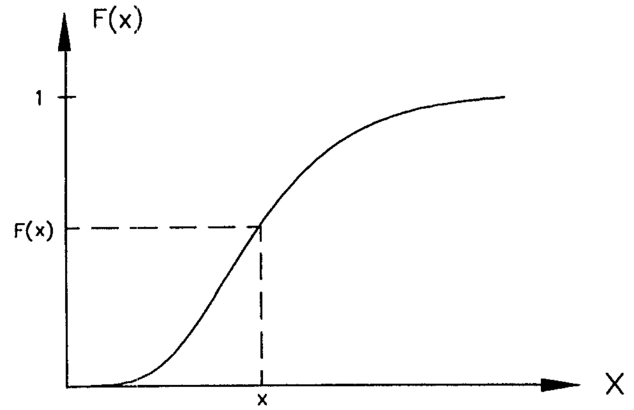

Fig.1. Cumulative distribution function of X.

If the total number of observations is n, The number of observations where $(X > x)$ is

$$k = n(1 - F(x)) = t\lambda(1 - F(x)) \tag{1}$$

The return period T of x is defined as

$$T \; = \; t\Big|_{k=1} \; = \; \frac{1}{\lambda\;(\;1\;-\;F(x)\;)} \tag{2}$$

i.e. on average x will be exceeded once in every T years. x is also called T-year event.

<u>Encounter probability p</u>

Based on the fact that on average x will be exceeded once in every T years, the exceedence probability of x in 1 year is $1/T$. Therefore

non-exceedence probability of x in 1 year	$\text{Prob}(X \le x) \; = \; 1 \; - \; \frac{1}{T}$
non-exceedence probability of x in 2 years	$\text{Prob}(X \le x) \; = \; \left(1 \; - \; \frac{1}{T}\right)^2$
non-exceedence probability of x in L years	$\text{Prob}(X \le x) \; = \; \left(1 \; - \; \frac{1}{T}\right)^L$

and the encounter probability, i.e. the exceedence probability of x within a structure lifetime of L years is

$$p \; = \; 1 \; - \; \left(1 \; - \; \frac{1}{T}\right)^L \tag{3}$$

which in the case of larger T can be approximated

$$p \; = \; 1 \; - \; exp\left(-\frac{L}{T}\right) \tag{4}$$

<u>Design level</u>

Traditionally the design level for design wave height was the wave height corresponding to a certain return period T. For example, if the design wave height corresponding to a return period of 100 years is 10 m, the physical meaning is that on average this 10 m design wave height will be exceeded once in every 100 years.

In the reliability based design of coastal structures it is better to use encounter probability, i.e. the exceedence probability of the design wave height within the structure lifetime. For example If the structure lifetime L is 25 years, the encounter probability of the design wave height (10 meter) is

$$p \; = \; 1 \; - \; \left(1 \; - \; \frac{1}{T}\right)^L \; = \; 22\%$$

This means that this 10 m design wave height will be exceeded with 22% probability within a structure lifetime of 25 years.

2.2 General procedure

In practice engineers are often given a long-term significant wave height measurement/hindcast and required to determine the design wave height corresponding to a certain return wave period. The general procedure to perform the task is:

1) Choice of the extreme data set based on a long-term wave height measurement/hindcast
2) Choice of several theoretical distributions as the candidates for the extreme wave height distribution
3) Fitting of the extreme wave heights to the candidates by a fitting method. If the least square fitting method is employed, a plotting position formula must be used
4) Choice of the distribution based on the comparison of the fitting goodness among the candidates
5) Calculation of the design wave height corresponding to a certain return period
6) Determination of the confidence interval of the design wave height in order to account for sample variability, measurement/hindcast error and other uncertainties

If structure lifetime and encounter probability are given in stead of return period, we can calculate the return period by eq (3) and proceed as above.

2.3 Data sets

The original wave data are typically obtained either from direct measurements or from the hindcasts based on the meteorological information. Most of the measurements/hindcasts cover a rather short span of time, say less than 10 years in the case of direct measurements and less than 40 years in the case of hindcasts.

In practice three kinds of extreme data sets have been used.

Complete data set	containing all the direct measurements of wave height usually equally spaced in time.
Annual series data set	consisting of the largest wave height in each year of measurements/hindcasts, cf. Fig.2.
Partial series data sets	composed of the largest wave height in each individual storm exceeding a certain level (threshold). The threshold is determined based on the structure location and engineering experience, cf. Fig.2. It is also called POT data set (Peak Over Threshold).

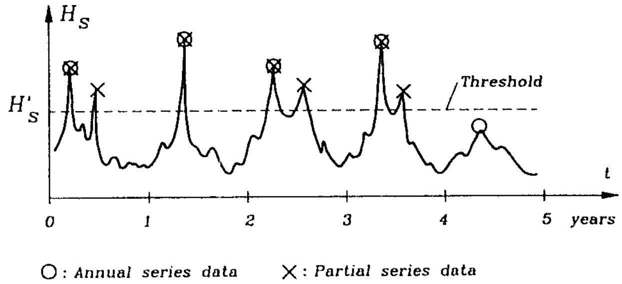

Fig.2. Illustration of the establishment of annual series data set and partial series data set.

The extreme data sets, established based on the original wave data, should fulfill the following 3 conditions:

Independence There must be no correlation between extreme data. The annual series data set and the partial series data set meet the independence requirement because the extreme data are from different storms.

Homogeneity The extreme data must belong to the same statistical population, e.g. all extreme data are from wind-generated waves.

Stationary There must be stationary long-term climatology. Studies of wave data for the North Sea from the last 20 years give evidence of non-stationarity as they indicate a trend in the means. Average variations exist from decades to decades or even longer period of time. However, until more progress is available in investigating long-term climatological variations, the assumption of stationary statistics might be considered realistic for engineering purpose, because the long-term climatological variation is generally very weak.

The complete data set cannot fulfill the required independence between data. Goda (1979) found correlation coefficients of $0.3 - 0.5$ for significant wave heights (measurement duration is 20 minutes and time interval between two succeeding measurements is 24 hours). Moreover, what is interesting in the case of design waves is the wave height corresponding to a very high non-exceedence probability, i.e. the very upper tail of the distribution. If the chosen distribution is not the true one, the very upper tail value will be distorted severely because in the fitting process the chosen distribution will be adjusted to the vast population of the data. For these reasons the complete data set is seldom used.

Most engineers prefer the partial series data set over the annual series data set simply because the former usually gives larger design wave height and hence, more conservatively designed structures.

2.4 Candidate distributions

Generally the exponential distribution, the Weibull distribution, the Gumbel (FT-I) distribution, the Frechet distribution and the Log-normal distribution are the theoretical distributions which fit the extreme wave data well.

$$\text{Exponential} \quad F = F_X(x) = P(X < x) = 1 - e^{-\left(\frac{x-B}{A}\right)} \tag{5}$$

$$\text{Weibull} \quad F = F_X(x) = P(X < x) = 1 - e^{-\left(\frac{x-B}{A}\right)^k} \tag{6}$$

$$\text{Gumbel} \quad F = F_X(x) = P(X < x) = e^{-e^{-\left(\frac{x-B}{A}\right)}} \tag{7}$$

$$\text{Frechet} \quad F = F_X(x) = P(X < x) = e^{-\left(\frac{x}{A}\right)^k} \tag{8}$$

$$\text{Log-normal} \quad F = F_X(x) = P(X < x) = \Phi\left(\frac{\ln(x) - B}{A}\right) \tag{9}$$

where X — A characteristic wave height, which could be the significant wave height H_s or the one-tenth wave height $H_{\frac{1}{10}}$ or the maximum wave height H_{max}, depending on the extreme data set.

x — Realization of X.

F — Non-exceedence probability of x (cumulative frequency).

A, B, k — Distribution parameters to9 be fitted. In the log-normal distribution A and B are the standard deviation and the mean of X respectively.

Φ — Standard normal distribution function.

No theoretical justification is available as to which distribution is to be used. The author have tried to fit 7 sets of partial series data to all these distributions. These data sets are real data representing deep and shallow water sea states from Bilbao in Spain, Sines in Portugal, the North Sea, Tripoli in Libya, Pozzallo and Follonica in Italy and Western Harbour in Hong Kong. The results show that the Weibull and the Gumbel distributions provide the closest fits. Therefore the following discussion is exemplified with these two distributions.

2.5 Fitting methods and procedure

Four generally applied methods of fitting the extreme data set to the chosen distributions are the maximum likelihood method, the method of moment, the least square method and the visual graphical method. The most commonly used methods are the maximum likelihood method and the least square method.

Least square method

Eqs (6) and (7) can be rewritten as

$$X = A\,Y + B \tag{10}$$

where Y is the reduced variate defined according to the distribution function

$$Y = (-ln(1-F))^{\frac{1}{k}} \quad \text{Weibull distribution} \tag{11}$$

$$Y = -ln(-lnF) \quad \text{Gumbel distribution} \tag{12}$$

The fitting procedure is summarized as the follows:

1) Rearrange the measured/hindcast extreme data (total number n) in the descending order, (x_i), $i = 1, 2, \cdots, n$ (X_1=max).

2) Assign a non-exceedence probability F_i to each x_i by an appropriate plotting position formula (cf. next section), thus obtaining a set of data pairs, $(F_i,\ x_i)$, $i = 1, 2, \cdots, n$.

3) Calculate the corresponding y value by eq (11) or eq (12), thus obtaining a new set of data pairs, $(y_i,\ x_i)$, $i = 1, 2, \cdots, n$.

4) Determine the regression coefficients of eq (10) by

$$A = \frac{Cov(Y,X)}{Var(Y)} \qquad B = \overline{X} - A\overline{Y}$$

$$Var(Y) = \frac{1}{n}\sum_{i=1}^{n}\left(y_i - \overline{Y}\right)^2$$

$$Cov(Y,X) = \frac{1}{n}\sum_{i=1}^{n}(y_i - \overline{Y})(x_i - \overline{X})$$

$$\overline{Y} = \frac{1}{n}\sum_{i=1}^{n} y_i \qquad \overline{X} = \frac{1}{n}\sum_{i=1}^{n} x_i$$

In the case of the Weibull distribution various k values are predefined and A and B are fitted accordingly. The final values of the three parameters are chosen based on the fitting goodness.

Maximum likelihood method

The 2-parameter Weibull distribution is

$$\text{Weibull} \quad F(x) = 1 - e^{-\left(\frac{x-x'}{A}\right)^k} \tag{13}$$

where x' is the threshold wave height, which should be smaller than the minimum wave height in the extreme data set. For unexperienced engineers several threshold values can be tried, and the one which produces best fit is finally chosen.

the maximum likelihood estimate k is obtained by solving the following equation by an iterative procedure:

$$N + k \sum_{i=1}^{N} \ln(x_i - x') = N k \sum_{i=1}^{N} \left((x_i - x')^k \ln(x_i - x')\right) \left(\sum_{i=1}^{N}(x_i - x')^k\right)^{-1} \tag{14}$$

The maximum likelihood estimate of A is

$$A = \left[\frac{1}{N} \sum_{i=1}^{N} (x_i - x')^k\right]^{1/k} \tag{15}$$

For the Gumbel distribution, the maximum likelihood estimate of A is obtained by solving the following equation by an iterative procedure:

$$\sum_{i=1}^{N} x_i \exp\left(-\frac{x_i}{A}\right) = \left[\frac{1}{N} \sum_{i=1}^{N} x_i - A\right] \sum_{i=1}^{N} \exp\left(-\frac{x_i}{A}\right) \tag{16}$$

The maximum likelihood estimate of B is

$$B = A \ln\left[N \left(\sum_{i=1}^{N} \exp\left(-\frac{x_i}{A}\right)\right)^{-1}\right] \tag{17}$$

2.6 Plotting position formulae

When the least square method is applied a plotting position formula must be chosen. The plotting position formula is used to assign a non-exceedence probability to each extreme wave height. The plotting position is of special importance when dealing with very small samples.

The non-exceedence probability (F_i) to be assigned to (x_i), can be determined based on three different statistical principles, namely sample frequency, distribution of frequency and order statistics, cf Burcharth et al (1994).

Mean, median and mode

The definition of mean, median and mode of a random variable X is given in the following because they are involved in some of the plotting position formulae.

Take the Gumbel distribution as an example. The distribution function $F_X(x)$ and density function $f_X(x)$ of a Gumbel random variable X reads

$$F_X(x) = P(X < x) = e^{-e^{-\left(\frac{x-B}{A}\right)}} \qquad f_X(x) = \frac{dF_X(x)}{dx} \tag{18}$$

The definition and value of the mean, the median and the mode are

$$\text{Mean} \quad \bar{X} = E[X] = \int_{-\infty}^{+\infty} x f_X(x)dx \approx B + 0.577A \tag{19}$$

$$\text{Median} \quad \hat{X} = x\Big|_{F_X(x)=0.5} = B + 0.367A \tag{20}$$

$$\text{Mode} \quad \tilde{X} = x\Big|_{f_X(x)=max} = B \tag{21}$$

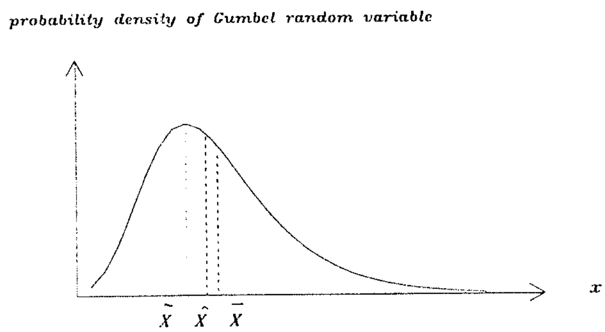

Fig. 3. Mean, median and mode of the Gumbel random variable.

Order statistics

Assume that a random variable X has a cumulative distribution function F_X, and probability density function f_X, i.e.

$$F_X(x) = P(X < x) \tag{22}$$

Furthermore, assume n data sampled from X and arranged in the descending order, x_1 being the largest value in n data.

Here x_1 is one realization of the ordered random variable X_1, defined as the largest value in each sample. The distribution function of X_1 is

$$F_{X_1}(x) = P(X_1 < x) = (F_X(x))^n = (P(X < x))^n \tag{23}$$

$F_{X_1}(x)$ may also be interpreted as the probability of the non-occurrence of the event ($X > x$) in any of n independent trials.

The density function of X, f_X, and the density function of X_1, f_{X_1}, are sketched in Fig.4.

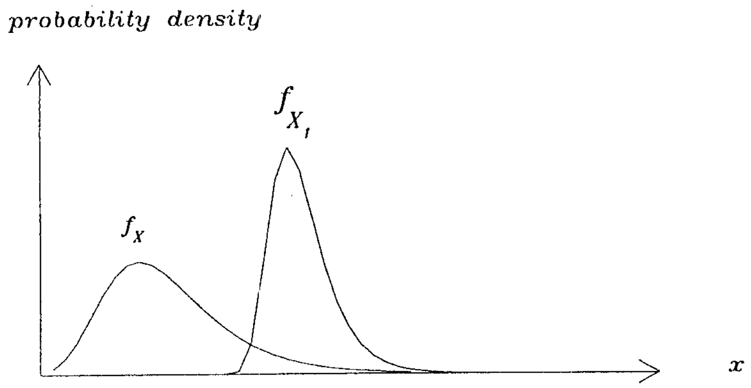

Fig. 4. f_X : Density function of X. f_{X_1} : density function of X_1.

For other ordered random variables X_i, $i = 2, 3, \cdots, n$, The distribution functions $F_{X_i}(x)$ can also be expressed as the function of $F_X(x)$, cf. Thoft-Christensen et al.(1982).

2.6.1 Plotting position based on sample frequency

This method is based solely on the cumulative frequency of the samples. The widely used formula is the so-called California plotting position formula

$$F_i = 1 - \frac{i}{n} \qquad i = 1,\ 2,\ \cdots,\ n \tag{24}$$

where	x_i	Extreme data in the descending order (x_1=max)
	F_i	Non-exceedence probability of x_i.
	n	Sample size, i.e. total data number.

The disadvantage of this plotting position formula is that the smallest extreme data x_n cannot be used because $F_n = 0$.

2.6.2 Plotting position based on distribution of frequencies

Assume that the random variable X has a cumulative distribution function F_X. The i'*th* highest value in n samples, X_i, is a random variable, too. Consequently, $F_{X_i}(x_i)$, the cumulative frequency of x_i, is a random variable, too. The philosophy of this method is to determine the plotting position of x_i via either the mean, the median or the mode of the random variable $F_{X_i}(x_i)$. The plotting position formula by this method is independent of the parent distribution (distribution-free).

Weibull (1939) used the mean of $F_{X_i}(x_i)$ to determine the cumulative frequency F_i to be assigned to x_i

$$\text{Weibull} \quad F_i == 1 - \frac{i}{n+1} \tag{25}$$

There is no explicit formula for the median of $F_{X_i}(x_i)$. However, Benard (1943) developed a good approximation

$$\text{Benard} \quad F_i \approx 1 - \frac{i - 0.3}{n + 0.4} \tag{26}$$

The plotting position formula based on the mode of $F_{X_i}(x_i)$ has not drawn much attention, because the chance of the occurrence of mode is still infinitesimal even though mode is more likely to occur than the mean and median,

2.6.3 Plotting position based on order statistics

The philosophy of this method is to determine the plotting position of x_i via the mean, the median and the mode of the ordered random variable X_i.

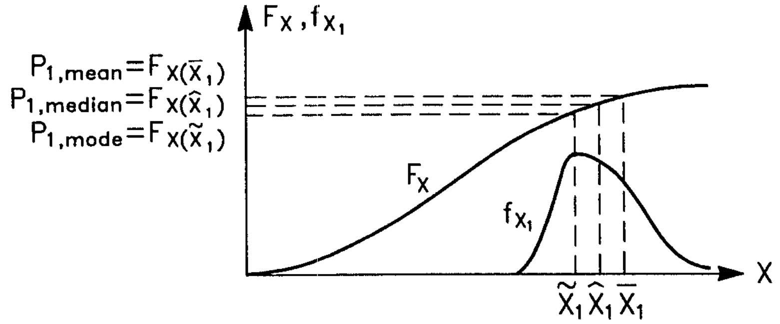

Fig. 5. Illustration of the determination of F_1 based on the mean, the median and the mode of X_1.

Plotting positions based on the mean value are distribution-dependent and not explicitly available. The best known approximations are

Blom	$F_i = 1 - \frac{i-3/8}{n+1/4}$	Normal distribution	(27)
Gringorten	$F_i = 1 - \frac{i-0.44}{n+0.12}$	Gumbel distribution	(28)
Petrauskas	$F_i = 1 - \frac{i-0.3-0.18/k}{n+0.21+0.32/k}$	Weibull distribution	(29)
Goda	$F_i = 1 - \frac{i-0.2-0.27/\sqrt{k}}{n+0.20+0.23/\{sqrtk}$	Weibull distribution	(30)

The plotting position based on the median value of the ordered random variable is the same as that based on the median value of distribution of frequency.

<u>Summary on plotting position formulae</u>

The choice of the plotting position formula depends on engineer's personnel taste.

From the statistical point of view the plotting position formula based on the mean (unbiased) is preferred because the expected squared error is minimized. Rosbjerg (1988) advocates the choice of the median plotting position formula (Benard formula) because it is distribution-free and is based both on the distribution of frequency and the order statistics. In practice the Weibull plotting position formula is most widely used.

2.7 Design wave height: x^T

The design wave height x^T is the wave height corresponding to the return period T. The Weibull and Gumbel distributions, eqs (6) and (7), are rewritten as

$$x = A(-ln(1 - F))^{\frac{1}{k}} + B \quad \text{Weibull distribution} \tag{31}$$

$$x = A(-ln(-ln(F))) + B \quad \text{Gumbel distribution} \tag{32}$$

Define the sample intensity λ as

$$\lambda = \frac{\text{number of extreme data}}{\text{number of years of observation}} \tag{33}$$

and employ the definition of return period T

$$T = \frac{1}{\lambda(1 - F)} \quad \text{or} \quad F = 1 - \frac{1}{\lambda T} \tag{34}$$

Inserting eq (34) into eqs (31) and (32), we get (now x means the wave height corresponding to return period T, and therefore is replaced by x^T)

$$x^T = A\left(-ln(\tfrac{1}{\lambda T})\right)^{\frac{1}{k}} + B \quad \text{Weibull distribution} \tag{35}$$

$$x^T = A\left(-ln(-ln(1 - \tfrac{1}{\lambda T}))\right) + B \quad \text{Gumbel distribution} \tag{36}$$

where A, B and k are the fitted distribution parameters.

2.8 Fitting goodness

Normally several candidate distributions will be fitted and the *best* one is chosen. The linear correlation coefficient, defined as

$$\rho = \frac{Cov(X,Y)}{\sqrt{Var(X)\ Var(Y)}} \tag{37}$$

is widely used as the criterion for the comparison of the fitting goodness. However, ρ is defined in the linear plotting domain (y, x), where the reduced variate y is dependent on the distribution function. Therefore, the interpretation of this criterion is less clear.

With the fitted distribution functions, the wave heights corresponding to the non-exceedence probability of the observed wave heights can be calculated, cf. eqs (31) and (32). The *average relative error* E, defined as

$$E = \frac{1}{n}\sum_{i=1}^{n}\frac{|\ x_{i,estimated} - x_{i,observed}\ |}{x_{i,observed}} \tag{38}$$

is a good simple criterion with a clear interpretation. $E = 5$ % means that on the average, the central estimation of wave height deviates from the observed wave height by 5 %. Obviously a smaller E-value indicates a better fitted distribution.

The statistical hypothesis test can also be used in the comparison of the fitting goodness (Goda et al. 1990)

2.9 Example

Delft Hydraulics Laboratory performed a hindcast study for the Tripoli deep water wave climate and identified the 17 most severe storms in a period of 20 years. The ranked significant wave heights are listed in Table 2.

Table 2. Tripoli storm analysis

rank i	Significant wave height x_i (m)	non-exceedence probability F_i	Reduced variate y_i Gumbel	Reduced variate y_i Weibull
1	9.32	0.944	2.86	1.57
2	8.11	0.889	2.14	1.40
3	7.19	0.833	1.70	1.28
4	7.06	0.778	1.38	1.18
5	6.37	0.722	1.12	1.11
6	6.15	0.667	0.90	1.04
7	6.03	0.611	0.71	0.98
8	5.72	0.556	0.53	0.92
9	4.92	0.500	0.37	0.86
10	4.90	0.444	0.21	0.80
11	4.78	0.389	0.06	0.74
12	4.67	0.333	-0.09	0.68
13	4.64	0.278	-0.25	0.62
14	4.19	0.222	-0.41	0.55
15	3.06	0.167	-0.58	0.49
16	2.73	0.111	-0.79	0.40
17	2.33	0.056	-1.06	0.30

You are required to find the design wave height which has 22% exceedence probability within a structure lifetime of 25 years.

The steps in the analysis are as follows:

1) Calculate the sample intensity by eq (33) $\lambda = \frac{17}{20}$
2) Calculate the return period by eq (3) $T = 100$ years
3) Assign a non-exceedence probability F_i to each observed wave height x_i according to the Weibull plotting position formula. Results are shown in Table 2.

4) Choose the Weibull and the Gumbel distributions as the candidate distributions. Calculate the values of the reduced variate $\{y_i\}$ according to eqs (11) and (12) respectively. For the Weibull distribution $\{y_i\}$ involves the iterative calculation. $\{y_i\}$ of the two distributions are also shown in Table 2.

5) Fit data (y_i, x_i) to eq (10) by the least square method and obtain the distribution parameters:
Weibull, k = 2.35, A = 5.17, B = 0.89
Gumbel, A = 1.73, B = 4.53
The fitting of the data to the Gumbel and the Weibull distributions is shown in Fig. 6.

6) Compare the goodness of fitting according to the value of the average relative error E, eq (38)
E = 4.72 % for the Weibull distribution fitting
E = 6.06 % for the Gumbel distribution fitting
Because of a clearly smaller E-value the Weibull distribution is taken as the representative of the extreme wave height distribution

7) Calculate the wave height corresponding to a return period of 100 years X^{100} by eq (35) x^{100} = 10.64 m

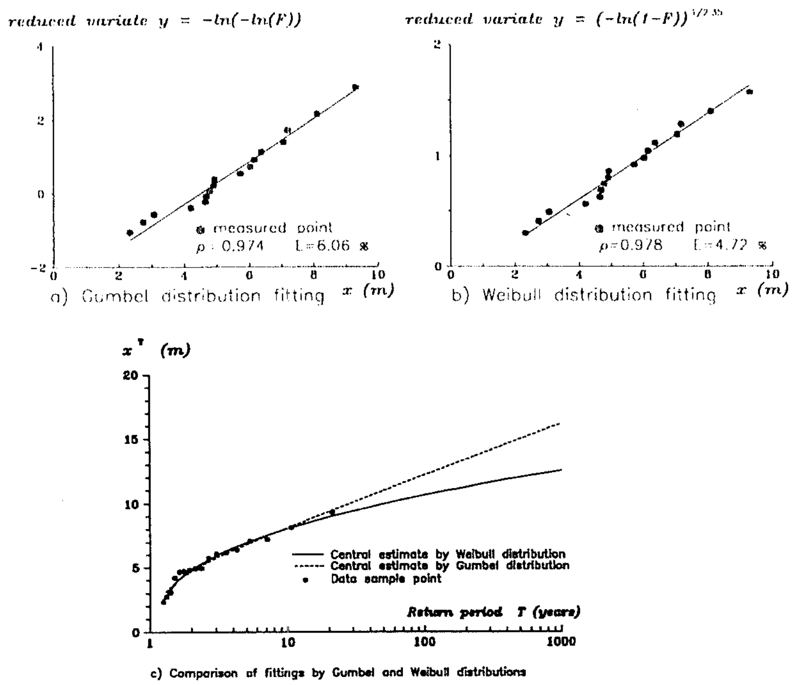

Fig. 6. Fitting to the Gumbel and the Weibull distributions and comparison.

2.10 Sources of uncertainties and confidence interval

Sources of uncertainties

The sources of uncertainty contributing to the uncertainty of the design wave height are:

1) Sample variability due to limited sample size.
2) Error related to measurement, visual observation or hindcast.
3) Choice of distribution as a representative of the unknown true long-term distribution
4) Variability of algorithms (choice of threshold, fitting method etc.
5) Climatological changes

The uncertainty sources 1) and 2) can be considered by numerical simulation in the determination of the design wave height.

Wave data set contains measurement/hindcast error. Measurement error is from malfunction and non-linearity of instruments, such as accelerometer and pressure cell, while hindcast error occurs when the sea-level atmospheric pressure fields are converted to wind data and further to wave data. The accuracy of such conversion depends on the quality of the pressure data and on the technique which is used to synthesize the data into the continues wave field. Burcharth (1986) gives an overview on the variational coefficient C (standard deviation over mean value) of measurement/hindcast error.

Visual observation data should not be used for determination of design wave height because ships avoid poor weather on purpose. With the advance of measuring equipment and numerical model, generally C value has been reduced to below 0.1.

Table 1. variational coefficient of extreme data C

Methods of determination	Accelerometer Pressure cell Vertical radar	Horizontal radar	Hindcast by SPM	Hindcast other	Visual
Variational Coe. C	0.05-0.1	0.15	0.12-0.2	0.1-0.2	0.2

Confidence interval of design wave height x^T

We use an example to demonstrate how the confidence interval of the design wave height is determined. The gumbel distribution curve in Fig.7 is obtained by fitting Tripoli significant wave height to Gumbel distribution by the least square fitting method and the Weibull plotting position formula.

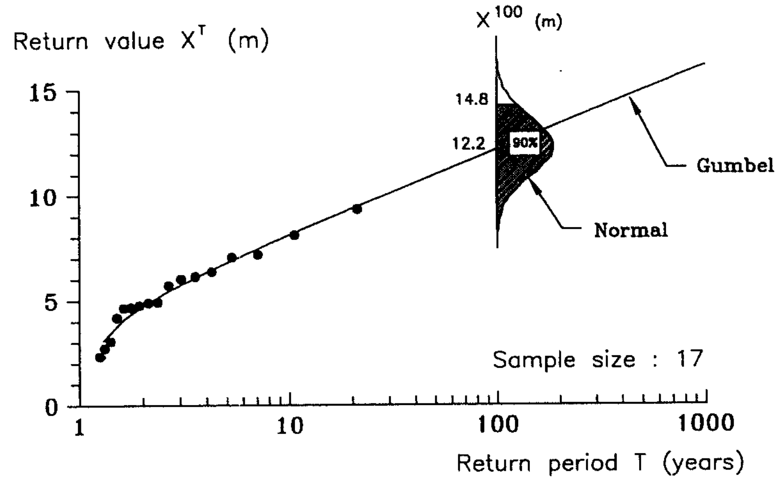

Fig.7. Design wave height.

If the design level for design wave height is a return period of 100 years, i.e. $T = 100$, the design wave height is $x^{100} = 12.2\ m$.

If other uncertainties, e.g. sample variability, is included, the design wave height x^{100} becomes a random variable. The distribution of the design wave height x^{100}, which is usually assumed to follow the normal distribution, can be obtained by numerical simulation to be described in the next section, cf. Fig.7. In order to account sample variability, a confidence band is often applied. For example, the design wave height is 14.8 m which corresponds to the 90% one-sided confidence interval, cf. Fig.7.

<u>Numerical simulation</u>

To exemplify the discussion, it is assumed that the extreme wave height follows the Gumbel distribution

$$F = F_X(x) = P(X < x) = exp\left(-exp\left(-(\frac{x-B}{A})\right)\right) \tag{39}$$

where X is the extreme wave height which is a random variable, x a realization of X, A and B the distribution parameters.

Due to the sample variability and measurement/hindcast error, the distribution parameter A and B become random variables,

In order to account the sample variability and measurement/hindcast error, a numerical simulation is performed as explained in the followings.

A sample with size N is fitted to the Gumbel distribution. The obtained distribution parameters A_{true} and B_{true} are assumed to be the true values.

1) Generate randomly a data between 0 and 1. Let the non-exceedence probability F_1 equal to that data. the single extreme data x is obtained by (cf. Fig.8)

$$x = F_X^{-1}(F_1) = A_{\text{true}}[-\ln(-\ln F_1)] + B_{\text{true}} \tag{40}$$

2) Repeat step 1) N times. Thus we obtain a sample belonging to the distribution of eq (39) and the sample size is N.

3) Fit the sample to the Gumbel distribution and get the new estimated distribution parameters A and B.

4) Calculate the wave height x^T corresponding to the return period T by eq (36)

5) Repeat steps 2) to 4), say, 10,000 times. Thus we get 10,000 values of x^T.

6) Choose the wave height corresponding to the specified confidence band.

In order to include the measurement/hindcast error the following step can be added after step 1). This step is to modify each extreme data x generated by step 1), based on the assumption that the hindcast error follows the normal distribution, cf. Fig.8

1*) Generate randomly a data between 0 and 1. Let the non-exceedence probability F_2 equal to that data. the modified extreme data x_{modified} is obtained by

$$x_{\text{modified}} = x + C\ x\ \Phi^{-1}(F_2) \tag{41}$$

where Φ is the standard normal distribution and C is the coefficient of variation of the measurement/hindcast error. C ranges usually from 0.05 to 0.1.

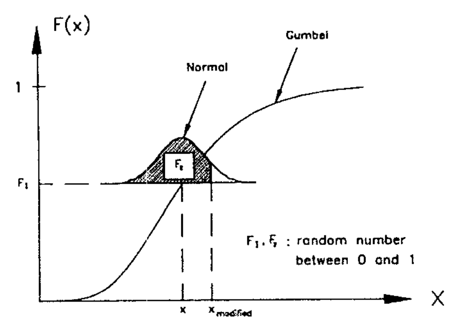

Fig.8. Simulated wave height taking into account measurement/hindcast error.

Example

Again the Tripoli deep water wave data is used as an example to demonstrate the determination of the design wave height and the influence of sample variability.

By fitting the extreme data to Gumbel distribution we obtain the distribution parameters $A = 1.73$ and $B = 4.53$, cf. Fig.9. The design wave height corresponding to a return period of 100 years is 12.2 m.

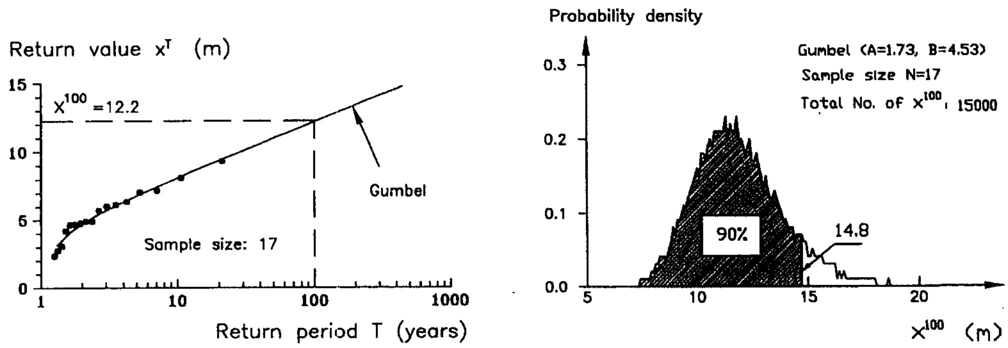

Fig.9. Simulated distribution of x^{100} (sample variability).

If sample variability is included, the design wave height x^{100} becomes a random variable. The distribution of the design wave height x^{100} can be obtained by numerical simulation, cf. Fig.9. In order to account sample variability, an 80% confidence band is often applied. In the case of wave height estimate, one-sided confidence interval is preferred over two-sided confidence interval because the lower bound of the confidence band is of less interest. Therefore, the design wave height is 14.8 m which corresponds to 90% one-sided confidence interval.

2.11 Physical consideration of design wave height

Wave breaking

The design wave height must be checked against wave breaking condition. Wave breaking occurs due to wave steepness (Stokes wave theory) or limited water depth (Solitary wave theory). Based on laboratory and field observations, many empirical formulae for wave breaking condition have been proposed, e.g. Goda (1985).

Structural response characteristics

The choice of design wave height depends not only on the structure life time, but also on the character of the structural response.

Fig.10 indicates as an example the differences in armour layer damage development for various types of rubble structures. The figure illustrates the importance of evaluation of prediction and confidence limits related to the estimated design wave height, especially in case of structures with brittle failure characteristics. To such cases a lower damage level must be chosen for the mean value design sea state. The figure is illustrative. In reality also the confidence bands for the damage curves should be considered.

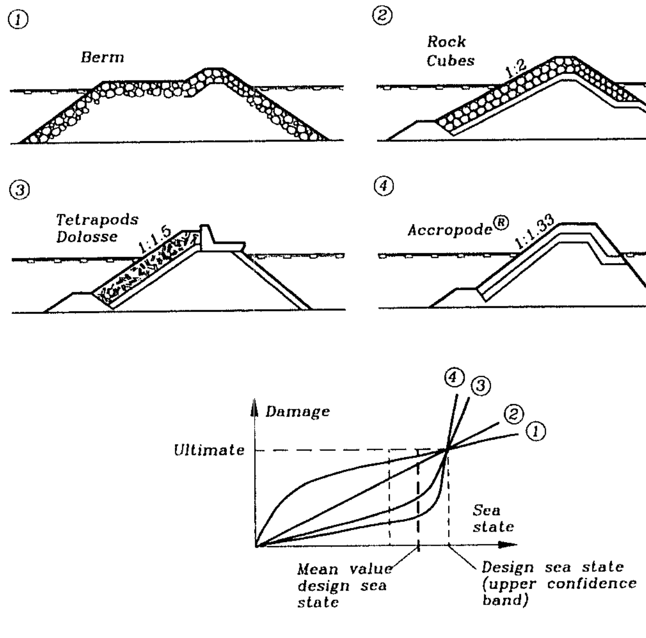

Fig.10. Illustration of typical armour layer failure characteristics for various types of rubble mound structures.

2.12 Wave period

There is no theory to determine the design wave period corresponding to the design wave height obtained by the extreme analysis, due to the complexity and locality of the joint distribution between wave height and wave period.

Fig.11 shows examples of scatter diagrams representing the joint distribution of significant wave height, H_s, and mean wave period, T_m, and still water level, z, respectively. The numbers in the scatter diagrams are the number of observations falling in the corresponding predefined intervals of H_s, T_m and z.

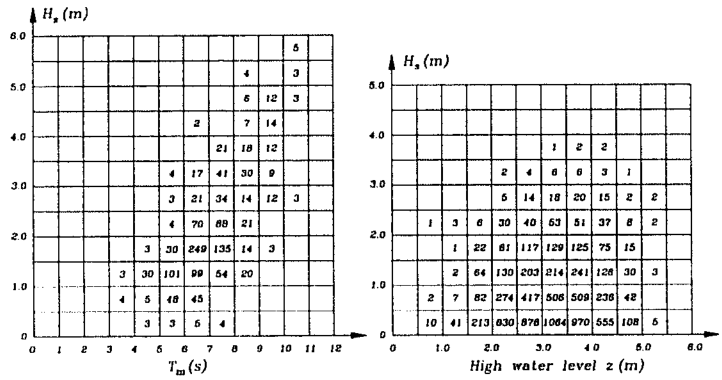

Fig.11. Scatter diagrams signifying examples of joint distributions of H_s and T_m, and H_s and water level, z.

In practice, several wave periods within a realistic range are simply assigned to the design wave height to form the candidates of the design sea state conditions. Then by theoretical consideration and/or laboratory investigation, the one which is most dangerous is chosen.

DS449 gives the range of peak wave period

$$\sqrt{\frac{130\ H_s}{g}} < T_p < \sqrt{\frac{280\ H_s}{g}} \tag{42}$$

2.13 Water level

The sea water level is affected by the following effects:

1) Astronomical effect: Tides generated by the astronomical aspect is the best understood due to their extreme regularity and the simplicity of observations. At a site without any previous tidal records usually one or a few month of recording will be sufficient to analyze the astronomical effect on the water level. The astronomical tidal variations can be found in the Admiralty Tide Tables.
2) Meteorological effect: In shallow water the water level is also affected by the meteorological effects, namely,
   i) Barometric: The higher barometric pressure causes a lower water level and vise versa.
   ii) Wind: Strong wind creates a set-up of the water level on the downwind side and a set-down on the upwind side.

   It is difficult to determine the meteorological effect on the water level. If water level records are available for a long period of time, the meteorological effect can be isolated from the astronomical effect and subjected to the extreme analysis in order to establish the long-term statistics of the water level. If such records are not available, numerical models can, using wind and/or barometric chart, give reliable results.
3) Earthquake

The water depth read from the Chart Datum is the one corresponding to the Lowest Astronomical Tide, which is the lowest tide level under the average meteorological conditions, cf. Fig.12, which gives also the widely used terminology and abbreviation of the various sea water levels.

The extreme analysis should be performed on both the high water level and the low water level. Based on the established long-term statistics is given the design low water level and the design high water level.

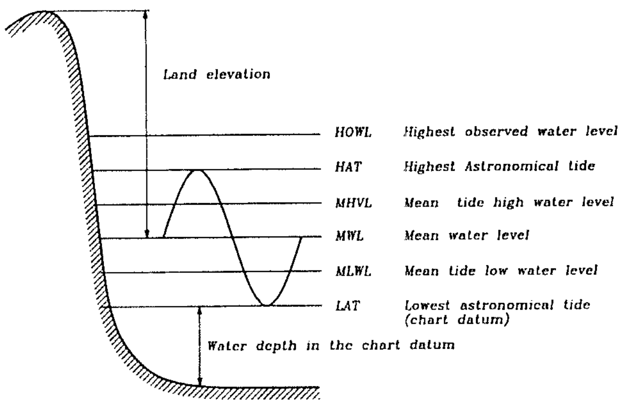

Fig.12. Water depth.

2.14 Multiparameter extreme analysis

A sea state should be characterized at least by some characteristic values of wave height (e.g. H_s), wave period (e.g. T_m), the wave direction, and the water level, because these four parameters are the most important for the impacts on the structures. Of importance is also the duration of the sea state and sometimes also the shape (type) of the wave spectrum.

When more sea state parameters have significant influence on the impact on the structure considerations must be given to the probability of occurrence of the various possible combinations of the parameter values.

For the general case where several variables are of importance but the correlation coefficients are not known the best joint probability approach would be to establish a long-term statistics for the response in question, e.g. for the run-up, the armour unit stability, the wave force on a parapet wall, etc.

If we assume that the variables of importance are H_s, T_m, α (wave direction) and z (water level) then by hindcasting or/and measurements several data sets covering some years can be established

$$(H_{s,i},\ T_{m,i},\ \alpha_i,\ z_i)\,,\quad i = 1,\ 2,\ \ldots\ n$$

For each data set the response in question is either calculated from formulae or determined by model tests. If for example run-up, R_u, is in question a single variable data set is obtained

$$(R_{u,i})\,,\quad i = 1,\ 2,\ \ldots\ n$$

The related long-term statistics can be established by fitting to a theoretical extreme distribution (extreme analysis).

2.15 References

Benard, L.R. , 1943. *Statistical analysis in hydrology.* Trans. Am. Soc. Civ. Eng., 108, pp 1110-1160

Burcharth, H.F. , 1986. *On the uncertainties related to the estimation of extreme environmental conditions.* Proceeding of Seminar on Uncertainties Related to the Design and Construction of Offshore Jacket Structures, Copenhagen, 1986, Published by Danish Society of Hydraulic Engineering

Burcharth, H.F. and Zhou Liu , 1994. *On the extreme wave height analysis.* Proceedings of HYDRO-PORT'94, Yokosuka, Japan, 19-21 October, 1994

Cunnane, C. , 1978. *Unbiased plotting positions - a review.* J. Hydrology, 37, pp 205-22.

Goda, Y. , 1979. *A review on statistical interpretation of wave data.* Port and Harbour Research Institute, 18(1), 1979

Goda, Y. , 1985. *Random seas and design of marine structures* . University of Tokyo Press, Japan, 1985

Goda, Y. , 1988. *On the methodology of selecting design wave height.* Proc. 21st Int. Conf. on Coastal Engr., Spain.

Goda, Y., Kobune, K. , 1990. *Distribution function fitting for storm wave data.* Proc. 22nd Int. Conf. on Coastal Engr., The Netherlands.

Le Mehaute, B. and Shen Wang , 1984. *Effects of measurement error on long-term wave statistics.* Proceedings of the 19th International Conference on Coastal Engineering, Houston, USA, 1984.

Liu, Z. and Burcharth, H.F , 1996. *Design wave height related to structure lifetime.* Proceedings of the 25th International Conference on Coastal Engineering, Orlando, USA, 1996.

Rosbjerg, D. , 1985. *Estimation in partial duration series with independent and dependent peak values.* Journ. of Hydrology, 76, pp 183-195.

Rosbjerg, D. , 1988. *A defence of the median plotting position.* Progress Report 66, ISVA, Technical University of Denmark

Ross, S.M., , 1987. *Introduction to probability and statistics for engineers and scientists.* John Wiley & Sons, Inc., 1987, PP 245-305. ISBN 0-471-60815-7.

Thoft-Christensen, P. and Michael J. Baker , 1982. *Structural reliability theory and its application.* ISBN 3-540-11731-8, Springer-Verlag, 1982.

Weibull, W. , 1939. *A statistical theory of strength of material.* Ing. Vet. Ak. Handl. (Stockholm), 151.

3 RUBBLE MOUND BREAKWATERS

3.1 Introduction

Rubble mound breakwaters are used for protection of harbours and beaches against wave action. They are also used for protection of navigation channels and beaches against sediment transportation.

The energy of incident waves are mainly dissipated by wave breaking, partly reflected back to the sea and partly transmitted into harbour due to penetration and overtopping, cf Fig.1.

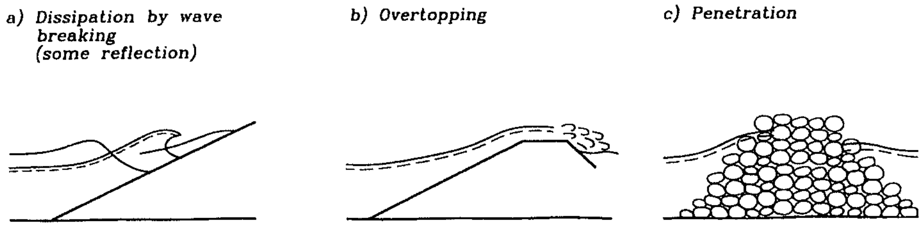

Fig.1. Illustration of incident wave energy transformation in front of a rubble mound breakwater.

3.1.1 Components of a rubble mound breakwater

A rubble mound breakwater is composed of core, berm, filter layer, armour layer and superstructure, cf. Fig.2.

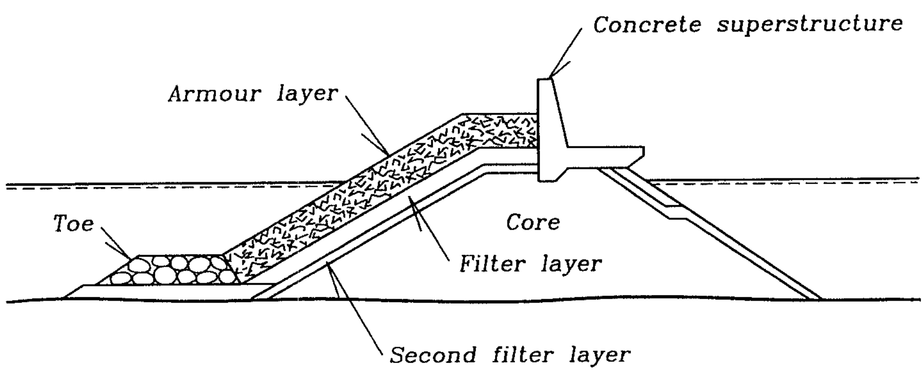

Fig.2. Components of a conventional rubble mound breakwater.

The purpose of the core is to prevent wave transmission into harbour, therefore, it is of importance that core material is not too coarse. The core is usually constructed of natural gravel or quarry run.

The berm functions as the foundation for the armour layer. Besides, the berm may catch armour units displaced from armour layer, by which the slope of the armour layer becomes more gentle and the breakwater stability may improve. The berm is normally constructed of large stones of quarry run.

The objective of the filter layer is to prevent the core material from being washed out through armour layer. Sometimes it is necessary to design multi filter layers. Filter layer is also called underlayer. It is built of quarry run.

The purpose of armour layer is to protect the core from direct wave attacks by the dissipation of wave energy. Historically armour layer was built of large rocks. Today the increasing size of vessels make it necessary to construct a rubble mound breakwater in deep water. This calls for larger armour units. If stones of sufficient size are not available, concrete armour units, such as cubes, Tetrapods, Dolosse are used, cf. Fig.3. Compared to rocks, concrete armour units, especially the slender type, have the advantage of being interlocked with high permeability and porosity as armour layer, which make them more stable and more effective in dissipating wave energy. This leads to the adoption of steeper cross sections and hence, the reduction of the construction volume. However, slender types of units can be easily broken.

The superstructure is used either in order to reduce the crest elevation or to reduce wave overtopping, or as a roadway for traffic or pipelines. The superstructure are usually constructed of concrete. Superstructure is also called wave screen, crown wall or parapet wall.

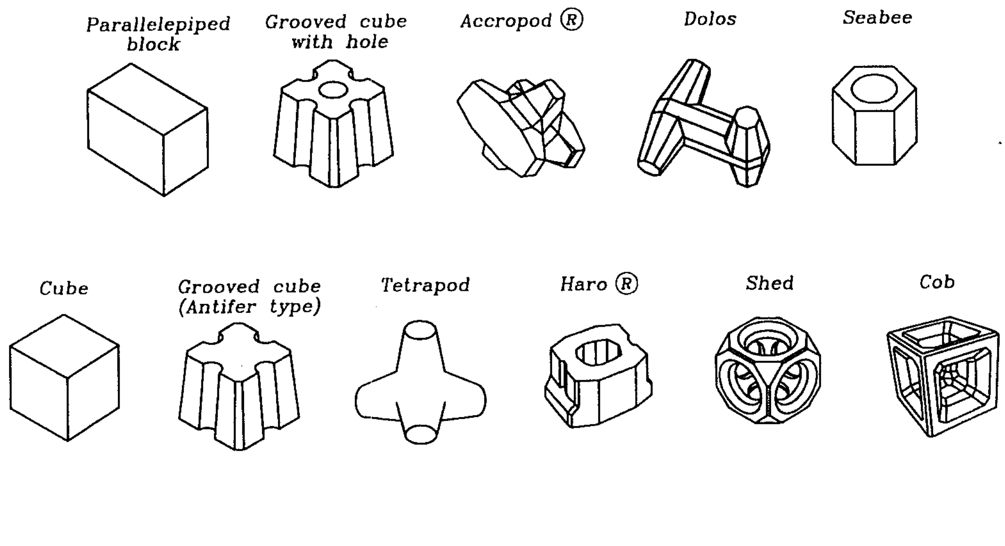

Fig.3. Examples of concrete armour units.

3.1.2 Types of rubble mound breakwaters

Various kinds of rubble mound breakwaters are shown in Fig.4.

Fig.4-a.is the most simple rubble mound breakwater, consisting of a mound of stones. However, a homogeneous structure built of stones large enough to resist displacements due to wave forces is very permeable and will cause too much penetration not only of waves but also of sediments if present in the area. Moreover, large stones are expensive because most quarries yield a lot of finer material and only relatively few large stones.

Consequently a real structure will consist of a core of fine material covered by big stones To prevent the finer material from being washed out, filter layers must be constructed, cf. Fig.4-b.

In Fig.4-c. a superstructure and concrete armour units are introduced. Note that the slope built of concrete armour units is steeper than that of stones. This means a great reduction of the construction volume.

The armour units in conventional multilayer structures, Figs.4-b and 4-c, are designed to stay in place as built, i.e. the profile remains unchanged with only minor displacements of armour units. In the case of rock armour a design can also be based on some natural reshaping of the seaward profile during wave action (self-adjusted profile). In this way relatively smaller rocks can be used because nature will optimize the profile to be the most resistant to wave action. If the mound is large enough to prevent complete erosion of the crest, then an S-shaped profile will develop as indicated in Fig. 4-d. This type of structure is often called a berm breakwater due to the large berm of armour stones placed during construction, and is designed for no overtopping.

Multilayer rubble mound structures might be given an S-shaped or bermed profile as shown in Fig. 4-e in order to reduce the wave forces, run-up and overtopping.

Completely submerged breakwaters are called reef breakwaters, which is mainly for the protection of beaches. They are constructed either as conventional multilayer structures or as homogeneous structures as shown in Fig.4-f. Most of the existing submerged breakwaters are actually the remains of normal breakwaters that were not repaired after severe damage.

The selection of the types of rubble mound breakwaters depend on availability of materials, construction methods, maintenance methods.

Usually two or more types of rubble mound breakwaters will be chosen for the subsequent design phase and model tests. The final is chosen based on economy versus reliability.

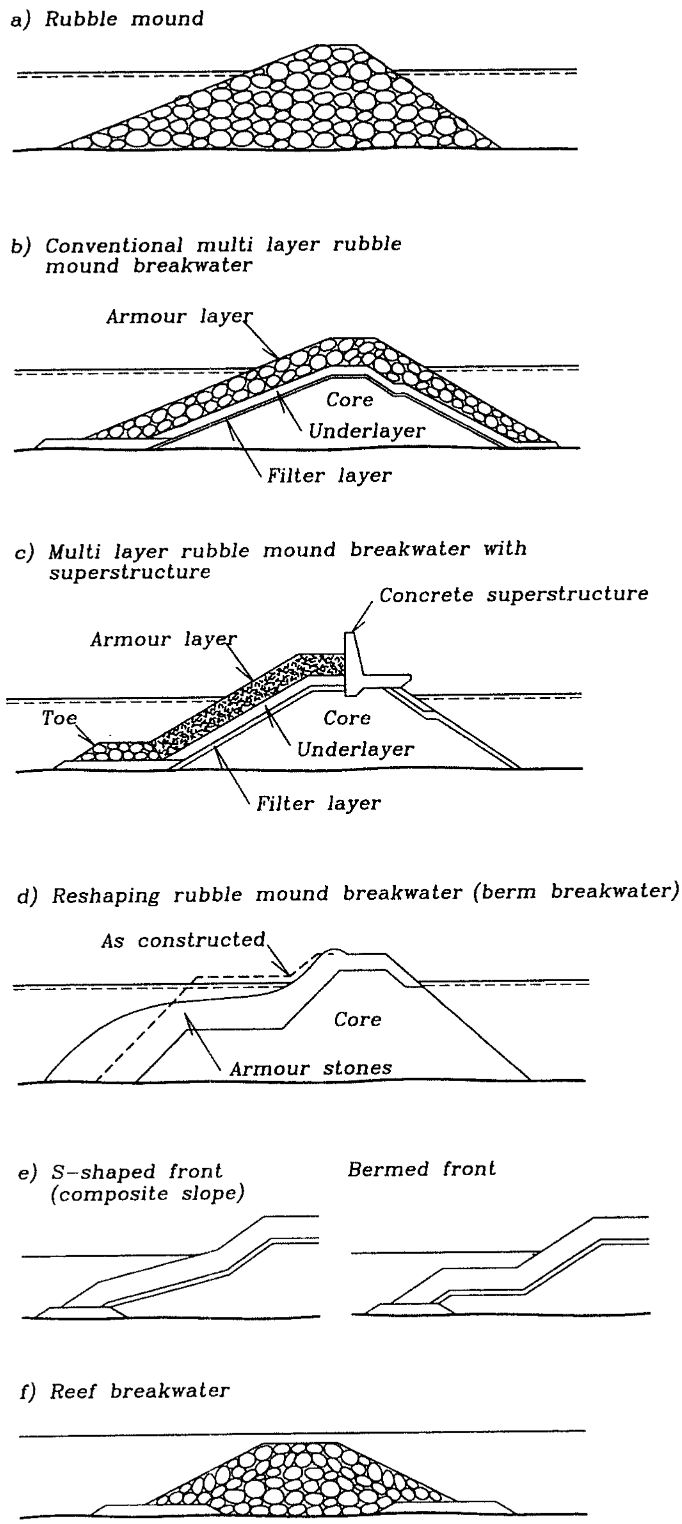

Fig.4. Types of rubble mound breakwaters (Burcharth, 1993).

3.2 Construction of rubble mound breakwaters

Contractors bidding for the breakwater constructions are free to choose the method of the construction within certain limitations. This means that the choice of construction methods is handed over to the contractors. However, it is always necessary in the design process to consider how the breakwater is to be built. For example, a wider berm should be designed if the berm is to be constructed by a less accurate construction method in order to assure the berm to support the armour layer.

3.2.1 Construction methods

There are in principle three construction methods.

Dry	To construct the breakwater in the dry behind a cofferdams or at extreme low tide. It is the most accurate construction method. However, it is seldom the case because cofferdams are available only if they are built for other purposes, and the construction should not wait for the extreme low tide.
Land	To place or dump the material from the equipment standing on the breakwater. The top of the breakwater serves as a roadway during the construction. This may makes the width at the top of the breakwater wider than required by The superstructure of breakwaters may form an excellent foundation for crane rails in the construction of large breakwaters for which huge cranes are necessary. It is necessary that the roadway is at such a high level that the safety of equipment is not endangered by waves.
Floating	To place or damp the material from floating equipment, such as barges. It is the most inaccurate construction method. It requires a positioning system to guide barges. Besides, waves and currents hamper barges from accurate placement of materials. But it is often the most economical construction method, especially if materials are delivered to the site on barges. Barges are often used to place the large volumes of materials needed for the core and the lower part of a breakwater. Sometimes barges are also equipped with a crane in order to make it possible to place the material at higher level and to place the armour units.

In practice the combination of floating equipments and breakwater-based equipments will normally be the most economical and efficient way to construct a rubble mound breakwater.

3.2.2 Construction procedure

Rubble mound breakwaters are in general very vulnerable during construction. The construction strategy should aim at the completion of the armour layer at the earliest possible stage.

Fig.5 shows an example of the construction procedure of a rubble mound breakwater. The construction method is the combination of floating equipments and breakwater-based equipment.

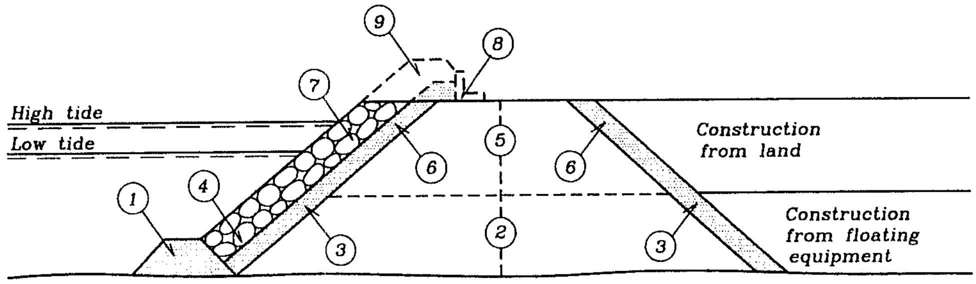

Fig.5. Construction procedure of a rubble mound breakwater (Agerschou, et al. 1983).

The berm stones are placed either by barge crane or breakwater-based crane, not dumped. The berm is usually built first because it forms the boundary for the core and filter to be dumped.

The core and filter materials were dumped either from barges or from the free end of the breakwater. The core and filter materials tend to stand with a rather steep slope (natural angle of repose). This means that it is often necessary to use other equipment to make the slope flatter. For the construction of the filter layer the breakwater-based equipment is preferred in order to control the filter layer thickness.

The armour units are placed by a crane, usually from the breakwater, but sometimes also from barges. The free drop height of the concrete armour units should be specified so that the units do not break. In order to assure the uniform distribution of armour units to be placed randomly, a grid system indicating the position of each unit can be used.

Superstructure is normally cast in-situ in elements of app. 5 - 10 meter length.

3.2.3 Quarry run

Rubble mound breakwaters require very large quantities of rock materials of various gradings and qualities.

Because natural stones are seldom available in sufficient quantities and sizes the materials must in most cases be supplied from quarries. The output from a quarry in terms of sizes and shapes is, however, not only dependent on the applied blasting technique but to a large extent on the type of rock and the degree of weathering.

A sample of quarry blocks will cover a range of block weights (or masses). The cumulative distribution of block weights is the basis for the definition of characteristic block weights, sizes and gradings, cf. Fig.6.

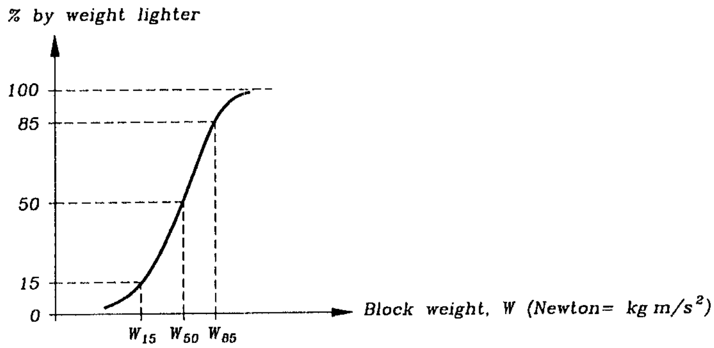

Fig.6. Illustration of cumulative block weight distribution.

The equivalent cube length $D_{n,50}$ used is defined as

$$D_{n,50} = \left(\frac{W_{50}}{\rho_s g}\right)^{1/3} \tag{1}$$

where W_{50} is the *median weight* and ρ_s is the mass density of the stone.

As an indicator of the gradation (grading width) is often used the ratio, $D_{85}/D_{15} = (W_{85}/W_{15})^{1/3}$ or W_{85}/W_{15}.

In breakwater engineering the following classes are often used, cf. Table 1.

Table 1. Conventional gradings and their application.

Gradation	D_{85}/D_{15}	Application (conventional)
Narrow	≤ 1.5	Armour layer, berms, filter layer
Medium	1.5 – 2.5	Filter layers, (maybe berms and armour layer)
Wide	2.5 – 5 (or more)	Core material

3.3 Wave-structure interaction

This section discusses the wave structure interaction. Functional relationships between the main environmental parameters, structural parameters and the structural responses are given in terms of formulae, when they exist. The formulae are derived mainly from physical considerations and scale model tests and are valid only for the tested parameter ranges.

3.3.1 Types of wave breaking on slope

The kinematics of regular waves breaking on smooth, impermeable slopes can be qualitatively described by the so-called surf-similarity parameter or Irribarren number, ξ, which characterizes the type of wave breaking.

$$\xi_0 = \frac{1}{\sqrt{\frac{H_0}{L_0}}\cot\alpha} \quad \text{or} \quad \xi_b = \frac{1}{\sqrt{\frac{H_b}{L_0}}\cot\alpha} \tag{2}$$

where H_0 wave height in deep water
H_b wave height at the breaking point
L_0 wave length in deep water $L = \frac{gT^2}{2\pi}$
α slope angle

The breaker types and related ranges of ξ-values are given in Table 2.

Table 2. Types of wave breaking and ξ-values.
Regular waves, smooth and impermeable slope.

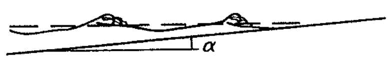	*Spilling*	$\xi_o<0.5$	$\xi_b<0.4$
	*Plunging*	$0.5<\xi_o<3.3$	$0.4<\xi_b<2.0$
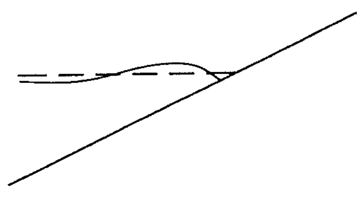	*Surging or collapsing* *(No real wave breaking on the slope)*	$\xi_o>3.3$	$\xi_b>2.0$

For irregular waves some characteristic values of wave parameters, e.g. significant wave height H_s, peak wave period T_p or mean wave period T_m are used for the determination of ξ-values. Moreover, Table 2 can be used only as a reference.

3.3.2 Wave run-up and run-down

Wave breaking on a slope causes up-rush and down-rush. The maximum and minimum elevation of the water surface measured vertically from still water level are denoted by R_u, run-up, and R_d, run-down, respectively, see Fig.7.

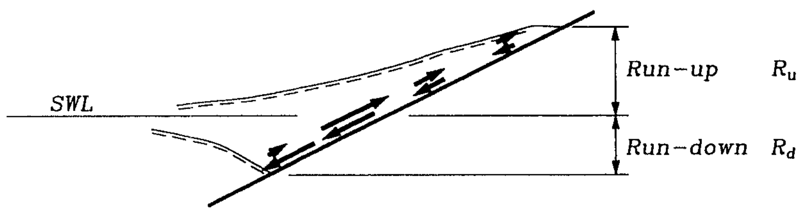

Fig.7. Definition of wave run-up and run-down.

The value of R_u helps to determine the crest elevation of rubble mound breakwaters. And the value of R_d gives hint on the range where the slope should be covered by armour units.

R_u and R_d depend on the water depth, wave climate (wave height, wave period and wave attack angle), and the structure (slope angle, the surface roughness and the permeability and porosity of the slope).

The following dimensional analysis shows that wave run-up is proportional to the wave height. $\propto$ should be read as *proportional to.*

It is reasonable to assume that the velocity of up-rush at still water level is proportional to the maximum horizontal velocity of water particle when wave breaks, i.e.

$$v \propto u_{max}$$

u_{max} equals the wave celerity c when the wave breaks.

$$u_{max} = c \quad \Longrightarrow \quad v \propto c$$

In shallow water the wave celerity depends on water depth

$$c = \sqrt{gh} \quad \Longrightarrow \quad v \propto h^{1/2}$$

And the wave height is proportional to water depth when the wave breaks

$$H \propto h \quad \Longrightarrow \quad v \propto H^{1/2}$$

If there is no energy loss during the process, by energy conservation

$$\frac{1}{2}mv^2 = mgR_u \quad \Longrightarrow \quad R_u \propto v^2 \propto H$$

Obviously the conclusion holds for wave run-down.

The empirical formula for regular wave run-up on smooth and impermeable slope reads

$$\frac{R_u}{H} = \begin{cases} \xi & \text{if} \quad \xi \leq 2.3 \\ 2.3 & \text{if} \quad \xi \geq 2.3 \end{cases}$$

where H wave height in front of structure

ξ $\quad \xi = \frac{1}{\sqrt{\frac{H}{L_0}}\cot\alpha}$

The empirical formula for irregular wave run-up on smooth and impermeable slope reads

$$\frac{R_{u,2\%}}{H_s} = \begin{cases} 1.5\,\xi_p & \text{if} \quad \xi_p \leq 2 \\ 3 & \text{if} \quad \xi_p \geq 2 \end{cases}$$

where H_s significant wave height in front of structure

ξ_p $\quad \xi_p = \frac{1}{\sqrt{\frac{H}{L_p}}\cot\alpha}$

L_p $\quad L_p = \frac{gT_p^2}{2\pi}$

$R_{u,2\%}$ 2% of wave run-up will exceed $R_{u,2\%}$

There are also empirical formulae taking into considerations rough, permeable slopes, bermed slopes, oblique waves and 3-D waves.

Wave run-down can be positive as well as negative. A positive run-down means that the down-rush process is interrupted by the up-rush from the proceeding wave, and the water level on slope is always above the still water level. Regular wave run-down on smooth, impermeable slope can be calculated by the empirical formula

$$\frac{R_d}{H} = R_u\,(1 - 0.4\xi) \tag{3}$$

3.3.3 Wave overtopping

Wave overtopping is often represented by $\overline{Q}$, the average volume of water overtopping the crest of the breakwater per second per meter length of the breakwater, even though the amount of overtopping varies considerably from wave to wave and in most cases the bulk of the average discharge is caused by a limited fraction of the waves.

No standards for overtopping exist. However, some critical $\overline{Q}$ values structure, $\overline{Q}$ $m^3/s/m$, have be established on the basis of field observations, cf. Table 3, which corresponds to targets situated few meters behind the breakwater crest.

Table 3. Critical values of average overtopping discharges, $\overline{Q}$ $m^3/s/m$

Pedestrians	wet, but safe	$< 4 \cdot 10^{-6} <$	very uncomfortable	$< 3 \cdot 10^{-5} <$	unsafe
Vehicles	safe driving	$< 10^{-6} <$	difficult to drive	$< 2 \cdot 10^{-5} <$	unsafe to drive
Buildings and installations	no damage	$< 10^{-6} <$	minor damage to sign posts, fittings windows etc.	$< 3 \cdot 10^{-5} <$	damage to structural parts

Fig.8 shows the parameters related to $\overline{Q}$. The relative free board $\frac{R}{H_s}$ is the most important dimensionless parameter, because model tests show that the dimensionless $\overline{Q}$ is decreasing proportionally to the exponential function of $\frac{R}{H_s}$, i.e.

$$\frac{\overline{Q}}{g\, H_s\, T_m} = a\; exp\left(-b\,\frac{R}{H_s}\right) \tag{4}$$

where a and b are empirical coefficients depending on the geometry of the structure.

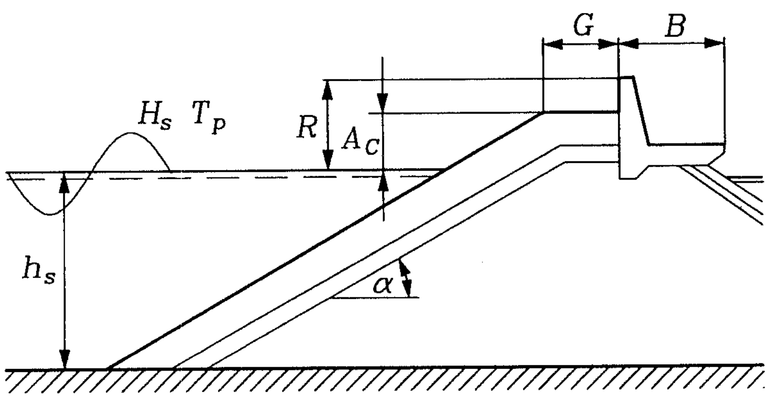

Fig. 8. Parameters related to overtopping.

3.3.4 Wave reflection

Rubble mound breakwaters reflect some proportion of the incident wave energy. If significant, the interaction of incident and reflected waves can create a very confused sea with very steep and often breaking waves. It is a well known problem in many harbour entrance areas where it can cause considerable manoeuvring problems to smaller vessels. A strong reflection also increases the sea bed erosion potential in front of the structure (scour). Moreover, waves reflected from breakwaters can in some cases create or increase erosion of neighbour beaches.

The reflection can be quantified by the reflection coefficient

$$C_r = H_{s,r}/H_s \tag{5}$$

where H_s significant wave height of incident wave

$H_{s,r}$ significant wave heights of incident wave

The reflection coefficient for smooth, impermeable and non-overtopped slope reads

$$C_r = 0.1\,\xi^2 \qquad \xi < 2.5 \tag{6}$$

and for non-overtopped rock slope reads

$$C_r = 0.14\,\xi_p^{0.73} \qquad \xi_p < 8 \tag{7}$$

3.3.5 Wave transmission

Waves behind a rubble mound breakwater are caused mainly by overtopping, but also by wave penetration. Wave transmission can cause ship maneuver problem inside a harbour.

Wave transmission can be characterized by a transmission coefficient, C_t, defined as

$$C_t^{H_s} \;=\; H_{s,t}/H_s \tag{8}$$

$H_{s,t}$ is the significant wave height on the harbour side of structures.

3.3.6 Wave force on armour layer and armour unit stability

Wave breaking on slopes causes up-rush and down-rush, which are characterized by the velocity v. v is highly non-stationary with respect to both velocity and direction.

The flow forces acting on an armour unit by up-rush and down-rush is schematized in Fig.9. The flow is assumed to be quasi-stationary, i.e. the inertia force F_I is neglected.

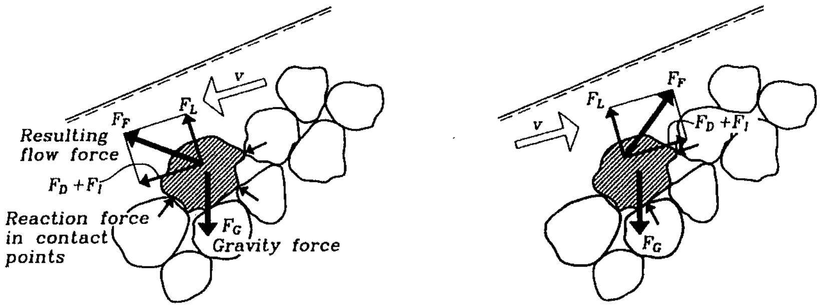

Fig.9. Illustration of forces on armour units.

The armour unit size is characterized by an equivalent cube length D_n

$$D_n = \left(\frac{M}{\rho_a}\right)^{1/3} \tag{9}$$

M and ρ_a are the mass and density of the armour unit respectively. The gravity force is the submerged weight of the armour unit

$$F_G = (\rho_a - \rho_w) g D_n^3 \tag{10}$$

The lift force F_L is caused by the difference in pressure on the upper and lower side of the unit due to the velocity difference.

The drag force F_D consists two parts: skin friction force acting on the surface of the unit and form drag force due to the difference in pressure on the up-flow and down-flow side of the unit. For the case of rubble mound breakwater armour unit, the form drag force is many times larger than the skin friction force.

Applying the Morison equation the flow forces on a resting unit can be expressed as follows:

$$F_D \approx C_D \, \rho_w \, A \, v^2$$

$$F_L \approx C_L \, \rho_w \, A \, v^2$$

where A cross sectional area at right angles to v

C_D , C_L drag and lift coefficients respectively

Because $A \propto D_n^2$ and $v \propto H$ (cf. section on wave run-up and run-down), the resultant flow force may be written

$$F_R = C\, \rho_w\, g\, D_n^2\, H \tag{11}$$

C is a coefficient.

There are several armour unit displacement modes, cf. Fig.10.

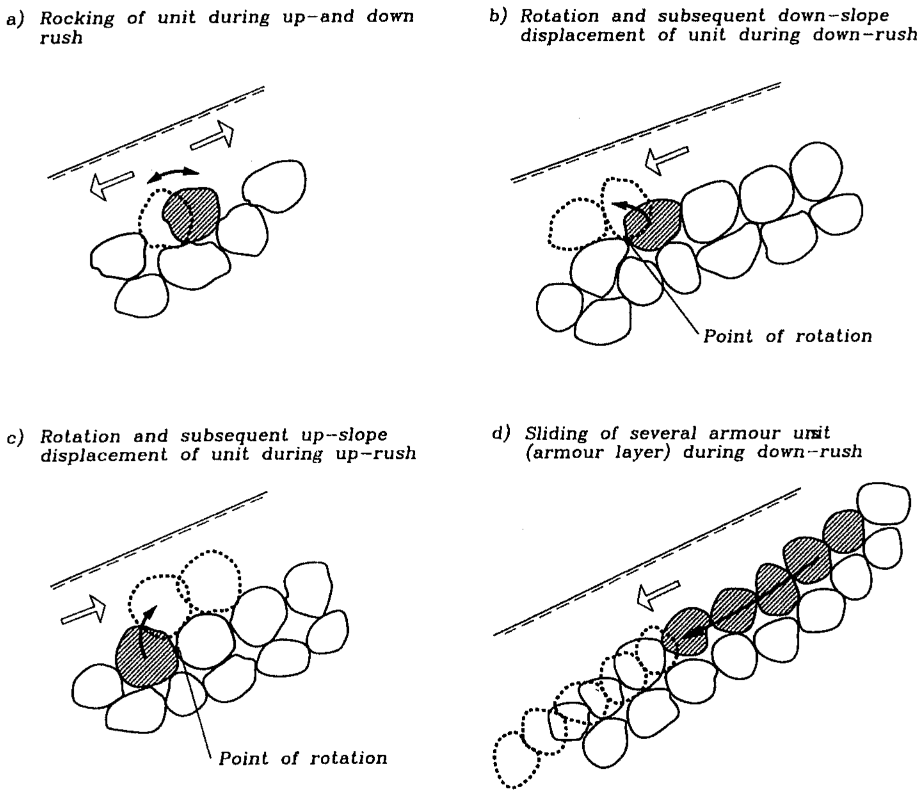

Fig.10. Armour unit displacement modes.

Take the sliding of armour unit during down-rush as an example, cf. Fig.11.

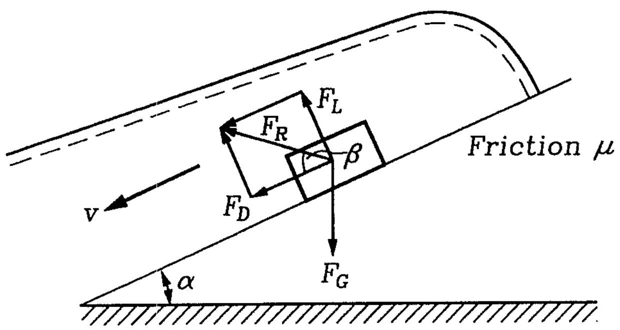

Fig.11. Unit sliding during down-rush.

The criterion for stability may be expressed

$$F_R \cos\beta + F_G \sin\alpha \le \mu(F_G \cos\alpha - F_R \sin\beta) \qquad \text{or}$$

$$F_G(\sin\alpha - \mu\cos\alpha) \le -F_R(\cos\beta + \mu\sin\beta)$$

by inserting the expressions for F_R and F_G and $M = \rho_a D_n^3$

$$\frac{\rho_a H^3}{M\left(\frac{\rho_a}{\rho_w} - 1\right)^3 \cot\alpha} \le \frac{1}{C^3 \cot\alpha}\left(\frac{\mu\cos\alpha - sin\alpha}{\cos\beta + \mu\sin\beta}\right)^3 = K_D$$

or write into the form of the well-known Hudson formula

$$M = \frac{\rho_a H^3}{K_D\left(\frac{\rho_a}{\rho_w} - 1\right)^3 \cot\alpha} \qquad (12)$$

The stability coefficient K_D is an empirical coefficient depending on the type of armour unit, wave steepness, etc.

For other armour unit displacement modes the stability formulae are basically the same as the one derived above.

However, Hudson formula, which was developed for rock armour, where the stabilizing force is the weight of rocks, cannot represent the stability of concrete armour unit layer, whose stability depends both on weight and interlocking. With respect to the contribution of the weight of concrete armour unit to the hydraulic stability, the more gentle the slope, the bigger the contribution, as expressed in Hudson formula. But on the other hand, the interlocking ability increases with the increase of slope angle (before the slope reaches its natural angle of repose). This means that there is an optimum slope which maximize the stability of concrete armour unit layer.

Today it becomes more popular to use the stability number N_s, defined as

$$N_s = \frac{H_s}{\Delta D_n} = (K_D \cot\alpha)^{1/3} \qquad (\Delta = \frac{\rho_a}{\rho_w} - 1) \qquad (13)$$

3.3.7 Wave force on superstructure

The wave forces on a superstructure exposed to irregular waves are of a stochastic nature. The forces acting on a superstructure at a given instant are schematized in Fig. 12.

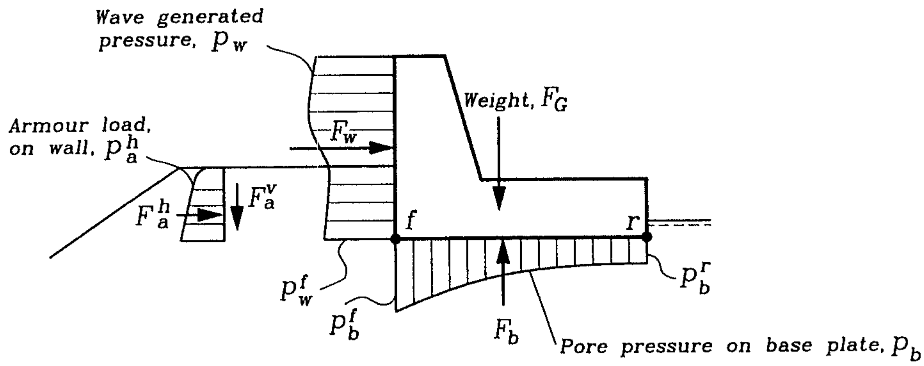

Fig. 12. Wave forces on a superstructure.

The wave generated pressure, p_w, acting perpendicular to the front of the wall is the one, which would be recorded by pressure transducers mounted on the front face. F_w is the instantaneous resultant of the wave generated pressures p_w.

The instantaneous uplift pressure, p_b, acting perpendicular to the base plate is equal to the pore pressure in the soil immediately under the plate. The resultant is F_b.

At the front corner, f, the uplift pressure p_b^f, equals the pressure on the front wall p_w^f.

At the rear corner, r, the uplift pressure, p_b^r, equals the hydrostatic pressure at r.

The actual distribution of p_b between p_b^f and p_b^r depends on the wave generated boundary pressure field and on the permeability and homogeneity of the soil. The distribution cannot be determined in normal wave flume scale tests because of strong scale effects related to porous flow. However, the corner pressures p_b^f and p_b^r can be measured or estimated, and in case of homogeneous and rather permeable soils and quasi-static conditions, a safe estimate on the most dangerous uplift can be found assuming a linear pressure distribution between a maximum value of p_b^f and a minimum value of p_b^r.

Armour and filter stones resting against the front of the wave wall will introduce an armour load, p_a, on the front through the contact points. Both a normal soil mechanics load and a proportion of the dynamic wave loads on the armour contribute to p_a. The resultant force F_a is generally not perpendicular to the front due to friction between the armour and filter stones and the wall, and must be split into the two orthogonal components F_a^h and F_a^v.

3.4 Structural design of rubble mound breakwaters

3.4.1 Failure modes of rubble mound breakwaters

In this context failure means excess of a design damage criterion, e.g. excess in displacement of armour units or excess in overtopping. All possible failure modes must be identified and considered in the design process.

The failure modes of a rubble mound breakwater are indicated in Fig.13. They can be classified into

Geotechnic	Core settlement. Slip failure of various components.
Hydraulic	Erosion of armour layer, rear slope layer and toe berm. Too much overtopping. Sliding and tilting of superstructure.
Structural	Breakage of armour units. Breakage of superstructure.

It should be stressed that these failure modes interact with each other, e.g. the erosion of toe berm and the breakage of armour units will speed up the erosion of the armour layer, excessive overtopping might cause the failure of the rear slope.

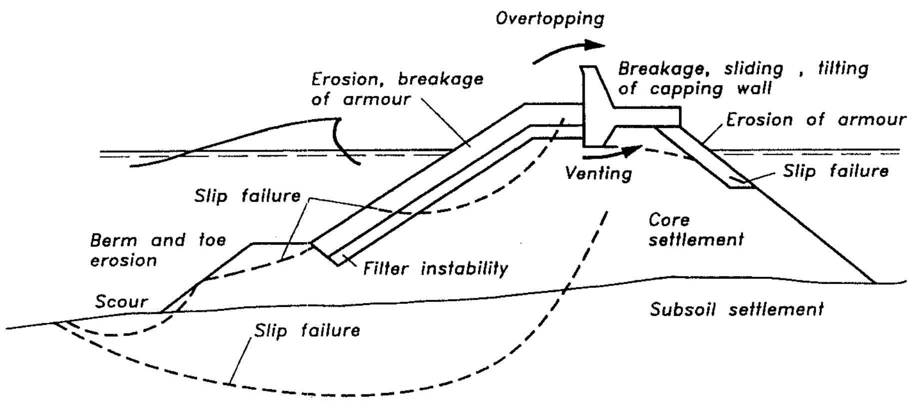

Fig.13. Failure modes of a rubble mound breakwater (Burcharth, 1993).

3.4.2 Definition of armour layer damage

Categories of the unit movement are

1) No movements
2) Rocking
3) Small movement: displaced by less than $2D_n$
4) Displacement: displaced by more than $2D_n$

There are 3 parameters defined to represent the armour layer damage.

1) The relative displacement D is defined as

$$D = \frac{n_d \text{ (number of displaced units)}}{n \text{ (total number of units)}} \tag{14}$$

2) The strip displacement N_{od} is defined as the number of the units displaced within a strip of one D_n width.

$$N_{od} = \frac{n_d}{\frac{B}{D_n}} \qquad (B : \text{Length of the breakwater}) \tag{15}$$

3) The relative eroded area S is (cf. Fig.14)

$$S = \frac{A_e}{D_n} \tag{16}$$

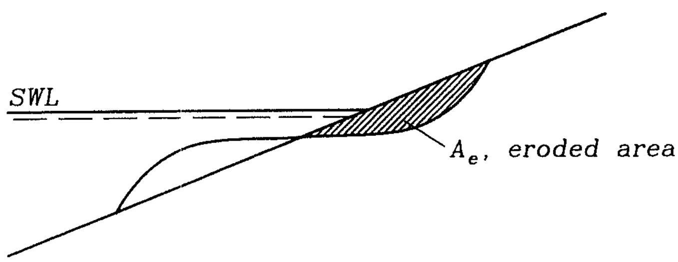

Fig.14. Definition of the eroded area A_e.

The relative displacement D has been used for long time. But the use of the total number of units as a reference has the disadvantage that D values depend on the height of the slope. The strip displacement N_{od} was presented recently in order to overcome the disadvantage. But it cannot account the effect of the packing density, e.g. N_{od} values are the same if two identical slopes have the same number of displaced units, even though the one is covered by, say 100 units and the other by 200 units.

The relative eroded area was first introduced in the study of b each erosion. For the slope formed of uniform concrete armour units, if settlement is disregarded, then

$$N_{od} = (1 - p)\,S \qquad (p : \text{Porosity of the armour layer}) \tag{17}$$

Unfortunately the relationship between N_{od} and S depends on the type of units and the slope angle due to the settlements.

There are 3 stages of the damage

1) Initial damage. There are very limited number of displaced units.
2) Moderate to severe damage. There are some displaced units. the armour layer remains stable as a whole. Usually it is the design criterion.
3) Failure. The damage is so severe that the filter layer is exposed directly to wave attack.

Table 4 gives the values of D, N_{od} and S corresponding to the damage stages.

Table 4. Damage parameters and damage stages.

Damage parameters		Initial damage	Moderate to severe damage	Failure
D		< 2	5-10	15
N_{0d}		< 0.5	2-3	5
S	slope 1 : 1.5	2	3-5	8
	slope 1 : 2.0	2	4-6	8
	slope 1 : 4.0	3	8-12	17

3.4.3 Armour layer

The weight of the individual armour unit is determined by Hudson formula,

$$M = \frac{\rho_a H^3}{K_D \left(\frac{\rho_a}{\rho_w} - 1\right)^3 \cot\alpha}$$

K_D values, corresponding to moderate damage and determined from model tests, are listed in Table 5.

For the armour units to be located at the round-head of the breakwater, the mass should be increased by 50 %.

There are also other stability formulae developed recently for various types of concrete armour units, cf. Appendix.

The lower bound of armour layer is app. $1.5 \times H_s$ below the still water level. In the case where superstructure is applied, the horizontal width of armour layer in front of the superstructure should be at least 3 times the equivalent cube length of the armour units in order to avoid severe wave impact on the superstructure.

Armour layer is usually composed of two layers of armour units placed randomly on the slope. Table 5 lists the packing density of armour units, porosity and layer thickness coefficient of armour layer. The number of armour unit per unit area, the concrete volume per unit area and layer thickness are determined by

$$\begin{array}{lll} \text{number of armour units per unit area} & N_a & = \frac{\varphi}{D_n^2} \\ \text{layer thickness} & t_a & = 2\,c\,D_n \\ \text{concrete or rock volume per unit area} & V & = N_a\,D_n^3 \end{array} \qquad (18)$$

where D_n equivalent cube length, $D_n = \left(\frac{M}{\rho_a}\right)^{1/3}$

φ packing density, cf. Table 5

c layer thickness coefficient, cf. Table 5

Table 5. Characteristic parameter values of armour units two layer random placement

type of armour unit		rock	cubes	Tetrapods	Dolosse
stability coefficient	k_D	3	6	10	12
packing density	φ	1.26	1.3	1.0	0.83
porosity	p	0.37	0.33	0.5	0.56
layer thickness coefficient	c	1	1	1.02	0.94

3.4.4 Filter layer

The purpose of filter layer(s) is to prevent the finer material in the core and the sea bed from being pulled out through the armour layers. Significant migration of finer material into the coarser material will lead to settlements and might cause reduced porosity and permeability of the filter layers resulting in reduced hydraulic stability of the cover layers.

It is easy to formulate filter rules which assure no or marginal migration. However, such restrictive rules necessitate more filter layers to overcome a certain difference in size of core and armour layer. Table 6 gives more applicable rules for filter layer.

Table 6. Filter rules.

Type of armour unit	$\frac{\text{(average) mass of armour unit}}{\text{average mass of filter stones}}$
Rock	15
Massive (cubes etc.)	10
Slender (Tetrapods etc.)	5

The thickness of the filter layer should be at least twice of the average equivalent length of filter stone. Moreover, it should also be at least half of the equivalent cube length and armour units in order to prevent filter damage during the placement of armour units.

3.4.5 Core

The core material is generally quarry run, which usually has a wide gradation.

The core should not be constructed of too coarse materials in order to avoid undesirable transmission of waves and sediment transport through the breakwater. Coarse core material might also facilitate venting underneath superstructures.

On the other hand a lower limit for the size of material should also be set in order to prevent wash-out of the finer material. This is due to the consequent risk of larger settlements and inconvenient deposition of the materials. Also, if very fine material is used for the core it might be necessary to use several filter layers to avoid out-wash. Finer materials are also less suitable for construction due to the smaller natural angle of repose (very gentle slopes) and the vulnerability to erosion in waves and currents.

In practice the mass of core materials ranges

$$\frac{\text{(average) mass of armour units}}{\text{mass of core material}} = 200 \sim 6000 \tag{19}$$

3.4.6 Berm

The main function of berm is to provide support for the armour layer. The width of the berm should be at least 5 to 10 times the stone dimension of the berm. If less accurate construction methods are used, such as dumping of stones from floating equipment, a wider berm is recommended.

In the case of shallow water, concrete armour units are used for the construction of the berm.

It is normally recommended to construct the berm with a trough on the inner side. This trough gives better support for the armour layer. Moreover, it makes the placement of filter and armour layer easier.

Berm stone size can be estimated by

$$N_s = \frac{H_s}{\Delta D_{n,50}} = \frac{1.6}{N_{0d}^{-0.15} - 0.4\frac{h_t}{H_s}} \tag{20}$$

where $D_{n,50}$ $D_{n,50} = \left(\frac{M_{50}}{\rho_s}\right)^{1/3}$

h_t Water depth above the berm

N_{od} Number of stones displaced within a strip of one $D_{n,50}$ width

$$N_{od} = \begin{cases} 0.5 & \text{no damage} \\ 2 & \text{moderate damage} \\ 5 & \text{collapse} \end{cases}$$

3.4.7 Rear slope

If there is no severe overtopping, the filter materials are used for the protection of the rear slope. Moreover, a rather steep slope, say 1:1.5 or even 1:1.25 can be applied.

If there is significant overtopping, larger stones are needed to protect rear slope. Generally model tests should be performed to check the rear slope stability, even though there are some research results.

3.4.8 Superstructure

The most common failure modes of concrete superstructures are shown in Fig. 15. Quite often the combinations of failure modes occur.

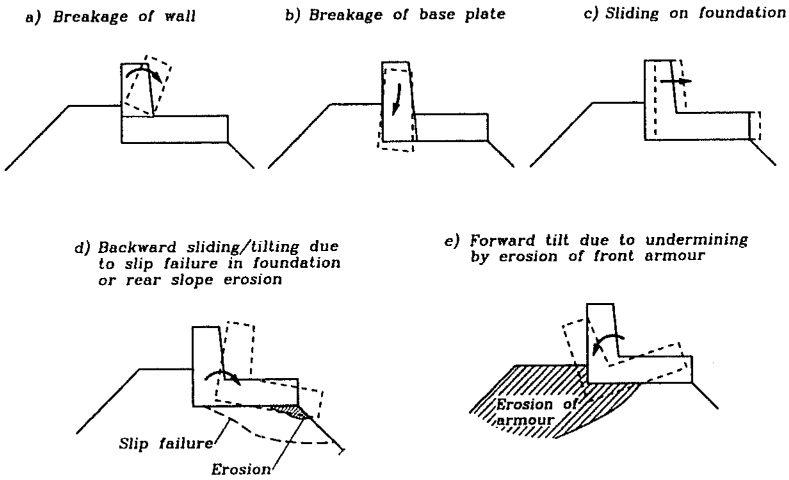

Fig.15. Common failure modes of concrete crown walls.

It is usually necessary to perform model tests in order to determine wave forces on the superstructure.

Prediction of the breakage of wall is the most simple case in the sense that only the wave loads on the front wall and the strength of the structure need to be known.

The total stability of the superstructure must be investigated by considering both the resistance to sliding and overturning and the bearing capacity of the foundation. They will be treated in the section on the overall stability of caissons.

Due to the uncertainty related both to wave loads, uplift pressure and coefficient of friction it is important to apply a safety coefficient in such calculation.

Severe wave impact on the superstructure can be avoided either by increasing the crest level of the armour layer or by increasing the width of the berm in front of the superstructure, cf. Fig.16.

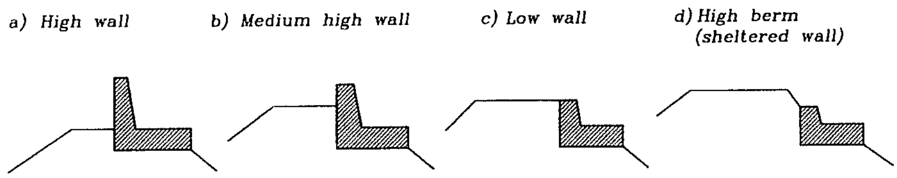

Fig.16. Typical superstructure configurations.

3.5 Examples of rubble mound breakwater failures

Anything, which might go wrong, will go wrong - *Marfian's Law*

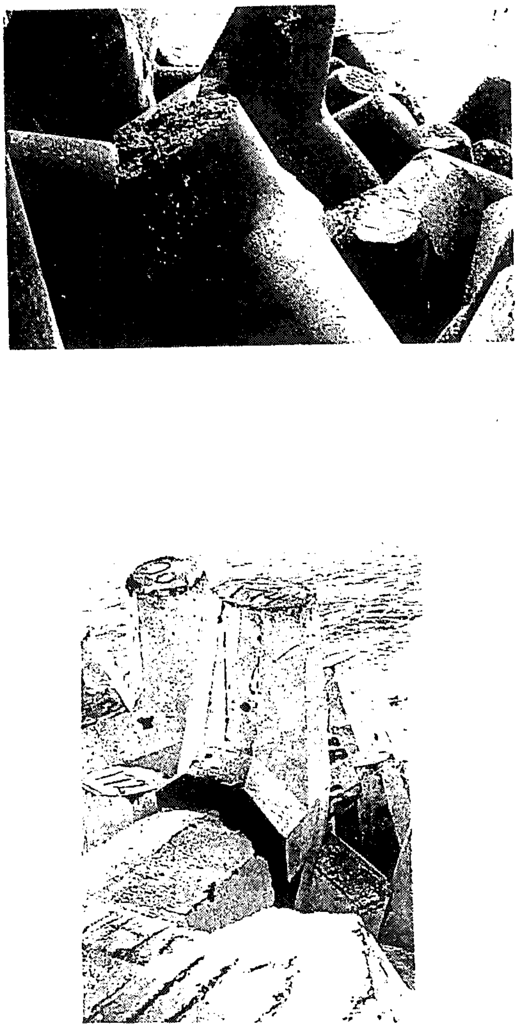

Breakage of 25 t Tetrapods and 38 t Dolosse
Crescent City Harbour, California, USA
(Magoon, et al. 1990)

Sinking of ships caused by wave overtopping
Oran City Harbour, Algeria
(Agerschou, et al. 1983)

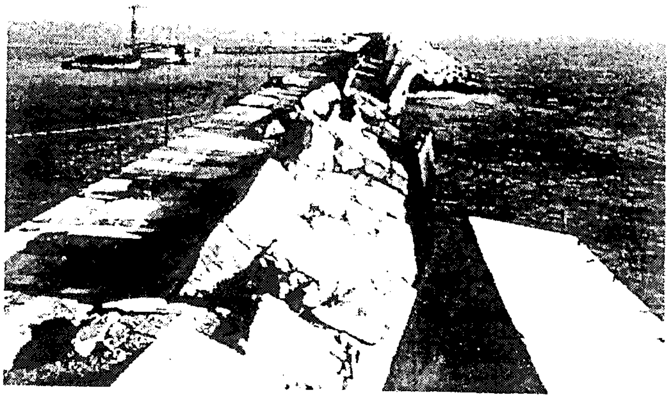

Armour layer is 42 t Dolosse on the slope 1:1.5
Failure started from breakage of Dolosse and erosion of armour layer
Sines Breakwater, Portugal
(Jensen, 1984)

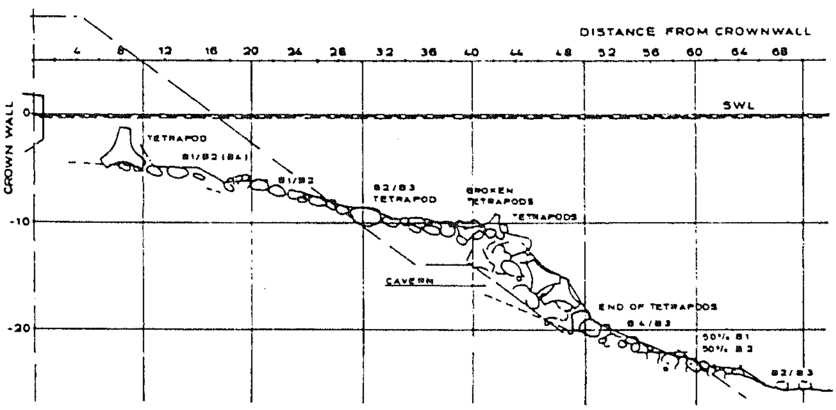

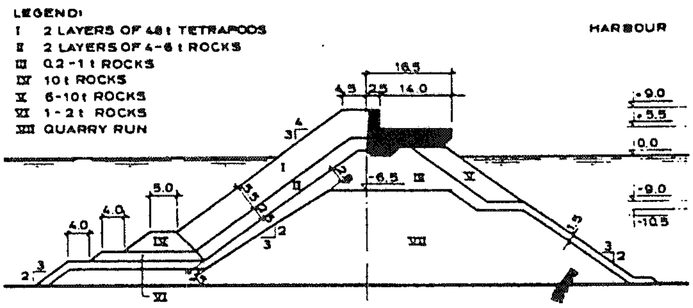

armour layer is 48 t Tetrapods on the slope 1:1.33
Failure stated from breakage of Tetrapods and erosion of armour layer
Port d'Azzew-EL-Djedid, Algeria
(Jensen, 1984)

4 VERTICAL BREAKWATERS

4.1 Introduction

Vertical breakwaters are used to protect harbours against wave actions. The round-head of rubble mound breakwaters are also often built of a vertical breakwater.

The energy of incident waves are partly reflected back to the sea, partly dissipated by wave breaking in front of vertical breakwaters and partly transmitted into harbour by penetration and overtopping, cf. Fig.1.

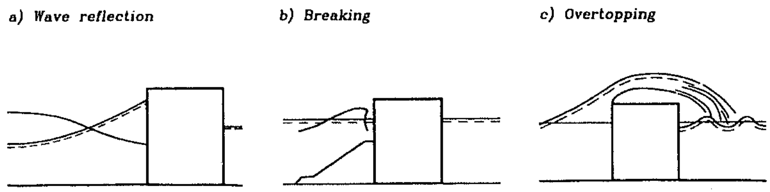

Fig.1. Illustration of incident wave energy deformation in front of a vertical breakwater.

4.1.1 Components of a vertical breakwater

A vertical breakwater is normally composed of rubble mound foundation, substructure and superstructure, cf. Fig.2.

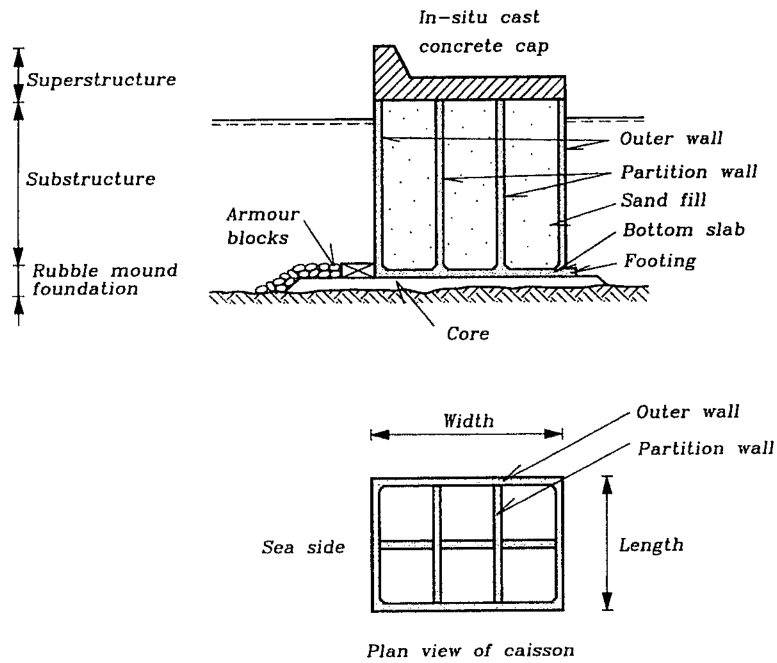

Fig.2. Components of a vertical breakwater.

The rubble mound foundation functions like a buffer between the substructure and the sea bed. It spreads the vertical load from the substructure over a wide area of sea bed. The rubble mound foundation consists of the armour layer, core and if necessary, filter layer.

The substructure can be composed of layers of rectangular rocks, of layers of solid concrete blocks, or of caissons.

A caisson is an open reinforced concrete box with a bottom slab and outer walls. A large caisson is usually divided into several inner cells by partition walls in order to reduce the span length of the outer walls. Moreover, the partition walls reduce the pressure of sands filled in caisson. A caisson has footings at the front and back heels in order to transfer the vertical loads to the foundation.

The super structure is composed of a parapet wall and deck. The parapet wall reduces water overtopping over the structure. The deck serves as a roadway. Oil and water pipeline are installed inside or under the deck.

In the analysis of overall stability, the superstructure and the substructure are called vertical structure.

4.1.2 Types of vertical breakwaters

Various cross sections of vertical breakwaters have been invented in order to improve the stability of the structure and reduce overtopping, but often structural measures in favor of the one criterion will worsen the other.

Traditionally the parapet wall has a vertical face, Fig.3-a1. It might be given a slope in order to reduce the horizontal impulsive wave forces, Fig.3-a2, but the amount of overtopping increases. Because the first rational consideration of this shape is related to the Hanstholm breakwater in Denmark this type is sometimes referred to in the literature as the Hanstholm type. A seaward curved parapet reduces overtopping by leading water jetting back to the sea, but the upward pressure causes the reduction of stability, Fig.3-a3. Fig.3-a4 reduces overtopping by entrapping water in the reservoirs. The water leaks back into the sea by the drainage system under the reservoirs.

Fig.3-b1 is the conventional type with an impermeable seaward face and is most often constructed of reinforced concrete caissons filled with sand or quarry rock and capped with in-situ cast concrete. Many old structures of this type were constructed of stacked precast mass concrete blocks, Fig.3-b2.

Fig.3-c1 is a dissipative type caissons with holes or slots in the front face and a wave chamber behind. Wave energy is dissipated by the turbulence created during in and out flow. The advantages obtained are the reduction of the overtopping and of the wave forces, especially of the large forces from waves breaking on the structure. Another advantage is the reduced reflection, often desirable from a navigational point of view. The same positive effects can be obtained by placing a mound of armour units in front of the wall, Fig.3-c2. This solution is suitable mainly in shallow water wave situations for combatting frequent high loads from breaking waves. It is a common structure in Japan where the armour units are called wave dissipation blocks. It is sometimes referred to as the Japanese type breakwater.

If sea bed is formed of clay, it must be removed before the foundation is built, Fig.3-d2. The skirt type is similar to the foundation method applied for the offshore reinforced concrete gravity structure in the North Sea in the water depth of $70-150$ meters, Fig.3-d3.

In the case of deep water an economical design often consists of caissons placed on a rubble mound foundation, Fig.3-e. This type is now referred to as a composite breakwater although this name was originally related to the functional circumstances where waves are reflected from the vertical face at high water and break on the rubble slope at low water. However, this idealized functional description is not realistic because the slope will increase the wave breaking and thereby the loads on the vertical wall.

The shape of caisson can be cylindrical or rectangular. The maximum horizontal wave force on the cylindrical caisson is only about half of that on the rectangular caisson, because the ventilated shock pressure does not occur with the cylindrical caisson.

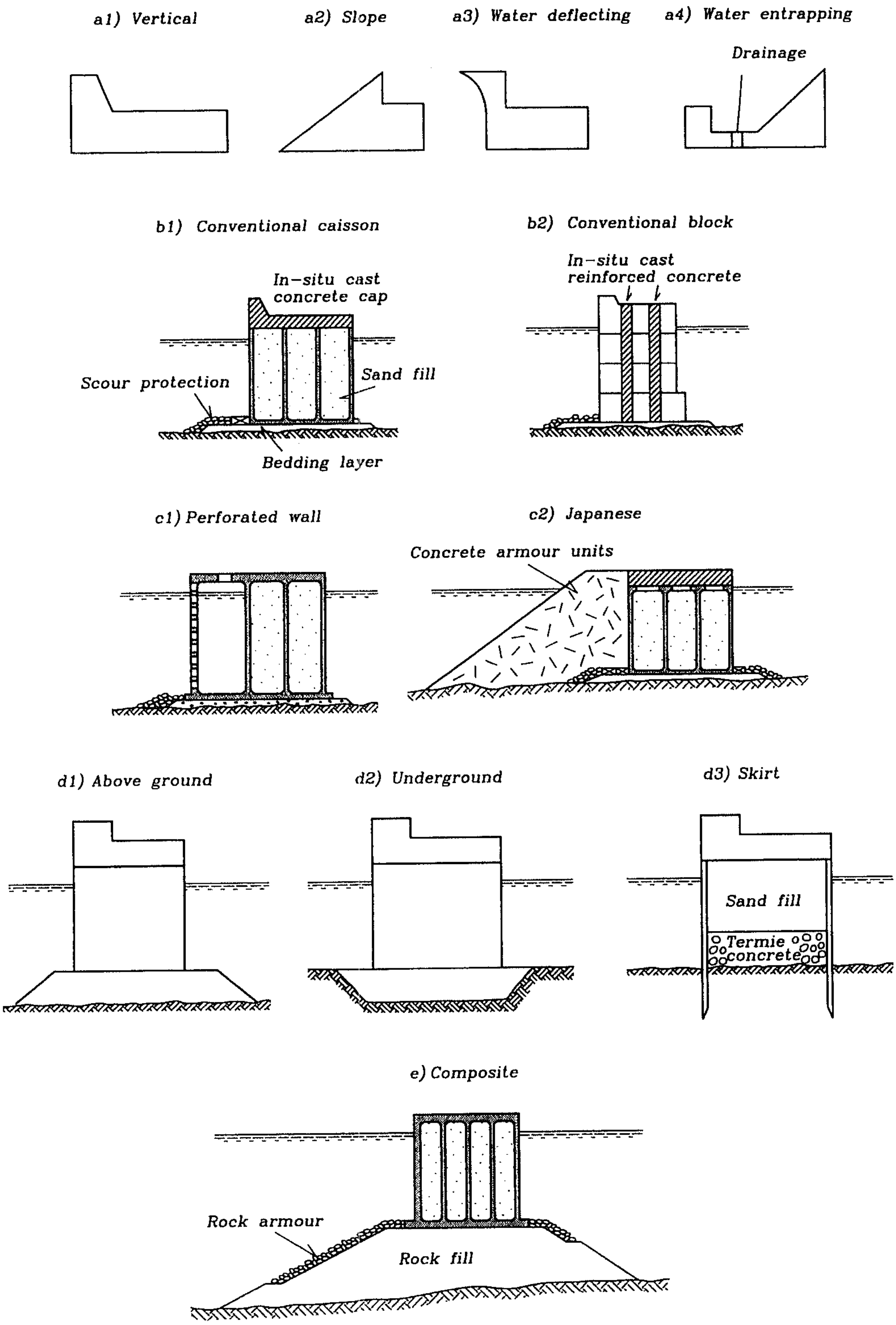

Fig.3. Various kinds of vertical breakwater cross sections.

4.2 Construction of vertical breakwaters

The construction of vertical breakwaters start from the land side. The construction procedure is

1) Production and transport of caissons.

   Design and production of caissons cannot be started before it is known how to transport the caissons from the production site to the breakwater.

   With respect to transport there are two types of caissons

   i) Non-floating caissons. Such caissons are normally rather small because they have to be transported by a crane.

      Non-floating caissons have the advantage of accurate and easy placement. Moreover, the placement can take place in a worse wave conditions than floating caissons.

      Non-floating caissons are produced on land, transported by trucks and placed by a crane standing at the temporary end of the breakwater.

   ii) Floating caissons. Floating caissons are towed from the production site to the construction site.

      Floating caissons are produced in an easy-launching place, such as in docks, on slipway, on platforms or on pontoons.

      As far as the construction time is involved, it is of importance that the average rate of production of caissons equals the average rate of placement. In most cases, the bottle-neck is the placement of caissons and subsequent armour blocks for the foundation, because both operation require good weather conditions.

      Because floating caissons are very large, slip forms can be applied. If one set of slip forms is used for the production of all caissons, the rate of the production is greatly influenced by the strength of concrete required when the form is removed. Sometimes, caissons are stored afloat in a basin for further concrete curing.

2) Preparation of caisson foundation.

   Caissons are sitting either on the filter layer or on the core of the foundation.

   Foundation materials are dumped either from barges or from the breakwater. However, the final supply of materials and the elevation of the foundation top must be controlled by divers, who build two horizontal guide rails at the designed elevation of the foundation, and follow a beam setting on and moving along the rails.

   It is customary to advance the foundation 10 to 30 meters further than the caisson to be placed in order to avoid erosion around the temporary end of the breakwater (scouring). If temporary scour protection is needed, the contractors must be prepared to place and remove such protection for each caisson, subsequent to the weather forecast information.

3) Placement of caissons.

A floating caisson is sunk by filling it with water. During the sinking process, the near end of the caisson must be held tight against the preceding one, and the far end moored.

If the caisson is not in the correct position when it reaches the sea bed, the water must be pumped out and the procedure repeated.

When the caisson is in its right position on the foundation, its compartments are filled with sands or gravels, and the armour blocks are placed by a crane.

The small caisson lowered from a crane can be sunk directly by filling sands and gravels.

4) Superstructure.

Superstructure is either cast in-situ or prefabricated together with caisson in the yard.

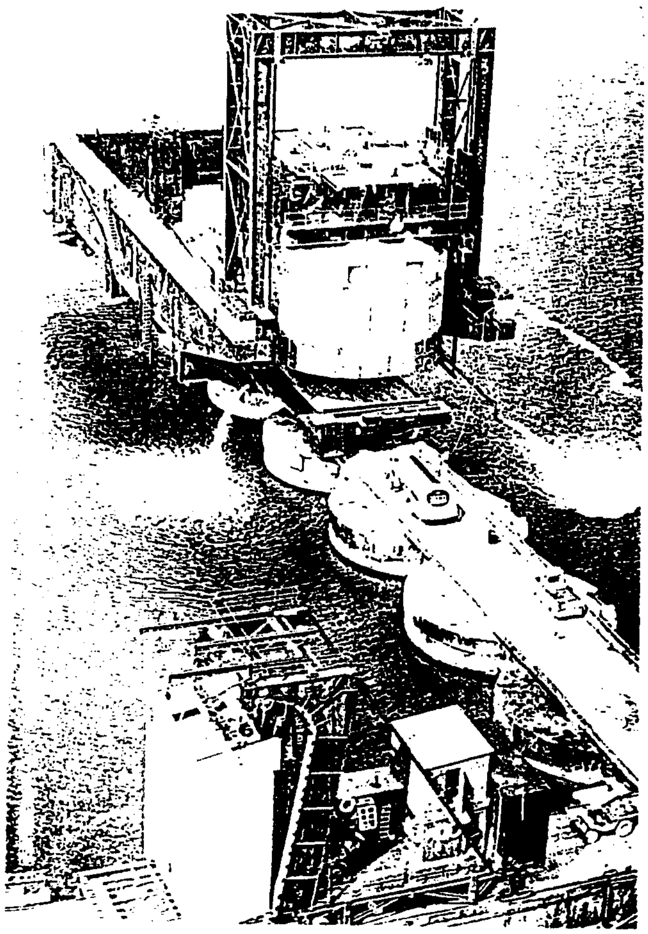

Fig.4. Placement of cylindrical reinforced concrete caissons by crane at Hanstholm. Weight: 800 *t, diameter:* 12.5 *m, height:* 12 *m, wall thickness:* 25 *cm. (Agerschou, et al. 1983)*

4.3 Wave-structure interaction

4.3.1 Wave reflection

Vertical breakwaters reflect large proportion of the incident wave energy. The interaction of incident and reflected waves can create a very confused sea with very steep and often breaking waves. It is a well known problem in many harbour entrance areas where it can cause considerable manoeuvring problems to smaller vessels. A strong reflection also increases the sea bed erosion potential in front of the structure (scour). Moreover, waves reflected from breakwaters can in some cases create or increase erosion of neighbour beaches.

The reflection can be quantified by the reflection coefficient

$$C_r = H_{s,r}/H_s \tag{1}$$

where H_s significant wave height of incident wave
$H_{s,r}$ significant wave heights of incident wave

C_r ranges typically between 0.9 and 1.0.

4.3.2 Wave overtopping

There is not much study on wave run-up. It seems that researchers are more interested in overtopping, because the harbour side of vertical breakwaters serves often as a berth. Large volume of overtopping causes also big wave agitation behind the breakwaters.

Wave overtopping is often represented by $\overline{Q}$, the average volume of water overtopping the crest of the breakwater per second per meter length of the breakwater. Like the case in rubble mound breakwater, the dimensionless overtopping is written as

$$\frac{\overline{Q}}{(g\,H_s^3)^{1/2}} = a\,exp\left(-b\,\frac{R}{H_s}\right) \tag{2}$$

where R is the free board of the breakwater, i.e. the vertical distance between SWL and the top elevation of the structure. a and b are empirical coefficients accounting geometries of the structure.

For the simple case of a plain vertical wall, $a = 0.19$ and $b = 4.2$.

4.3.3 Scour in front of vertical breakwaters

Due to the high reflective properties of vertical breakwaters, sea bed scour may constitute an importance source of damage, cf. Fig.5.

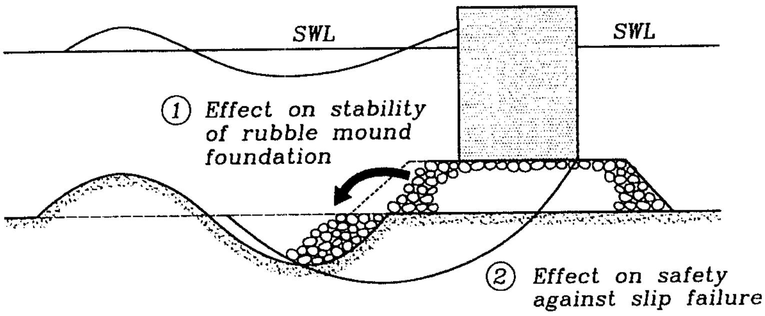

Fig.5. Effect of scour on stability of breakwaters.

One of the fundamentals for the scour of sea bed is that there are two distinct scour patterns under regular standing wave action in front of vertical structures,cf. Fig.6, namely

- A scour pattern for relatively find sand. The scour holes are located beneath the nodes of the standing wave while the ridges occur at the antinodes. The majority of sands is transported as suspended load.
- A scour pattern for relatively coarse sand. The ridges are beneath the nodes while the holes are located about half way between the nodes and antinodes. The majority of sands is transported as bed load.

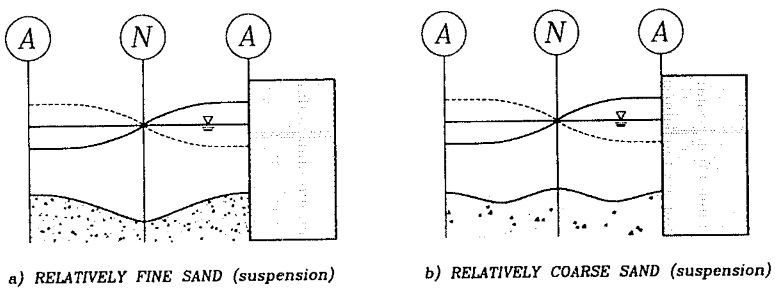

Fig.6. Scour pattern under regular standing wave.

4.3.4 Wave forces

It is a traditional approach in wave pressure calculation to classify the wave in front of caisson into standing wave and breaking wave, because the pressure of the breaking wave is much larger than that of the standing wave.

Sainflou developed the pressure formula of standing wave simplified from the trochoidal wave theory, Fig.7.

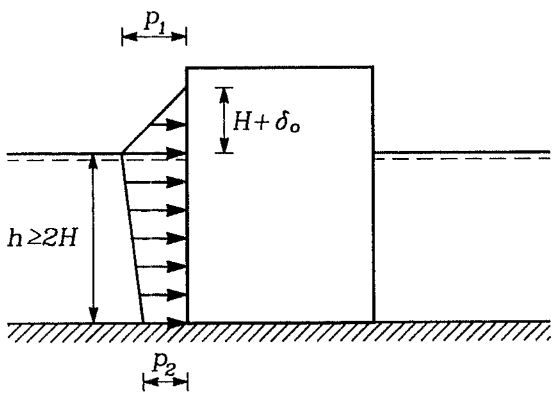

Fig. 7. Pressure distribution of standing wave by Sainflou.

$$p_1 = \frac{(p_2 + \rho_w g h)(H + \delta_0)}{h + H + \delta_0} \tag{3}$$

$$p_2 = \frac{\rho_w g H}{\cosh(\frac{2\pi h}{L})} \tag{4}$$

$$\delta_0 = \frac{\pi H^2}{L} \coth(\frac{2\pi h}{L}) \tag{5}$$

Horoi assume a uniform distribution of breaking wave pressure,cf. Fig.8.

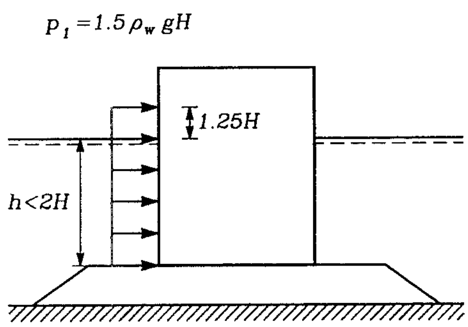

Fig. 8. Pressure distribution of breaking wave by Horoi.

Minikin proposed the following breaking wave pressure formula which consists of dynamic part p_d and hydrostatic part p_s.

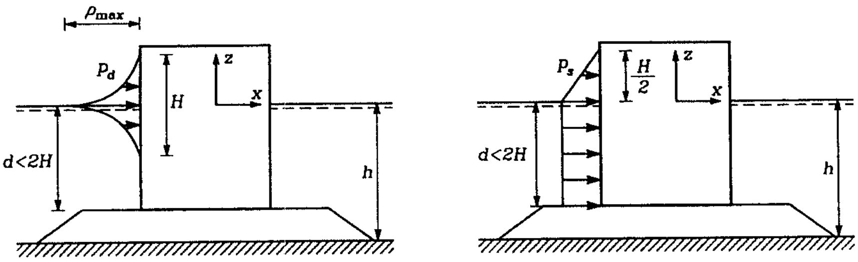

Fig.9. Pressure distribution of breaking wave by Minikin.

$$
\begin{aligned}
p_{max} &= 101\ \rho_w\ g\ d\left(1\ +\ \tfrac{d}{h}\right)\ \tfrac{H}{L} \\
p_d &= \left(1\ -\ 2\ \tfrac{|z|}{H}\right)^2\ p_{max} \qquad |\ z\ | \leq\ \tfrac{H}{2} \\
p_s &= \begin{cases} 0.5\ \rho\ g\ H\ (1\ -\ 2\ \tfrac{z}{H}) & 0 \leq z < \tfrac{H}{2} \\ 0.5\ \rho\ g\ H & z < 0 \end{cases}
\end{aligned}
\tag{6}
$$

The above wave pressure formulae were developed for regular waves. L is the wave length in front of vertical structure. With irregular waves the characteristic wave height and wave length, such as H_s, $H_{1/10}$, or $H_{1\%}$, L_p, or L_m are used in stead of H and L.

Based on the model tests, a universal formula for wave pressure on caissons was developed by Goda. Fig.10 shows the related definition sketch for the wave induced pressure under a wave crest.

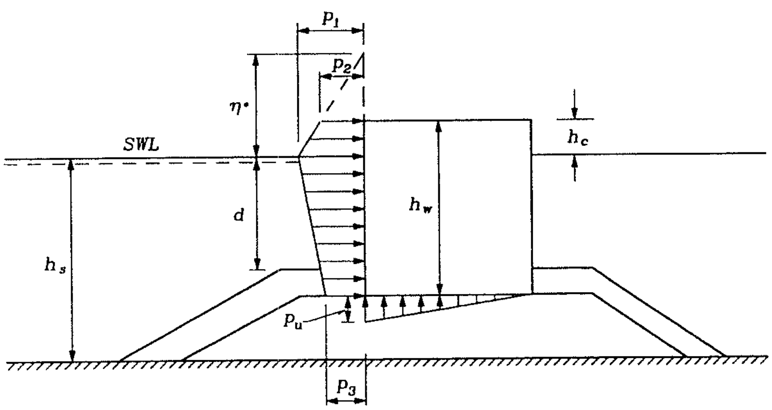

Fig.10. Universal wave pressure distribution by Goda.

$$
\begin{aligned}
\eta^* &= 0.75(1+\cos\beta)\,H_{max} && (7)\\
p_1 &= 0.5(1+\cos\beta)(\alpha_1+\alpha_2\cos^2\beta)\,\rho_w\,g\,H_{max} && (8)\\
p_2 &= \begin{cases} \left(1-\frac{h_c}{\eta^*}\right)p_1 & \text{for } \eta^* > h_c \\ 0 & \text{for } \eta^* \le h_c \end{cases} && (9)\\
p_3 &= \alpha_3\,p_1 && (10)\\
\alpha_1 &= 0.6+\frac{1}{2}\left[\frac{4\pi\,h_s/L_p}{\sinh\,(4\pi\,h_s/L_p)}\right]^2 && (11)\\
\alpha_2 &= \text{the smaller of } \frac{h_b-d}{3\,h_b}\left(\frac{H_{max}}{d}\right)^2 \text{ and } \frac{2d}{H_{max}} && (12)\\
\alpha_3 &= 1-\frac{h_w-h_c}{h_s}\left[1-\frac{1}{\cosh\,(2\pi\,h_s/L_p)}\right] && (13)
\end{aligned}
$$

where

β angle of incidence of waves (angle between wave crest and front of structure, 0^0 is perpendicular wave)

H_{max} maximum wave height.

$$
H_{max} = \begin{cases} 1.8\,H_s & \text{if the structure is outside surf zone} \\ H'_{max} & \text{if the structure is inside surf zone} \end{cases}
$$

H'_{max} The highest of the random breaking waves at a distance $5H_s$ seaward of the structure.

h_b water depth at a distance of $5H_s$ seaward of the break-water front wall.

L_p Deep water wave length corresponding to peak wave period.

Although the wave induced uplift pressure, p_u, at the front edge of the base plate is equal to p_3 it is suggested by Goda to use a somewhat reduced value

$$
p_u = \frac{1}{2}\,(1+\cos\beta)\;\alpha_1\,\alpha_3\,\rho_w\,g\,H_{max} \tag{14}
$$

This is because analyses of the behaviour of Japanese breakwaters revealed that the use of $p_u = p_3$ together with an assumed triangular distribution of the uplift pressure gave too conservative results.

The breakwater geometry is of paramount importance for the wave pressure. Fig.11 is an example with a high foundation. Many of the waves become plunging breakers. When a plunger hits the vertical face like a hammer head, the horizontal pressure on the vertical face is formed of two parts, namely hammer shock which depends on the velocity of the hammer head, and the compression shock which is due to the air pocket enclosed and compressed by the plunging breaker.

In most cases the sea bed has a gentle slope and the vertical breakwater has a low foundation. The type of wave breaking is surging. The entrapped air is ventilated upwards. The ventilated shock pressure is relatively small.

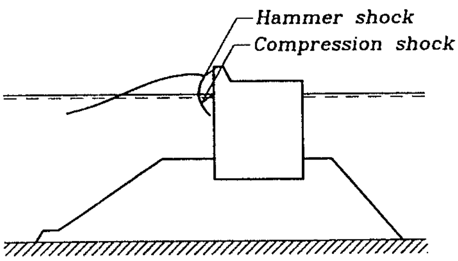

Fig.11. Types of shock pressure.

The coefficient α_2 of the Goda formula is replaced by α^* in order to include the shock pressure. α^* reaches a maximum of 2 when $\frac{B_M}{L} = 0.12$, $\frac{d}{h} = 0.4$ and $\frac{H_s}{d} = 2$.

$$\alpha^* = \text{the bigger of } \alpha_2 \text{ and } \alpha_I$$

$$\alpha_I = \alpha_{I0}\alpha_{I1}$$

$$\alpha_{I0} = \begin{cases} \frac{H_s}{d} & \text{if } H_s \le 2d \\ 2 & \text{if } H_s > 2d \end{cases}$$

$$\alpha_{I1} = \begin{cases} \frac{\cos\delta_2}{\cosh\delta_1} & \text{if } \delta_2 \le 0 \\ \left(\frac{1}{\cosh\delta_1 \cosh\delta_2}\right)^{1/2} & \text{if } \delta_2 > 0 \end{cases}$$

$$\delta_1 = \begin{cases} 20\,\delta_{11} & \text{if } \delta_{11} \le 0 \\ 15\,\delta_{11} & \text{if } \delta_{11} > 0 \end{cases}$$

$$\delta_2 = \begin{cases} 4.9\,\delta_{22} & \text{if } \delta_{22} \le 0 \\ 3\,\delta_{22} & \text{if } \delta_{22} > 0 \end{cases}$$

$$\delta_{11} = 0.93\left(\frac{B_M}{L} - 0.12\right) + 0.36\left(\frac{h-d}{h-0.6}\right)$$

$$\delta_{22} = 0.36\left(\frac{B_M}{L} - 0.12\right) + 0.93\left(\frac{h-d}{h-0.6}\right)$$

4.4 Structural design of vertical breakwaters

4.4.1 Failure modes of vertical breakwaters

Failure modes of vertical breakwaters are depicted in Fig.12. The figure indicates a distinction between failure modes related to the overall stability of the vertical structure and failure modes related to the integrity of the structural parts.

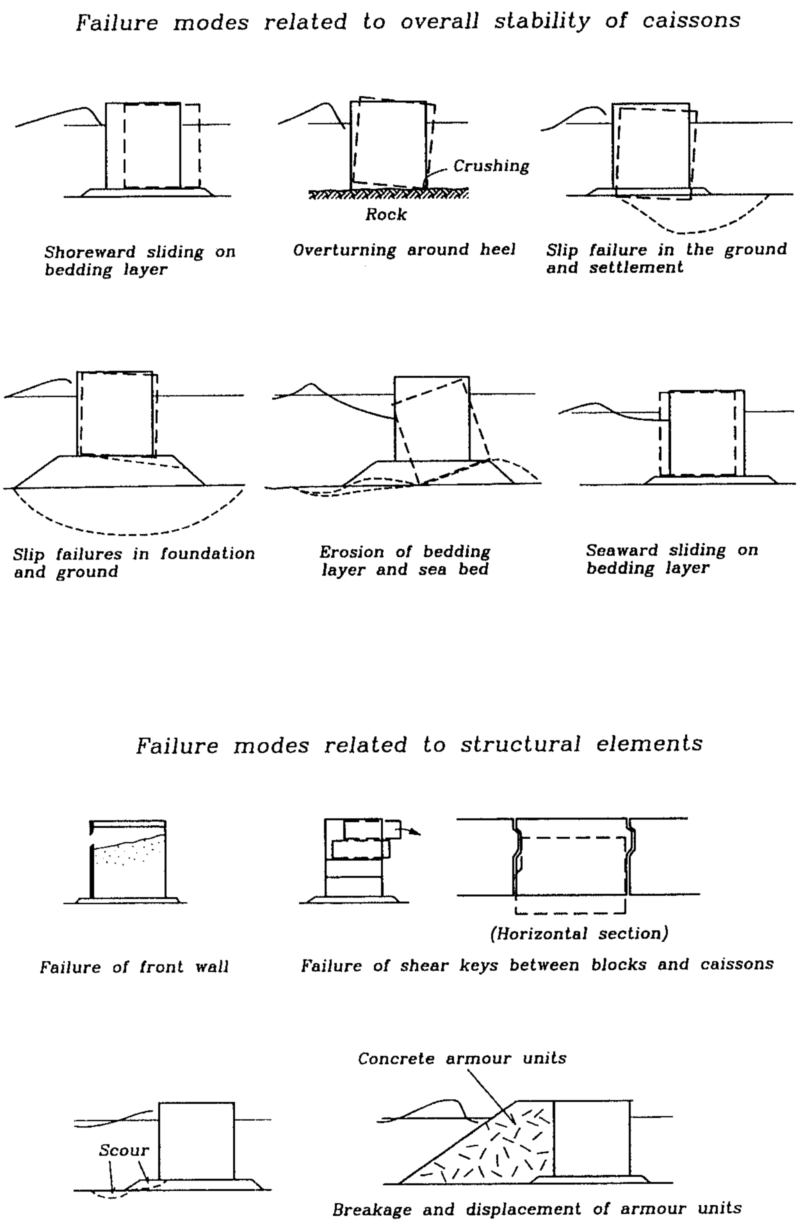

Fig.12 Failure modes of vertical breakwaters (Burcharth, 1993).

4.4.2 Overall stability of vertical structures

The stability of vertical structures relies heavily on the net its net weight, F_g, which is the weight of the structure minus the buoyancy, cf Fig.13.

F_f is the horizontal wave pressure on the front of vertical structure and F_b is the uplift force on the bottom of vertical structure. They are calculated by Goda formula. The horizontal wave pressure on the rear side can be taken as the hydrostatic difference between the mean water level and the wave trough. It is not taken into consideration.

The stability against sliding is expressed as

$$F_f \leq \mu (F_g - F_b) \tag{15}$$

where μ is the friction coefficient between the caisson and the foundation. The value of μ is usually taken as 0.6.

The *stability against overturning* around the heel of the caisson is expressed as

$$F_f \ a + F_b \ b \leq F_g \ c \tag{16}$$

It is recommended to apply a safety factor of not less than 1.2 against sliding and overturning.

The first step in the assessment of the bearing capacity of the foundation is to calculate the magnitude, position and direction of the resultant force on the foundation. The soil mechanics methods of analysing the bearing capacity of a foundation when exposed to eccentric inclined loads are then applied, i.e. slip failure analyses or bearing capacity diagrams.

Overturning of a caisson implies very high stresses at the point of rotation. In order to avoid the crush of the stones and caisson around the heel the bearing capacity of the stone around the heel should not be exceeded. As a first estimate of the allowable pressure under the heel values in the range $0.4 - 0.6$ MN/m^2 might be used, according to Japanese practice.

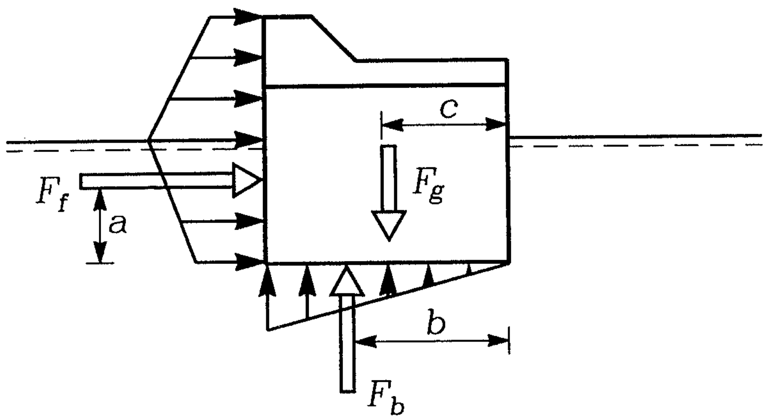

Fig.13. Forces acting on vertical structure.

4.4.3 Rubble mound foundation

It is best to set the height of the rubble mound foundation as low as possible to prevent impulsive wave pressure. However, for the foundation to fulfil the function as a buffer between the caisson and the sea bed, the height of the foundation should be at least 1.5 meter. Moreover, the top of the foundation should bot be very deep under water in order to facilitate diver's underwater operations. Besides, the height of the foundation depends on the availability of armour blocks and the limited height of caissons set by manufacture ability.

The berm in front of caissons provides protection against possible scouring of sea bed. But a wider berm increases cost and may cause impulsive wave pressure on the caisson. The berm at the rear side has the function of transmitting the vertical load to the sea bed. It also provides an allowance of the caisson sliding. The practical berm width ranges 5 to 10 meters.

The slope of the rubble mound foundation is usually 1:2 or 1:3 for the seaward side and 1:1.5 or 1:2 for the harbour side.

The minimum weight of armour units for the rubble mound foundation is calculated by Hudson formula

$$M = \frac{\rho_a H_{1/3}^3}{K_D^3 \left(\frac{\rho_a}{\rho_w} - 1 \right)^3}$$

$$K_D = \begin{cases} 1.8 & \text{if} \quad C \leq 1.8 \\ C & \text{if} \quad C \geq 1.8 \end{cases}$$

where C $\quad C = 1.3 \frac{1-k}{k^{1/3}} \frac{h'}{H_s} + 1.8 exp \left(-1.5 \frac{(1-k)^2}{k^{1/3}} \frac{h'}{H_s} \right)$

k $\quad k = \frac{\frac{4\pi h'}{L}}{\sinh(\frac{4\pi h'}{L})} \sin^2 \left(\frac{2\pi B_M}{L'} \right)$

h' Water depth over the berm

B_M Berm width

H_s Design significant wave height

L Wave length at deep water

L' wave length at the water depth of h'

4.4.4 Superstructure and caisson

The elevation of the top of the superstructure depends on the allowable overtopping. In practice it ranges from 0.6 H_s to 1.25 H_s above SWL.

The elevation of the bottom of the superstructure should be a little above SWL in order to assure not too much disturbance on the construction of the superstructure by waves.

The thickness of the parapet wall is required by the integrity of the parapet wall. The Japanese Standard demands the minimum thickness of 0.5 meter.

The height of the caisson is the elevation of the bottom of the parapet wall minus the elevation of the top of the foundation. The width of the caisson is assumed to be 2/3 of the height and should be checked with the overall stability of the caisson. The length of the caisson depends on the barge and crane ability for floating and non-floating caissons respectively, usually in the range of 0.5 – 2.0 times of the width.

The maximum dimension of the inner cells is usually designed to be less than 5 meters. Correspondingly the thickness of the outer walls and the partition walls are 40 – 50 and 20 – 25 cm respectively. The thickness of the bottom slab is normally 50 – 70 cm. The thickness of the footings is the same as the bottom slab. the length of the bottom slab is $\frac{1}{10} - \frac{1}{5}$ of the width of the cells.

All thickness should be checked for structural integrity.

The thickness of the covering of the reinforcements for outer walls, partition walls and bottom slab should not be less than

$$\begin{cases} 7 \text{ cm} & \text{Sea side} \\ 5 \text{ cm} & \text{Inside and land side} \end{cases}$$

Besides, the stability during transport of floating caissons should be checked.

$$\overline{GM} \geq 20 \text{ cm} \tag{17}$$

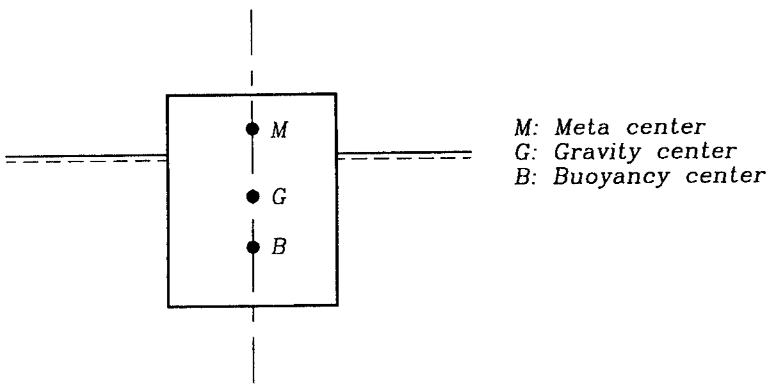

Fig.14. Floating stability of caisson.

4.5 Example of a caisson failure

Anything, which might go wrong, will go wrong - *Marfian's Law*

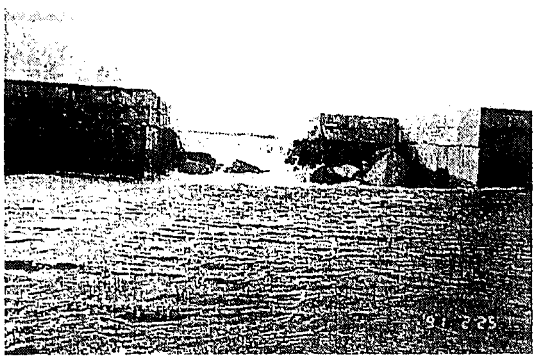

(From the Sea Side)

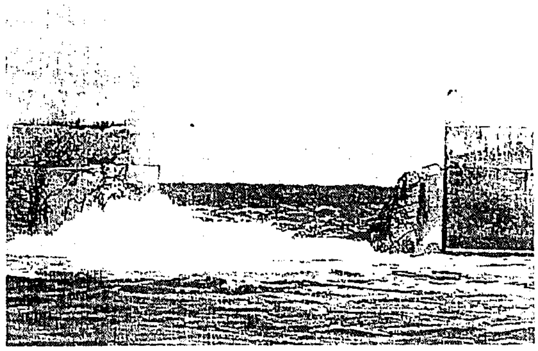

(From the Harbor Side)

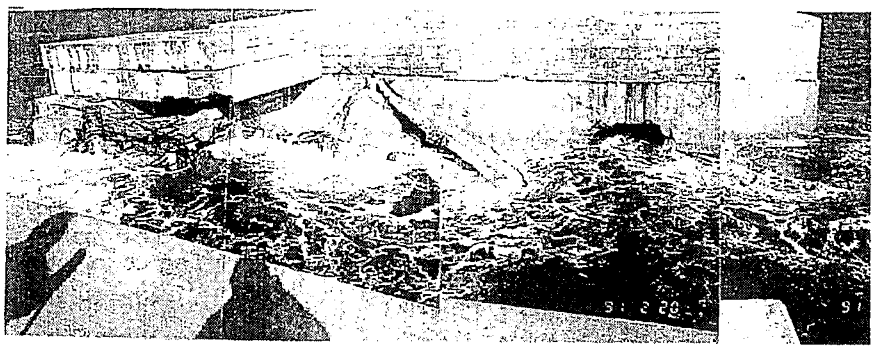

(To the No. 8 Caisson)

Failure of caisson breakwater at mutsu-Ogawara port, Japan.

Breakage and erosion of wave dissipating blocks Sliding of caisson.

Wave dissipating blocks are 50 t Tetrapods.

Caisson weight: 3660 *t* *Dimension* $24 \times 21 \times 15.5\ m$ *(width × length × height). (Hitachi, 1994)*

5 Berth structures

5.1 Introduction

5.1.1 Types of berth structure

The purpose of a berth structure is mainly to provide a vertical front where ships can be moored for loading and unloading operation.

Berth structures can be classified into 3 types with respect to their arrangement relative to the shore line.

Quay or wharf	:	parallel to the shore line
Pier or jetty	:	perpendicular or oblique to the shore line
Dolphine	:	isolated on open sea for mooring ships

On the other hand, according to the structure itself, berth structures can be classified into (cf.Fig.1)

$$\text{Quay}\left\{\begin{array}{l} \text{Gravity}\left\{\begin{array}{l}\text{Block wall}\\ \text{Caisson}\\ \text{Cells}\end{array}\right. \\ \text{Sheet pile quay} \\ \text{Open piled quay}\end{array}\right. \qquad \text{Pier}\left\{\begin{array}{l} \text{Gravity}\left\{\begin{array}{l}\text{Block wall}\\ \text{Caisson}\end{array}\right. \\ \text{Floating pier} \\ \text{Open piled pier}\end{array}\right.$$

Gravity quay and gravity piers are called gravity structure. gravity structure and sheet pile wall are also called solid structure, while open piled quay and open piled pier are called open structure.

The gravity structure resists to loading by its own weight. It is sensitive to settlement and therefore, require good soil condition.

The sheet pile wall distributes the earth pressure by bending of the sheet piles. The loads are absorbed by tie rods anchored to the slab or the batter piles and by the passive earth pressure in front of the toe of the wall. Due to the relative thin sheet piles, it cannot be applied in more than 10 meter water depth. It is often the most economical type.

In the case of the open structure, the vertical loads are carried by piles, while the horizontal loads are absorbed by the anchor or by the batter piles. It is often applied in connection with relatively deep water depth and poor soil conditions.

Open structures may be chosen rather than gravity structures, because gravity structure may develop unacceptable settlement, or because a non-reflecting structure is preferred for wave disturbance reason, or because of cost, especially if the structure is located at considerable water depth.

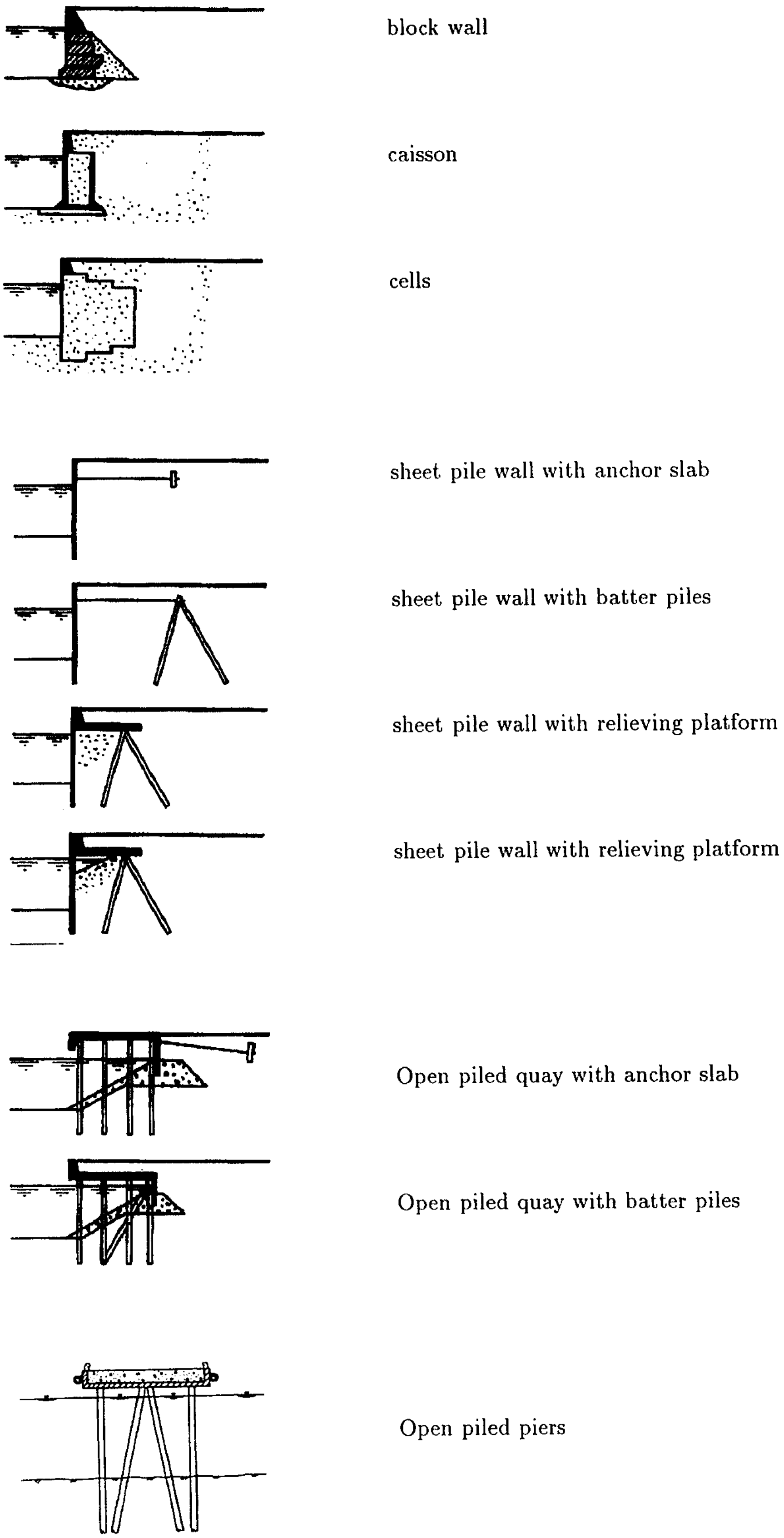

Fig.1. Types of berth structures

5.1.2 Design loads

The design loads can be classified into

- Design loads
  - from sea side
    - wind, wave, current and ice
    - ship impact during berthing
    - bollard force during mooring
  - from berth itself
    - weight of berth structure
    - dead load on berth structure (e.g. building)
    - live load on berth structure (e.g. crane)
  - from land side
    - dead load of filling
    - dead and live load on filling
    - hydrostatic force due to water level difference

The various loads acting on the berth structure should not be simply added together. Rather, they should be combined with regard to their probability of occurrence.

Wave force on berth structure is usually not considered since the most berth structures are sheltered against severe wave actions. With respect to the open piled structure, where the horizontal wave force on piles may be of importance, reference is made to Sarpakaya et al. (1981).

The study of forces acting on the berth structure due to formation of ice in the harbour basin has so far not been given high priority. However, when quays, dolphines, bridge pillars are surrounded by solid ice or exposed to drift ice, one must take into consideration that both horizontal and vertical ice forces can be of importance (Wortley 1984).

Geotechnical books should be referred for the calculation of the active and passive soil pressure from filling, as well as the bearing capacity of piles.

5.1.3 Factors affecting the choice of the type of berth structures

1 Soil conditions

The fact that the soil conditions can vary very much from one site to another led to the development of a wide spectrum of types of berth structures. For example, is the soil is loose and has a low bearing capacity, open piled structure should be applied because the piles can be driven down to rocks or other sufficiently firm stratum.

2 Water depth

When the structure is located in shallow water or even on land, i.e. dredging of the harbour basin is necessary, sheet pile walls, which can be constructed through the existing soils, is likely to be very competitive. When the existing water depth is close to the desired one, open piled structure may be more competitive.

3 Wave action

Open piled structures are normally more favorable than solid ones with respect to the reflection of the incoming waves.

4 Resistance to loads

Berth structures should be designed to resist the vertical loads by dead loads and live loads, as well as the horizontal loads from ship impacts, wind, filling behind the structure, etc. In general the gravity structures are considered more resistant to loadings than the open piled structures, both vertically and horizontally.

5 Materials

A berth structure can be constructed out of timber, steel and concrete or a combination of these materials. The general choice of the construction materials will depend on the purpose of the structure and economical reasons.

6 Underwater work

Underwater construction should be avoided as much as possible. In this respect the sheet pile walls and open piled structure are ideal.

5.2 Gravity berth structures

The gravity structures resist to loading by its own weight. It is sensitive to settlements and therefore, require reasonably good soil conditions.

5.2.1 Components of gravity berth structures

Gravity berth structures consist of vertical structures (superstructure + substructure), foundation and back fill, cf. Fig.2. The function of each component and the construction procedure are almost the same as those of vertical breakwaters, except for the back fill.

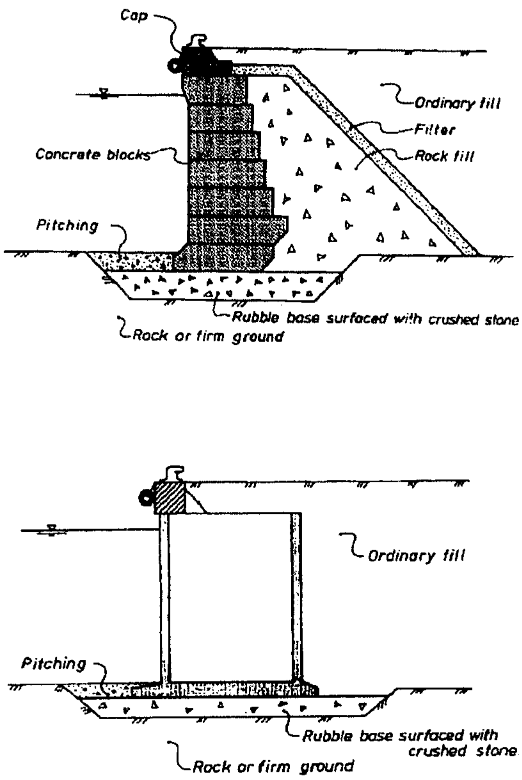

Fig.2. Components of gravity berth structures

5.2.2 Back fill

It is preferable to use quarry stones as back fill because

1 It has a relatively high internal friction angle and hence, low active earth pressure on the structures.

2 It has a relatively high porosity, which reduces water pressure on the vertical structure due to the water level difference between the front side and the back side of the structure.

3 It will not be easily washed away through the gaps between the concrete blocks or between caissons.

There should be filter between the rock fill and the ordinary fill, cf. Fig.2.

In the caisson quay o ordinary fill can be applied directly if special measures have been taken to prevent the back fill from being washed out through the gaps of caissons, cf.Fig.3. The gaps are designed to overcome the uneven settlement.

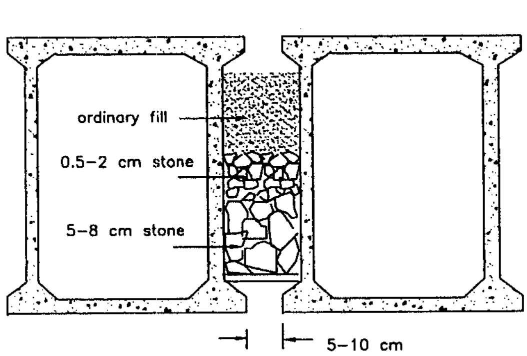

Fig.3. Connection between caissons.

In the case of concrete blocks, a relieving block is often applied in order to reduce the earth pressure from the back fill, cf.Fig.4.

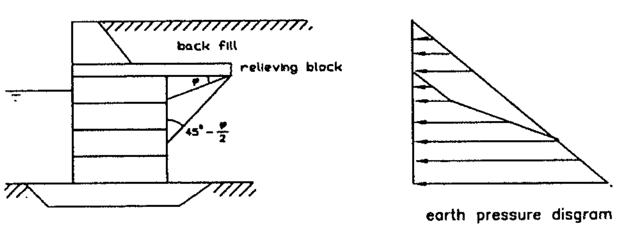

Fig.4. Relieving block and earth pressure diagram.

5.2.3 New type of gravity berth structures

Instead of using concrete blocks and caissons, reinforced concrete retaining wall has been developed recently. These L-blocks have been constructed in the same way as caissons, cf. Fig.5. But they are transported to and installed at the berth site by cranes. The length of the block varies between 3 to 12 meters, depending on the crane ability, which is 100 tons for mobile cranes and 200 tons for floating port cranes.

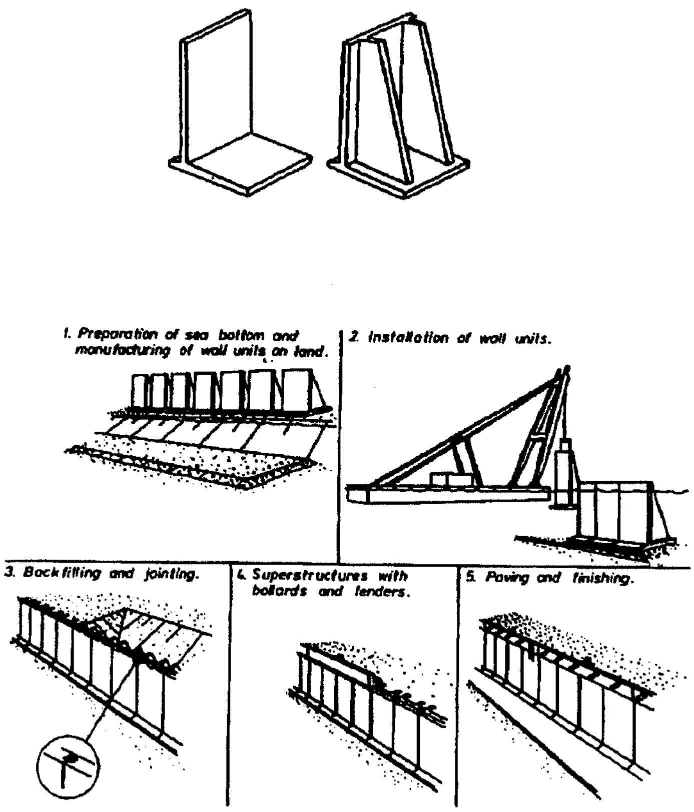

Fig.5. Construction of L-blocks quay (Thorsen, 1988).

Another alternative is steel sheet pile cells. Circular main cells connected with arched cells are the most popular form, cf. Fig.6.

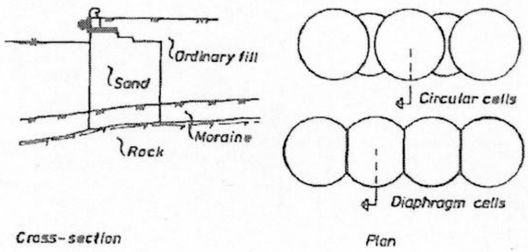

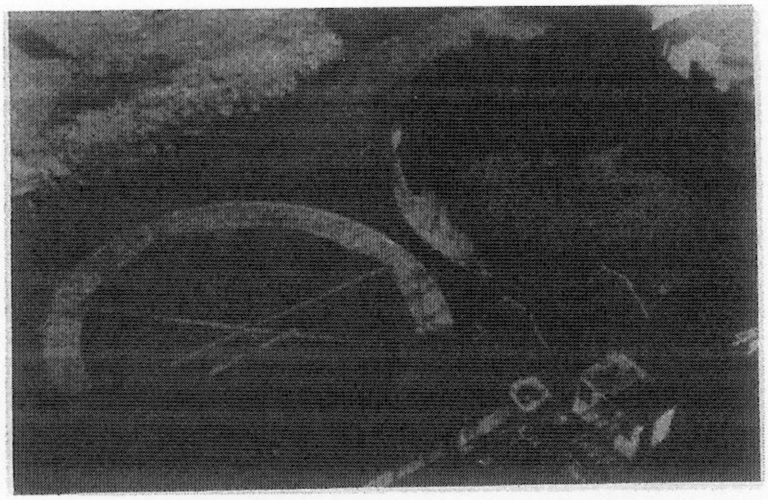

Fig.6. Construction of cell quay (Thorsen, 1988).

5.3 Sheet pile walls

In earlier times the materials of sheet piles were wood and reinforced concrete, but today steel sheet piles are mostly used.

5.3.1 Components and connection

Fig.7 is a typical cross section of sheet pile walls. In the case of shallow water and good soil conditions, the sheet piles may be driven deep enough to act as a cantilever and the tie rod support becomes unnecessary.

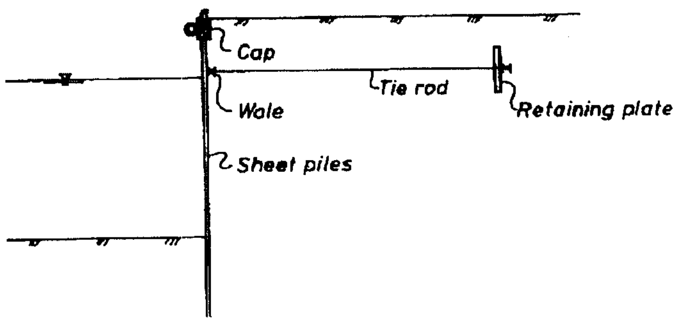

Fig.7. Sheet pile walls.

There are various connection patterns between sheet piles, cf. Fig.8. The locks are sand tight, which means that the ordinary back fill can be applied.

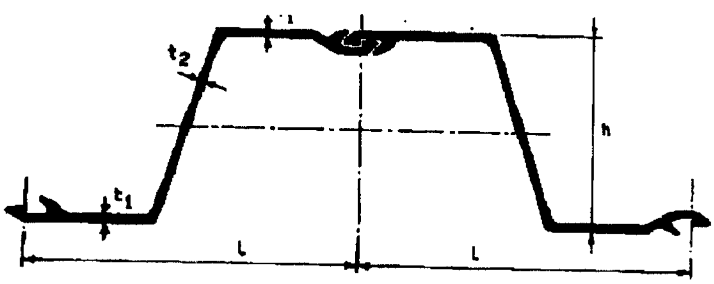

Fig.8. One of various steel sheet pile connections.

5.3.2 Forces acting on sheet pile wall

The friction between the soil and the sheet pile is an uncertain factor due to possible loose contact. Moreover, friction force is acting on the safe side. Therefore, it is often omitted n the design.

Fig.9 shows the forces and the bending moment diagram of the sheet pile, where

B	Bollard force. Often only the horizontal bollard force is considered.
I	Ship impact force. It is seldom a problem for this type of structures.
p	Live load on the apron.
E_a	Earth pressure from the back fill. E_a is usually active earth pressure and will increase with increasing live load p.
w	Hydrostatic pressure due to the water level difference.
A	Tension of the tie rod.
E_p	Earth pressure in front of the wall. E_p is the passive earth pressure and will depend on the penetration depth of the pile z.

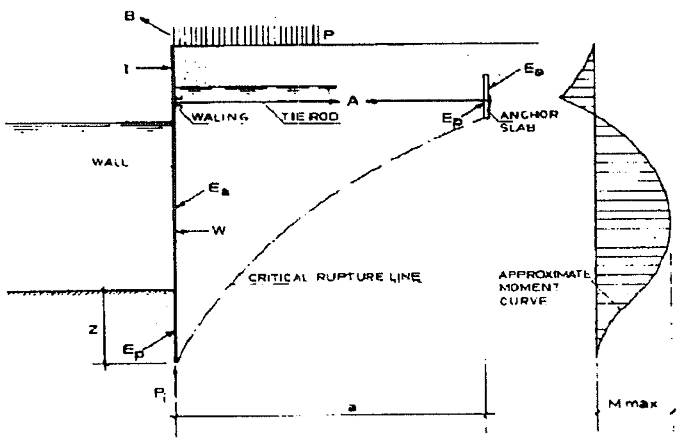

Fig.9. Forces and bending moment of sheet pile.

5.3.3 Structure design and construction procedure of sheet pile wall

By the force equilibrium analysis of the sheet pile can be obtained the necessary penetration depth z, the tension of the tie rod A which determines the diameter of the tie rod, and the bending moment diagram which decides the thickness of the sheet pile.

The tension of the tie rod is absorbed as the passive earth pressure in front of the anchor slab. The distance between the sheet pile and the anchor slab is determined as the minimum distance for which the overall stability of the structure can be obtained.

In order to reduce the maximum bending moment in the sheet pile, it is desirable to locate the anchor slab at the middle of the sheet pile. However, in practice the anchor slab is always located a little above the still water level for the convenience of construction.

Fig.10 illustrates the construction procedure of the sheet pile walls.

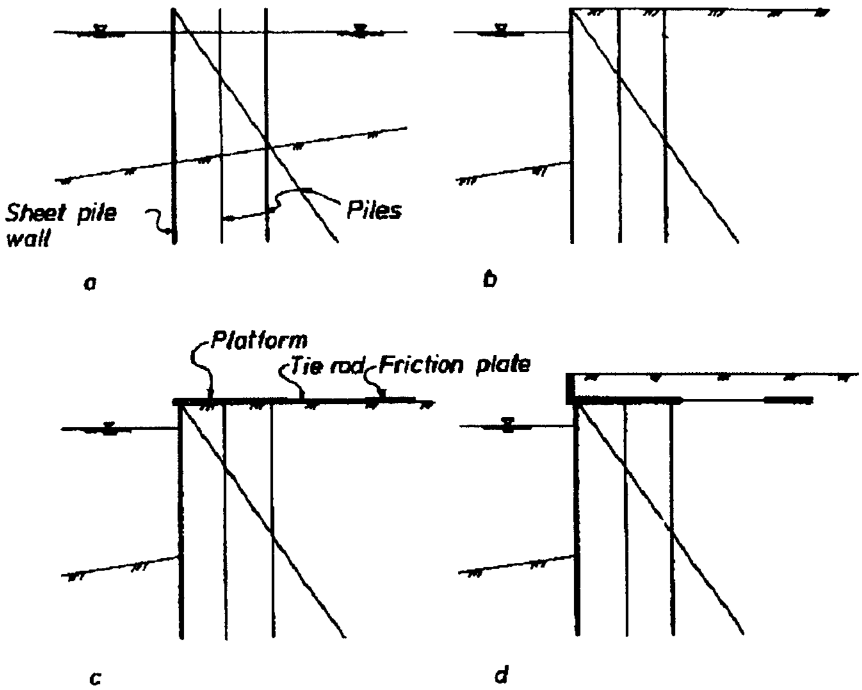

Fig.10. Construction of the sheet pile walls.

5.3.4 Other types of sheet pile walls

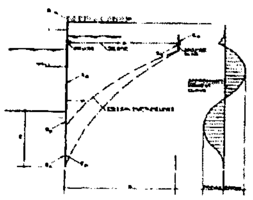

1 Fixed sheet pile wall

The sheet pile penetrates to such a depth that it is fixed in the ground. in order to reduce the maximum bending moment of the sheet pile and the tension of the tie rod.

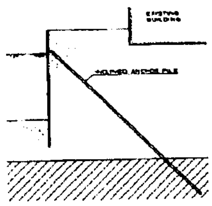

2 Batter friction pile

with good soil condition well underneath

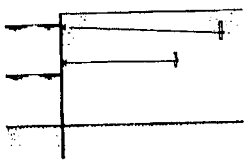

3 Double anchor slabs

suitable in the case of considerable tide range

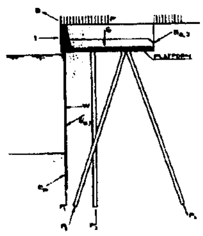

4 Relieving platform

The active soil pressure is absorbed by the batter piles

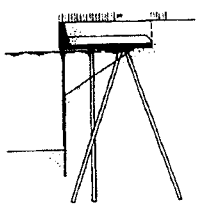

5 Relieving platform

smaller active soil pressure

Fig. 11. Other types of sheet pile walls.

5.4 Open piled quay

5.4.1 Components and principles

A typical open piled quay is composed of deck, piles, slope protection, earth retaining structure, anchor slab or batter piles, cf Figs.12 and 13.

Vertical dead and live loads are transmitted to the piles. Horizontal force from ship impacts is transmitted through the deck and absorbed as the passive earth pressure from the back fill. Mooring force and active earth pressure from the back fill are absorbed by the anchor slab.

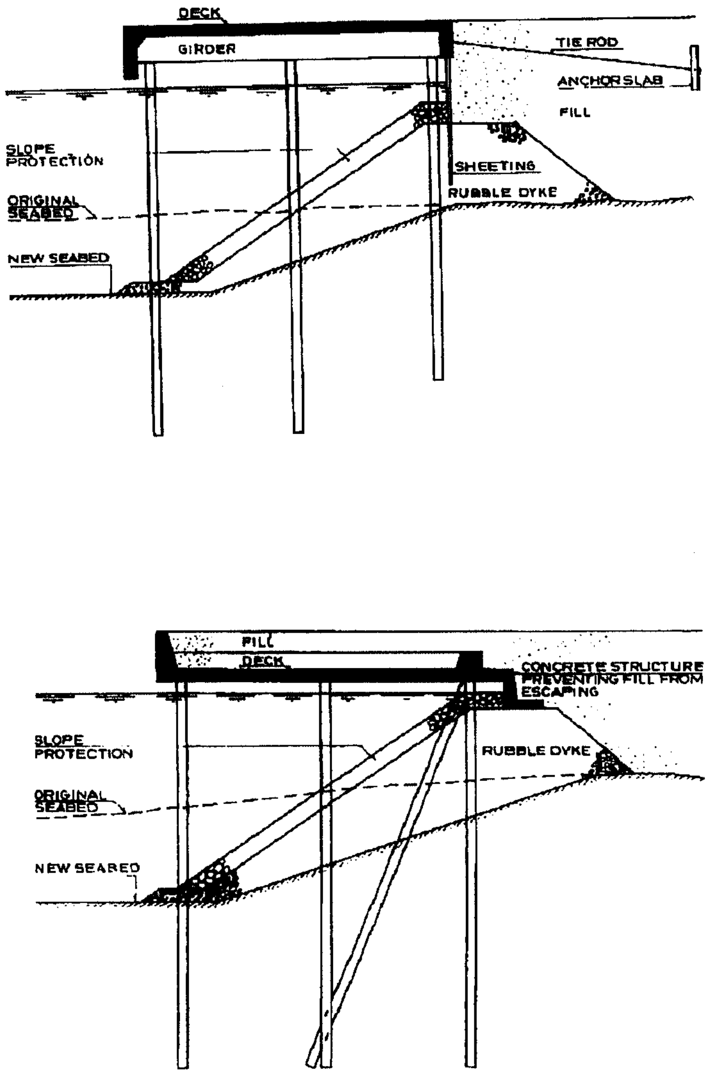

Fig.12. Open piled quay.

5.4.2 Design of open piled quay

The design water depth is the Lowest Astronomical Tide (LAT) read from the Chart Datum. Various dimensions of open piled quay shown in Fig.13 is determined as follows

- H_1 Water depth, including the maximum draft of the design ship, ship vertical movement due to winds, waves and currents, underkeel clearance, deposition of sediment and dredging techniques, cf. Fig.6 of section 1.
- H_2 Depending on the top elevation of the structure. It should be at least 0.5 meter above the Highest Observed Water Level (HOWL).
- a Should be at least 1 meter to ensure that the turbulence from ship propeller will not affect the stability of the slope, and the possible falling of the rock from the slope will not affect the berthing.
- e should be at least 2 meters to avoid the ship impact on the piles.
- b depends on the steepness of the slope, which is usually 1:1.5.
- c should be at least 1.0 - 1.5 meter.

The design of the rubble mound slope to prevent erosion is referred to Section 3 *Rubble Mound Breakwaters.* The arrangement and dimension of the piles are referred to the geotechnic books with respect to the loading conditions and the bearing capacity of the piles.

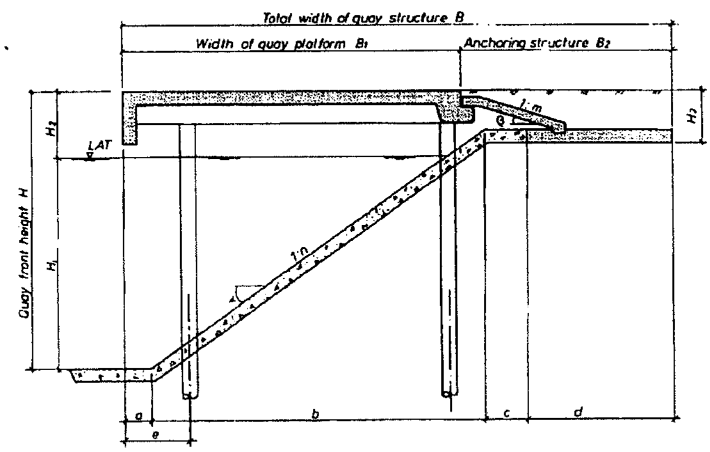

Fig.13. Dimensions of open piled quay.

5.5 Open piled pier

Piled piers may be chosen rather than gravity piers because of cost, e.g. if the pier is located at considerable water depth, gravity pier may develop unacceptable settlements, or because a non-reflecting structure is preferred for wave disturbance reason.

Piled piers consist of a deck supported on piles. Piles may be of steel, reinforced concrete or timber. The deck will normally be made of reinforced concrete, either cast in-situ or precast. It is often necessary to provide the edge of the deck with a curtain which will ensure that the small vessels will not be trapped underneath the deck at the low water level.

The static principle of a pier is illustrated in Fig.14. The vertical dead load and live load are carried by the deck and distributed to the piles. The horizontal loads from the ship impact and the mooring forces are decisive for piled piers. Depending on the number, stiffness and fixity in the ground of the piles this may be possible with vertical piles if the corresponding deflection is acceptable. More frequently, however, batter piles are used to transmit the horizontal forces.

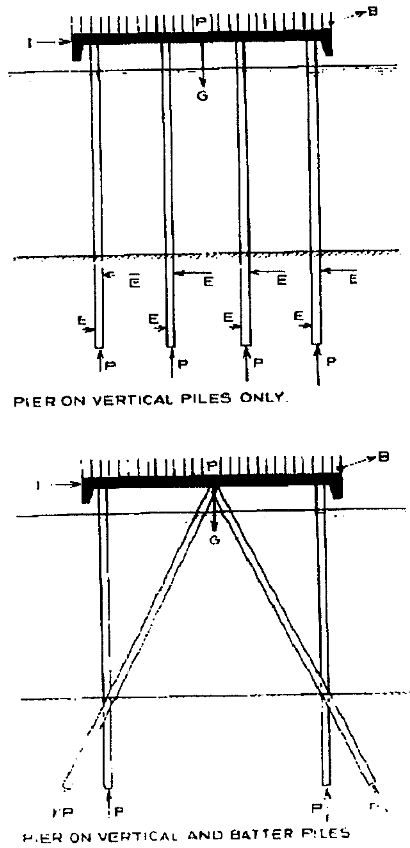

Fig.14. Open piled piers.

5.6 Fender

5.6.1 Principle and type

Fenders are installed for the following reasons:

1) To absorb berthing impact energy.

2) To prevent direct contact between vessels and quay while the vessel is moored.

The principle of the fender is to absorb the berthing energy and transmit an acceptable load to the structure. The great difference in berth structures results in different fenders. Generally, a solid quay will be able to resist a high horizontal force, while an open piled structure must have fenders which can absorb the energy and reduce the thrust to the structure.

There are numerous types of fenders. The two most popular are rubber fenders and pneumatic fenders. Rubber fenders utilize that rubber can deflect considerably under load and return to its original shape after unloading, cf. Fig.15, while in pneumatic fenders air is contained in a bag of rubber, the air pressure will increase when the bag is squeezed.

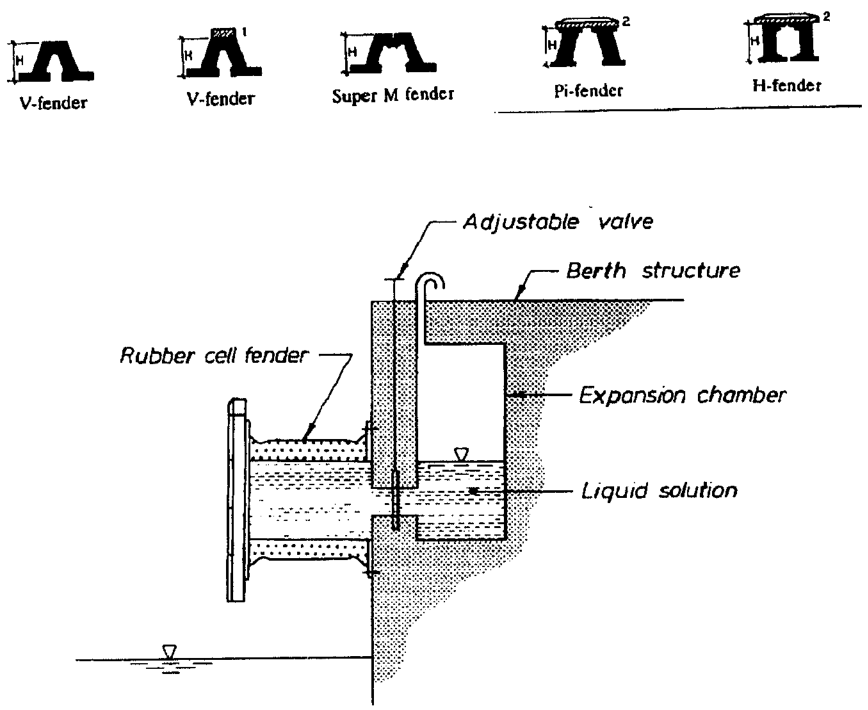

Fig.15. Rubber fenders and pneumatic fenders.

Various combination of fenders have been applied, e.g. double hollow cylindrical fenders with a panel suspended in chain, cf. Fig.16.

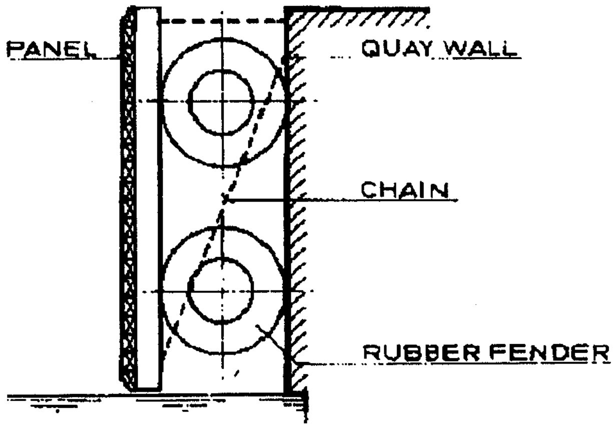

Fig.16. Hollow cylindrical fenders with a panel for increasing contact area.

5.6.2 Fender factors

The fender factor is the ratio between the force to be resisted by the berth structure and the energy to be absorbed by the fender. The ideal fender will be the one which absorbs large amount of energy and transmitted low reactive loads to the berth structure, i.e. low fender factor.

An illustration of the deformation diagram of fenders is shown in Fig.17.

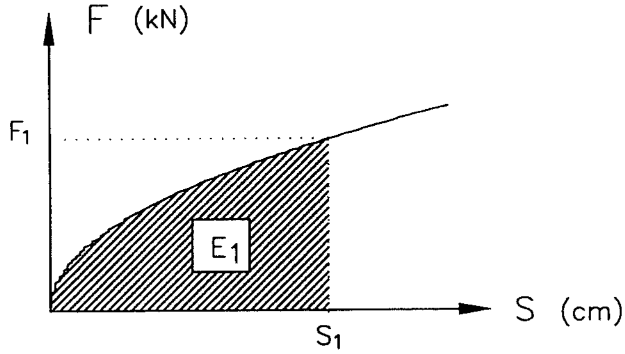

Fig.17. Deformation diagram of fenders.

The energy absorbed by fender corresponding to deformation s_1 is

$$E_1 \;=\; \int_0^{s_1} F(s)\,ds \tag{1}$$

where $F(s)$ instant force

s length of compression of the fender

s_1 final length of compression of fender

And the force transferred to the berth structure F_1 is obtained by the deformation diagram, cf. Fig.17. Therefore the deformation diagram of the fender can easily be converted to the fender factor diagram, cf. Fig.18. The manufacturer of fenders will provide the fender factor diagram.

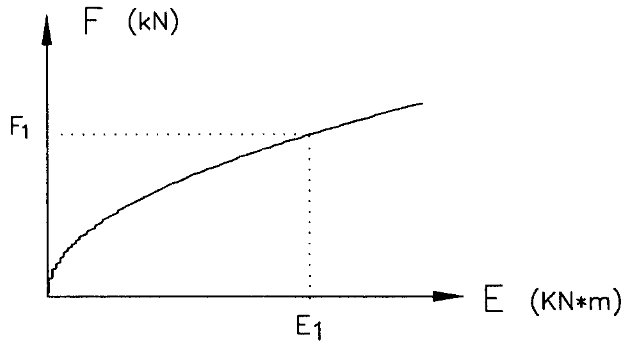

Fig.18. Fender factor diagram.

The choice of the fender proceeds as

1) Calculate the impact energy to be absorbed by the fenders.
2) Choose from the fender factor diagram the fender type which is economical and whose corresponding reaction force will not damage the berth structure.

5.6.3 Absorbed energy by fenders

The energy to be absorbed by fenders due to the impacts of the berthing ship can be estimated from the theoretical, empirical and statistical methods.

The theoretical method is based on the general kinetic energy equation due to the impact of a ship on a berthing structure (Vasco Costa, 1964). Here only empirical formulae are instroduced.

The energy which is to be absorbed by the fender during the impact is

$$E \;=\; C_h\, C_e\, C_c\, C_s\, \frac{mu^2}{2} \tag{2}$$

where E impact energy to be absorbed by the fender

C_h hydrodynamic mass factor, influenced by the ship shape, the underkeel clearance, the ship velocity and the water depth.
$C_h = 1.25 \sim 2.0$, often $C_h = 1.5$ is applied.

C_e eccentricity factor, describing the influence of the distance between the ship gravity center and the impact point, and the ship berthing angle.
$C_e = 0.4 \sim 0.6$

C_c cushion effect of water, describing the buffer effect of the water between the ship and the berth structure. If the berth structure is solid, where the water between the ship and the structure has to be squeezed aside before the ship can touch the structure, a lower value is recommended.
$C_c = 0.8 \sim 1.0$

C_s softening effect, describing the elastic deformation taking place in ship and the berth structure. $C_s = 0.9 \sim 1.0$

m mass of the design ship

u velocity of the berthing ship normal to the berth line, cf. Table 1

Table 1. Velocity of the berthing ship u.

DWT	20,000	40,000	60,000	80,000
u (m/s)	0.11~0.3	0.09 ~ 0.27	0.08 ~ 0.25	0.08 ~ 0.25

Another empirical formula reads

$$E = \frac{10\ m}{120 + \sqrt{m}} \quad (kN \times m) \tag{3}$$

where m is the total weight of the design ship in tonnage.

5.6.4 Ship's impact force on berth structure during berthing operation

Ship's impact force on berth structure during berthing operation is determined as follows

1) Calculate the impact energy to be absorbed by the fenders.
2) Find the impact force from the fender factor diagram.

5.7 Mooring facilities

The mooring facilities include wires or ropes attached to bollards which are fastened to concrete blocks in the berth structures.

There are many types of mooring wires or ropes with different size and strength. The strength of the mooring wires should be smaller than the bearing capacity of the bollards, so that if there is overloading the wires are broken in stead of bollards.

Bollards are usually placed just inside the front edge of the quay. The old wooden poles and stone bollard can still be seen in small structures. Cast steel bollards are a natural part of a modern quay, cf. Fig.19. The bollard load and the distance between bollards are shown in Table 2.

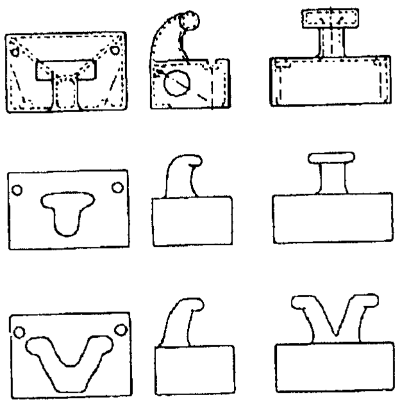

Fig.19. Different types of bollards.

Table 2. Bollard loads.

ship mass up to ton	bollard load kN	app. distance m	bollard load from the berth kN/running meter	bollard load along the berth kN/running meter
2,000	100	5-10	15	10
5,000	200	10-15	15	10
10,000	300	15	20	15
20,000	500	20	25	20
30,000	600	20	30	20
50,000	800	20-25	35	20
100,000	1000	25	40	25
200,000	1500	30	50	30

6 REFERENCE BOOKS

Agerschou, H., Lundgren, H., Sørensen, T. , 1983. *Planning and design of ports and marine terminals.* John Wiley and Sons Ltd., Chichester, UK, 1983.

Burcharth, H.F. , 1993. *The design of breakwaters.* Chapter 28, Coastal and Harbour Engineering Reference Book, Edited by M.B. Abbott and W.A. Price, E & FN SPON, UK, 1993.

Bruun, P. , 1981. *Port engineering (3rd edition).* Golf Publishing Company, Houston, Texas, USA, 1981.

Goda, Y. , 1985. *Random seas and design of marine structures.* University of Tokyo Press, Japan, 1985.

Jensen, O.J. , 1984. *A monograph on rubble mound breakwaters.* Danish Hydraulic Institute, Denmark, 1984.

Thoresen, C.A. , 1988. *Port design: Guidelines and recommendations.* Tapir Publishers, Trondheim, Norway, 1988

7 APPENDIX: New hydraulic stability formulae

Notation

The following notations are used:

D	relative number of displaced units (e.g. for 2% displacement $D = 0.02$)
D_n	equivalent cubic length.
D_{n50}	median equivalent cubic length.
H_s	significant wave height
N_{od}	number of units displaced within a strip with one D_n width.
N_s	stability number, $N_s = \frac{H_s}{\Delta D_{n50}}$.
N_z	number of waves. For $N_z \geq 3000$ use $N_z = 3000$.
P	notional permeability factor, $P = 0.4$ for 2 layer lock armour.
r	Dolos waist ratio
S	relative eroded area.
s_m	fritious wave steepness, $s_m = \frac{H_s}{gT_m^2/2\pi}$.
φ	packing density for two layer armour
α	slope angle.
Δ	$\Delta = \frac{\rho_{armour}}{\rho_{water}} - 1$.

Rock: van der Meer formulae

Deep water conditions

$$\text{Plunging waves, } \xi_m < \xi_{mc} \; : \; \frac{H_s}{\Delta D_{n50}} = 6.2 \cdot S^{0.2}\, P^{0.18}\, N_z^{-0.1}\, \xi_m^{-0.5} \tag{1}$$

$$\text{Surging waves, } \xi_m > \xi_{mc} \; : \; \frac{H_s}{\Delta D_{n50}} = 1.0 \cdot S^{0.2}\, P^{0.13}\, N_z^{-0.1} \cdot cot\alpha^{0.5}\, \xi_m^{P} \tag{2}$$

$$\text{where } \xi_m = tan\alpha\, s_m^{-0.5} \text{ and } \xi_{mc} = \left(6.2\, P^{0.31}\, tan\alpha^{0.5}\right)^{1/(p+0.5)} \tag{3}$$

Shallow water conditions (depth limited waves)

$$\text{Plunging waves} \quad \frac{H_{2\%}}{\Delta D_{n50}} = 8.7\, S^{0.2}\, P^{0.18}\, N_z^{-0.1}\, \xi_m^{-0.5} \tag{4}$$

$$\text{Surging waves} \quad \frac{H_{2\%}}{\Delta D_{n50}} = 1.4\, S^{0.2}\, P^{-0.13}\, N_z^{-0.1}\, cot\alpha^{0.5} \xi_m^{P} \tag{5}$$

The wave height distribution in shallow water conditions is truncated compared to the Rayleigh distribution for which $H_{2\%} = 1.4H_s$. (1) and (2) are equal to (4) and (5) for Rayleigh distributed wave heights.

Concrete cubes: van der Meer formula

Van der Meer (1988) tested a two layer cube armour with one steep slope angle, $cot\alpha = 1.5$. The stability number is given by

$$N_s = \frac{H_s}{\Delta D_n} = \left(6.7\, N_{od}^{0.4} / N_z^{0.3} + 1.0\right)\, s_m^{-0.1} \tag{6}$$

Tetrapods: van der Meer formula

Van der Meer (1988) tested a two-layer Tetrapod armour on a slope with one slope angle, $cot\alpha = 1.5$. The stability number is given by

$$N_s = \frac{H_s}{\Delta D_n} = \left(3.75\, N_{od}^{0.5} / N_z^{0.25} + 0.85\right)\, s_m^{-0.2} \tag{7}$$

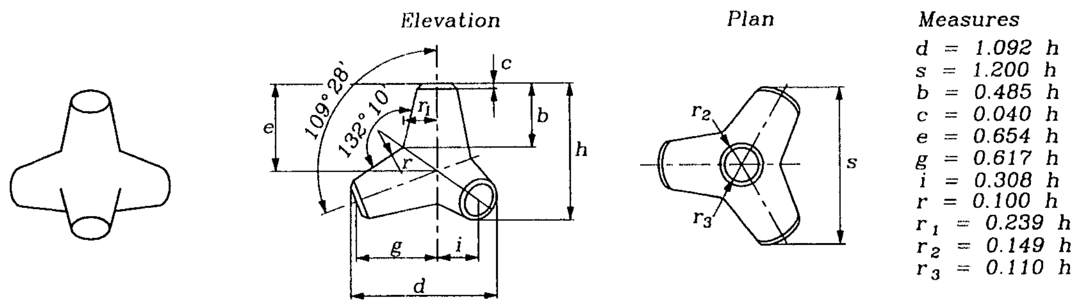

Volume: $V = D_n^3 = 0.280\ h^3$

$D_n = 0.655\ h$

A slightly more simple geometry of Tetrapods is given in SPM, 1984.

Dolosse: Burcharth formula

Based on the results of Brorsen et al. (1974), Burcharth et al. (1986), Holtzhausen et al. (1991) and Burcharth et al. (1992), Burcharth et al. (1992) presented the following formula for hydraulic stability of Dolosse on a slope of 1:1.5

$$
\begin{aligned}
N_s &= \frac{H_s}{\Delta Dn} = (47 - 72r)\,\varphi D^{1/3} N_z^{-0.1} \\
&= (17 - 26r)\,\varphi^{2/3} N_{od}^{1/3} N_z^{-0.1} \qquad (8)
\end{aligned}
$$

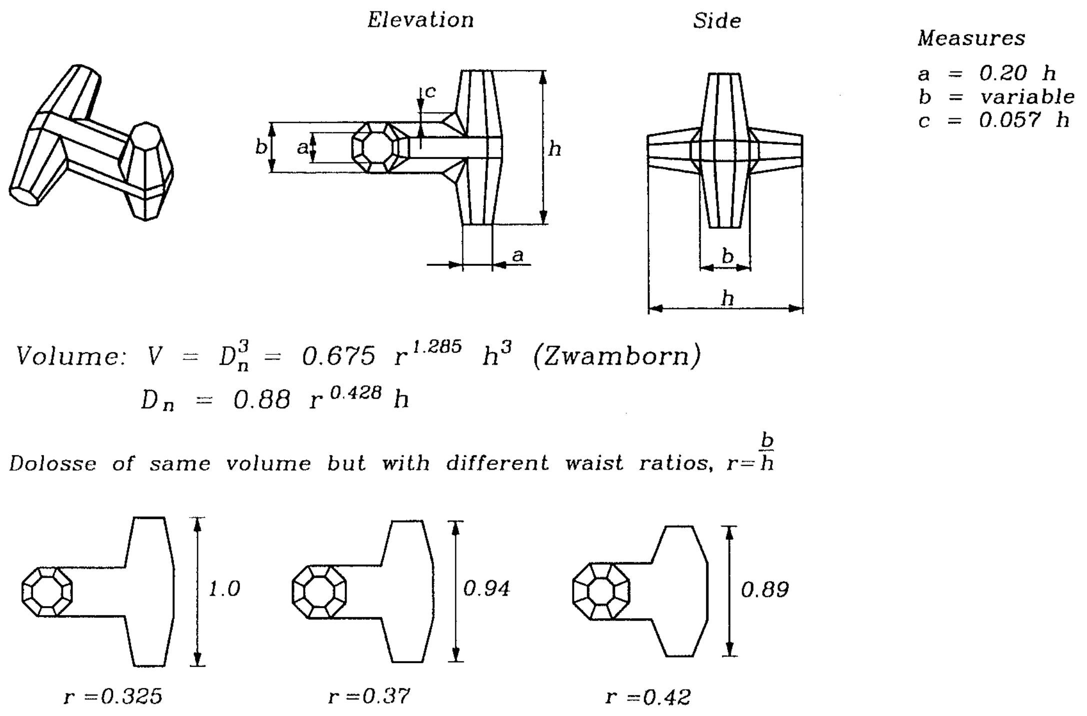

Accropodes (R)

Accropodes are placed in a regular pattern on a steep slope of 1:1.33. For initial choice SOGREAH recommends

$$N_s = \begin{cases} 2.52 & \text{breaking waves} \\ 2.71 & \text{non-breaking waves} \end{cases} \tag{9}$$

Van der Meer (1988) proposed

$$N_s = \begin{cases} 3.7 & \text{no damage} \\ 4.1 & \text{failure} \end{cases} \tag{10}$$

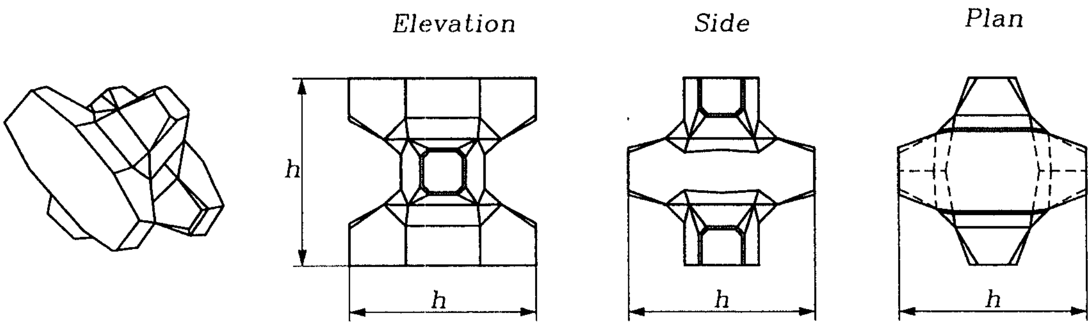

Volume: $V = D_n^3 = 0.343\ h^3$

$D_n = 0.700\ h$

References

Brorsen, M. Burcharth, H.F. and Larsen, T. , 1974. *Stability of Dolos Slopes.* Proc. 14th Coastal Engineering Conference, Copenhagen.

Burcharth, H.F. and Brejnegaard-Nielsen, T. , 1986. *The influence of waist thickness of dolosse on the hydraulic stability of dolos armour.* Proceeding of the 20th International Conference on Coastal Engineering, Taipei, Taiwan, Nov. 1986.

Burcharth, H.F. and Liu, Z. , 1992. *Design Dolos armour units.* To be published in Proc. 23th Coastal Engineering Conference, Venice, Italy, 1992.

van der Meer, J.W. , 1988. *Stability of cubes, Tetrapods and Accropodes.* Proceedings of Breakwater'88, Eastboune, 1988.

van der Meer, J.W. , 1988. *Rock slopes and gravel beaches under wave action.* Ph.D. thesis, Delft University of Technology, the Netherlands, 1988.